

**IMPRINTED FLUOROGENIC RECEPTORS COMPOSED OF
A POLYMERISABLE NAPHTHALIMIDE-BASED
OXYANION PROBE**

Ricarda Wagner

Technische Universität Dortmund
Institut für Umweltforschung der Fakultät Chemie

Technische Universität Dortmund
Institut für Umweltforschung der Fakultät Chemie

**IMPRINTED FLUOROGENIC RECEPTORS COMPOSED
OF A POLYMERISABLE NAPHTHALIMIDE-BASED
OXYANION PROBE**

Promotion am

Institut für Umweltforschung der Fakultät Chemie

Erstprüfer: PD Dr. Börje Sellergren
Zweitprüfer: Prof. Dr. Bernhard Lippert

Verfasser:
Dipl. Chem. Ricarda Wagner
105298
ricarda.wagner@uni-dortmund.de

Le doute n'est pas au-dessous du savoir, mais au-dessus. Le progrès est fils du doute.
L'esprit qui ne sait plus douter descend au-dessous de l'esprit.

-Alain, 1932, Propos sur l'éducation, S.147, 1969

Für meine Eltern

Contents

i. Table of Figures	V
ii. Table of Schemes/ Pictures	IX
iv. List of Tables	XI
v. List of Abbreviations	XIII

Abstract

Zusammenfassung

THEORETICAL PART

1. Introduction	1
2. Basic Spectroscopy	3
2.1 Spectroscopy	3
2.2 Solvatochromism	6
3. Chromogenic and Fluorogenic Sensors for Anions	7
3.1 Approaches towards Optical Sensors	8
3.1.1 Competitive or Displacement Approach	9
3.1.2 Chromogenic and Fluorogenic Sensors via coupling of a binding and signalling unit	9
3.2 Molecularly imprinted Optical Sensors	10
3.3 Molecular imprinting and Molecularly Imprinted Polymers (MIPs)	11
3.4 Approaches for the Preparation of MIPs	12
3.4.1 Covalent Approach	12
3.4.2 Non-covalent Approach	13
4. MIP Formats and Formation	15
4.1 Free Radical Polymerisation	15
4.2 Monolithic MIP Blocks by bulk Polymerisation	16
4.3 MIPs in thin-film Format	16
4.3.1 Living Polymerisation	17
4.4 Nanoparticles	20
5. Applications	21
6. Sensory MIPS via the non-covalent Approach	23
6.1 Templates	23
6.1.1 Amino Acids	24
6.1.2 Penicillin G	26
6.2 Cross-linker/ Commonly employed Co-Monomer/Cross-linker Systems	29
6.3 Solvents	31

6.4	Functional Monomers	35
6.4.1	Chromogenic and Fluorogenic Host Monomers	36
6.5	Initiators for Free Radical Polymerisation	41
7.	Characterisation Techniques	43
7.1	Elemental Analysis	43
7.2	Nuclear Magnetic Resonance (NMR) Spectroscopy	44
7.3	High-Performance liquid Chromatography (HPLC)	44
7.4	Absorption and UV/Vis-Spectrophotometric titrations/ Fluorescence spectra and titrations	46
7.5	Time-correlated Single Photon Counting (Life Time Measurements)	47
7.6	Scanning electron Microscopy (SEM)	47
7.7	Transmission electron Microscopy (TEM)	47
 RESULTS AND DISCUSSION		
8.	Naphthalimide-based Monomers	51
8.1	Design and Synthesis	51
8.2	Evaluation	53
8.2.1	Binding Behaviour	53
8.2.2	Spectroscopic Evaluation	54
9.	Indole-based Monomers	61
9.1	Binding Behaviour	62
9.2	Spectroscopic Evaluation	62
10.	Polymers	67
10.1	Monolithic Polymers via Bulk-Polymerisation	67
10.1.1	Monomers for bulk Synthesis	67
10.1.2	Template Molecules	69
10.1.3	Evaluation	70
10.1.3.1	Chromatographic Evaluation	72
10.1.3.2	Spectroscopic Evaluation of the bulk Polymers containing monomer 1	87
11.	Polymers with increasing Cross-Linking Level	99
11.1	High load Polymers	99
11.1.1	Evaluation	100
11.1.1.1	Response towards TBA Benzoate	100
11.1.1.2	Solvatochromism	104
11.2	Low load Polymers	105
11.2.1	Evaluation	106
11.2.1.1	Response towards TBA Benzoate	106
11.2.1.2	Solvatochromism	108

12. Molecularly Imprinted Polymers in thin-film Format	111
12.1 Films via RAFT Polymerisation Technique	111
12.1.1 Polymerisation of thin-layer Films	112
12.1.2 Response of drop Method Films	117
12.1.3 Response of dip Method Films	118
12.2 Films via Grafting	131
12.2.1 Solution studies of Pre-Polymerisation Mixtures	131
12.2.1.1 Monomer 1 in pentachloroethane	132
12.2.2 Solvent optimisation	138
12.2.3 Thin-film MIPs on glass cover-slips	140
12.2.3.1 MMA/EDMA 110°C Films prepared in Toluene	144
12.2.3.2 BMA/EDMA 110°C Films prepared in Toluene against TBA Z-L-Phe	151
12.2.3.3 BMA/EDMA 110°C Films prepared in Toluene against Penicillin G Potassium Salt	161
13. Conclusion	165
14. Experimental Part	171
15. References	187
Appendix	

i. Table of Figures

Figure 2.1:	Lambert - Beer Law	3
Figure 2.2:	Jablonski Diagram	4
Figure 3.1:	Built-up of a chemical sensor	7
Figure 3.2:	Schematic representation of the covalent imprinting approach	12
Figure 3.3:	Schematic representation of the non-covalent imprinting approach	13
Figure 4.1:	Schematic representation of RAFT polymerisation	14
Figure 4.2:	General structure of RAFT agents	14
Figure 4.3:	RAFT agent	14
Figure 6.1:	<i>L</i> -Phenylalanine anilide	23
Figure 6.1:	<i>L</i> -Glutamic acid	25
Figure 6.2:	<i>Z-L</i> -Glutamic acid	25
Figure 6.3:	<i>L</i> -Phenylalanine	26
Figure 6.4:	<i>Z-L</i> -Phenylalanine	26
Figure 6.5:	Penicillin G	26
Figure 6.6:	Penicillin G procain	27
Figure 6.7:	<i>N,N'</i> -methylenebisacrylamide	29
Figure 6.8:	EDMA	29
Figure 6.9:	DVB	33
Figure 6.10:	Commonly employed monomers for molecular imprinting	35
Figure 6.11:	Naphthalimides	37
Figure 6.12:	Indoles	37
Figure 6.13:	Phenoxazinones	38
Figure 6.14:	Benzoxadiazoles	38
Figure 6.15:	Commonly employed azo-initiators for free-radical polymerisation	41
Figure 8.1:	<i>p</i> -Vinylisocyanate	51
Figure 8.2:	NMR Spectra of 1 upon addition of 0, 0.25 and 6 eq of TBAB in DMSO- d_6	
Figure 8.3:	Absorption titration spectra of monomer 1 in DMSO and ACN	54
Figure 8.4:	Absorption titration spectra of monomer 1 in THF	55
Figure 9.1:	Complexation induced shift (CIS) as a function of the free concentration of TBA benzoate in DMSO- d_6	62
Figure 9.2:	Absorption spectra of monomer 2 in DMSO in presence of increasing concentration of TBA-benzoate	63
Figure 9.3:	Fluorescence emission of monomer 2 in DMSO in presence of increasing concentration of TBA-benzoate	64
Figure 10.1:	Monomer 3	68
Figure 10.2:	Monomer 4	68
Figure 10.3:	Monomer 5	68

Figure 10.4:	Maximum emission wavelength of <i>P_{IN}</i> , <i>P_{IGlu}</i> , <i>P_{IPhe}</i> and <i>P_{IPenG}</i> plotted against maximum emission wavelength of monomer 1 in Dioxane, THF, ACN, EtOH	88
Figure 10.5:	Fluorescence emission intensity of <i>P_{IGlu}</i> in water in presence of increasing concentration of Z-L-Glu	91
Figure 10.6:	Comparison of fluorescence emission intensities of <i>P_{IGlu}</i> in different solvents in presence of increasing concentration of Z-L-Glu	92
Figure 10.7:	Normalised fluorescence emission intensity of <i>P_{IGlu}</i> in water and in presence of 10 mM Z-L-Glu/PMP	93
Figure 10.8:	Normalised fluorescence emission intensity of <i>P_{IPhe}</i> in presence of water and PMP in water plotted against wavelength	95
Figure 10.9:	Normalised fluorescence emission intensity of <i>P_{IPhe}</i> in presence of water upon addition of Z-L-Phenylalanine/PMP, Z-D-Phenylalanine/PMP, Penicillin G potassium salt/PMP plotted against wavelength	96
Figure 11.1:	Normalised and background corrected fluorescence emission intensity of Polymer 1 upon increasing concentration of TBA Benzoat	101
Figure 11.2:	Solvatochromic behaviour of polymers of increasing cross-linking level	104
Figure 11.3:	Fluorescence emission upon addition of increasing concentration of guest on M1, M2, M3 and M4	107
Figure 11.4:	Solvatochromic behaviour of polymers of increasing cross-linking level (NIPs)	108
Figure 11.5:	Solvatochromic behaviour of polymers of increasing cross-linking level (MIPs)	108
Figure 12.1:	Maximum emission wavelength of NIP IV and MIP IV in presence of 1,4 Dioxane, THF, EtOH and ACN plotted against maximum emission wavelength of monomer 1	117
Figure 12.2:	Maximum emission wavelength of NIP II and MIP II in presence of 1,4 Dioxane, THF, EtOH and ACN plotted against maximum emission wavelength of monomer 1	119
Figure 12.3:	Maximum emission wavelength of NIP V and MIP V in presence of 1,4 Dioxane, THF, EtOH and ACN plotted against maximum emission wavelength of monomer 1	122
Figure 12.4:	Maximum emission wavelength of NIP VI and MIP VI in presence of 1,4 Dioxane, THF, EtOH and ACN plotted against maximum emission wavelength of monomer 1	123
Figure 12.5:	Maximum emission wavelength of NIP 30I and MIP 30I in presence of 1,4 Dioxane, THF, EtOH and ACN plotted against maximum emission wavelength of monomer 1	124
Figure 12.6:	Maximum emission wavelength of NIP 30II and MIP 30II in presence of 1,4 Dioxane, THF, EtOH and ACN plotted against maximum emission wavelength of monomer 1	125

Figure 12.7:	Normalised emission intensity of NIPIII and MIPIII slides recorded after polymerisation, washing and incubation with Z-L-Phe, Z-D-Phe, Benz and Z-L-Glu in dry state	126
Figure 12.8:	Normalised emission intensity of NIPVI and MIPVI slides recorded after polymerisation, washing and incubation with Z-L-Phe, Z-D-Phe, Benz and Z-L-Glu in dry state	127
Figure 12.9:	Background corrected intensity normalised emission intensity of NIPVI in ACN and increasing concentration of Z-L-Phe and Z-D-Phe	128
Figure 12.10:	Background corrected intensity normalised emission intensity of MIPVI in ACN and increasing concentration of Z-L-Phe and Z-D-Phe	129
Figure 12.11:	Absorption spectra of monomer 1, and the pre-polymerisation mixtures in pentachloroethane at varying temperatures	133
Figure 12.12:	Normalised fluorescence emission intensity of NIP and MIP MMA (50°C) upon addition of TBA-Z-L-Phe	
Figure 12.13:	Normalised fluorescence emission intensity of NIP and MIP MMA (110°C) upon addition of TBA-Z-L-Phe	135
Figure 12.14:	Normalised fluorescence emission intensity of NIP and MIP HEMA (110°C) upon addition of TBA-Z-L-Phe	135
Figure 12.15:	Excitation spectra of polymer film MIP HEMA/EDMA 50°C, $\lambda_{em} = 470, 485, 510$ nm; $\lambda_{ex} = 300 - 470$ nm	136
Figure 12.16:	Excitation spectra of polymer film MIP MMA/EDMA 50°C, $\lambda_{em} = 470, 485, 510$ nm; $\lambda_{ex} = 300 - 470$ nm	136
Figure 12.17:	Absorption spectra of monomer 1, and the pre-polymerisation mixtures in di-n-butylether	138
Figure 12.18a:	Absorption spectra of monomer 1, and the pre-polymerisation mixtures (HEMA/EDMA) in toluene	139
Figure 12.18b:	Absorption spectra of monomer 1, and the pre-polymerisation mixtures (MMA/EDMA) in toluene	139
Figure 12.18c:	Absorption spectra of monomer 1, and the pre-polymerisation mixtures (Styrene/DVB) in toluene	140
Figure 12.19:	Background corrected fluorescence emission intensity of MMA/EDMA MIP film prepared on RAFT cover-slip at 110°C in toluene in presence of increasing concentration of the template TBA Z-L-Phe in ACN	141
Figure 12.20:	Background corrected fluorescence emission intensity of MMA/EDMA MIP film prepared at 50°C in toluene in presence of increasing concentration of the template TBA Z-L-Phe in ACN	142
Figure 12.21:	Background corrected fluorescence emission intensity of MMA/EDMA MIP film prepared at 110°C in toluene in presence of increasing concentration of the template TBA Z-L-Phe in ACN	143
Figure 12.22:	Background corrected fluorescence emission intensity of Styrene/EDMA MIP film prepared at 110°C in toluene in presence of increasing concentration of the template TBA Z-L-Phe in ACN	144
Figure 12.23:	Comparison of background-corrected fluorescence emission intensity of NIP	

	films prepared in different batches and upon reuse after soxhlet extraction	145
Figure 12.24:	Comparison of background-corrected fluorescence emission intensity of MIP films prepared in different batches and upon reuse after soxhlet extraction	145
Figure 12.25:	Maximum emission wavelength of free monomer in solution plotted against maximum emission wavelength of the MMA/EDMA polymer films prepared at 110°C in toluene measured in Dioxane, THF, ACN and EtOH	145
Figure 12.26:	Normalised and background corrected fluorescence emission intensity of MMA/EDMA NIP and MIP films prepared in Toluene at 50°C in presence of increasing concentration of TBA Z-L-Phe and TBA Z-D-Phe	146
Figure 12.27:	α_Q for Z-L-Phe and Z-D-Phe on MMA/EDMA MIP	148
Figure 12.28:	Normalised and background corrected fluorescence emission intensity of MMA/EDMA NIP and MIP films prepared in Toluene at 110°C in presence of increasing concentration of TBA Z-L-Phe and TBA Z-D-Phe	148
Figure 12.29:	Quotient of titration curves of MMA/EDMA MIP in presence of Z-L-Phe and Z-D-Phe	150
Figure 12.30:	Benzyl methacrylate	151
Figure 12.31:	Maximum emission wavelength of free monomer in solution plotted against maximum emission wavelength of the BMA/EDMA polymer films prepared at 110°C in toluene measured in Dioxane, THF, ACN and EtOH	151
Figure 12.32:	Normalised and background corrected fluorescence emission intensity of BMA/EDMA NIP and MIP films prepared in Toluene at 110°C in presence of increasing concentration of TBA Z-L-Phe and TBA Z-D-Phe, TBA-Z-L-Glu, TBA Z-L-Tyr	152
Figure 12.33:	Titration curves of BMA/EDMA MIP in presence of Z-L-Phe, Z-D-Phe, Z-L-Glu and Z-L-Tyr	154
Figure 12.34:	Normalised and background corrected fluorescence emission intensity of BMA/EDMA NIP and MIP films prepared in Toluene at 110°C in presence of increasing concentration of TBA Z-L-Phe and in ACN:H ₂ O (50:50)	155
Figure 12.35:	Normalised and background corrected fluorescence emission intensity of BMA/EDMA MIP films prepared in Toluene at 110°C in presence of increasing concentration of TBA Z-L-Phe and TBA Z-D-Phe ACN:H ₂ O (10:90)	156
Figure 12.36:	Normalised and background corrected fluorescence emission intensity of BMA/EDMA NIP and MIP films prepared in Toluene at 110°C in presence of increasing concentration of TBA Z-L-Phe, TBA Z-D-Phe, TBA Z-L-Glu and TBA Z-L-Tyrosin ACN:TEA (99:1)	157
Figure 12.37:	Titration curves of BMA/EDMA MIP in presence of Z-L-Phe, Z-D-Phe, Z-L-Glu and Z-L-Tyr	160
Figure 12.38:	Normalised, background corrected fluorescence emission intensity of BMA/EDMA NIP and MIP films prepared in Toluene at 110°C in presence of increasing concentration of PenG pot in ACN	161

ii. Table of Schemes

Scheme 3.1:	Reaction scheme of RAFT polymerisation	15
Scheme 8.1:	Synthesis path of monomer 1	49
Scheme 9.1:	Synthesis path of monomer 2	59

iii. Table of Pictures

Picture 8.1:	Induced colour-change of a solution of monomer 1 in DMSO in presence of increasing concentration of TBA benzoate	52
Picture 9.1:	Colours of monomer 2 solutions in DMSO and in presence of increasing concentration of TBA-benzoate	62
Picture 10.1:	Colours of monomer 4 polymers prior and after extraction	68
Picture 10.2:	Colours of monomer 5 polymers prior and after extraction	69
Picture 10.3:	Colours of monomer 1 polymers prior and after extraction	69
Picture 10.4:	left: NIP in solvent, right: NIP in 2 mM Z-L-Glu	85
Picture 10.5:	left: MIP in solvent, right: MIP in 2 mM Z-L-Glu	85
Picture 10.6:	left: NIP in solvent, right: NIP in 2 mM PenG	86
Picture 10.7:	left: MIP in solvent, right: MIP in 2 mM PenG	86
Picture 10.8:	Colours of P_{1Glu} in water and 10 mM Z-L-Glu/PMP	91
Picture 10.9:	left: P_{6Phe} in water, right: P_{6Phe} in PMP in water	92
Picture 11.1:	Colour of polymer 1 in absence and in presence of 10 eq of TBA Benzoat	99
Picture 11.2:	Colour of polymer 2 in absence and in presence of 10 eq of TBA Benzoat	100
Picture 11.3:	Colour of polymer 3 in absence and in presence of 10 eq TBA Benzoat	100
Picture 11.4:	Colour of polymer 4 in absence and in presence of 10 eq TBA Benzoat	100
Picture 11.5:	Colour of polymer 6 in absence and in presence of 10 eq TBA Benzoat	101
Picture 11.6:	Colour in omission and upon addition of guest on left: M1, right: M2	105
Picture 11.7:	Colour in omission and upon addition of guest on left: M3, right: M4	105

Picture 12.1:	Unmodified glass cover-slip	112
Picture 12.2:	Activated glass cover-slip	112
Picture 12.3:	Amino-functionalised glass cover-slip	112
Picture 12.4:	Glass cover-slip with immobilised RAFT agent	112
Picture 12.5:	Polymer film (ACN)	114
Picture 12.6:	Polymer film (ACN: Toluene, 50:50)	114
Picture 12.7:	Polymer film (DMF)	114
Picture 12.8:	Polymer film (CHCl ₃)	114

iv. List of Tables

Table 6.1:	Properties of commonly-employed imprinting solvents	33
Table 8.1:	Maximum absorption of monomer 1 and precursor in different solvents	53
Table 8.2:	Association constants for monomer 1 in THF, ACN and DMSO derived from titration data	55
Table 8.3:	Maximum emission of monomer 1 and precursor in different solvents	56
Table 10.1:	Composition of the monolithic polymers P₁N , P_{Glu} , P_{Ph} , P_{PenG}	57
Table 10.2:	Retention times, capacity- and imprinting factors on P_{1Glu} and P_{1N}	71
Table 10.3:	Retention times, capacity- and imprinting factors on P_{4Glu} and P_{4N}	73
Table 10.4:	Retention times, capacity- and imprinting factors on P_{5Glu} and P_{5N}	74
Table 10.5:	Retention times, capacity- and imprinting factors on P_{3Glu} and P_{3N}	75
Table 10.6:	Retention times, capacity- and imprinting factors on P_{2Glu} and P_{2N}	76
Table 10.7:	Retention times, capacity- and imprinting factors on P_{1Ph} and P_{1N}	77
Table 10.8:	Retention times, capacity- and imprinting factors on P_{4Ph} and P_{4N}	78
Table 10.9:	Retention times, capacity- and imprinting factors on P_{5Ph} and P_{5N}	79
Table 10.10:	Retention times, capacity- and imprinting factors on P_{1PenG} and P_{1N}	80
Table 10.11:	Retention times, capacity- and imprinting factors on P_{4PenG} and P_{4N}	81
Table 10.12:	Retention times, capacity- and imprinting factors on P_{5PenG} and P_{5N}	82
Table 10.13:	Maximum emission wavelength of P_{1N} , P_{1Glu} , P_{1Ph} and P_{1PenG} in water and dry state	
Table 10.14:	IF_Q for P_{1Glu} in presence of increasing concentration of Z-L-Glu/PMP	90
Table 10.15:	Swelling ratios of the bulk polymers in different solvents	94
Table 11.1:	Polymer composition	97
Table 11.2:	Monomer to Template ratios	98
Table 11.3:	NIP compositions with increasing cross-linking level	103
Table 11.4:	MIP compositions with increasing cross-linking level	104
Table 12.1:	Recipes for thin-film polymers dip method	111
Table 12.2:	Polymer composition of drop method films	113
Table 12.3:	Dielectricity constants of the evaluated solvents	117
Table 12.4:	Maximum emission wavelegth of NIP IV and MIP IV in solvents of different polarity	117
Table 12.5:	Maximum emission wavelegth of NIP II and MIP II in solvents of different polarity	118
Table 12.6:	Maximum emission wavelegth of NIP V and MIP V in solvents of different polarity	119
Table 12.7:	Maximum emission wavelegth of NIP VI and MIP VI in solvents of different polarity	120
Table 12.8:	Maximum emission wavelegth of NIP 30I and MIP 30I in solvents of different polarity	121

Table 12.9:	Maximum emission waveleghth of NIP 30II and MIP 30II in solvents of different polarity	122
Table 12.10:	Maximum emission wavelength and intensity of the NIPVI and MIPVI at maximum emission wavelength after incubation with Z-L-Phe, Z-D-Phe, Benz and Z-L-Glu in dry state	125
Table 12.11:	Imprinting factors calculated from fluorecence titration of NIPVI and MIPVI in presence of Z-L-Phe and Z-D-Phe	127
Table 12.12:	Quenching factors calculated from fluorecence titration of NIPVI and MIPVI in presence of Z-L-Phe and Z-D-Phe	128
Table 12.13:	Pre-polymerisation compositions tested in pentachloroethane	130
Table 12.14:	Pre-polymerisation compositions investigated in di-n-butylether and toluene	135
Table 12.15:	Imprinting factors of System 3 calculated from fluorecence quenching in ACN upon addition of TBA Z-L-Phe	141
Table 12.16:	IF _Q and QF of MMA/EDMA films	146
Table 12.17:	Imprinting and quenching factor for MMA/EDMA films prepared in Toluene	147
Table 12.18:	Imprinting factors for BMA/ EDMA films prepared in Toluene	150
Table 12.19:	Quenching factors for BMA/ EDMA films prepared in Toluene	151
Table 12.20:	Imprinting factors calculated for BMA/EDMA films prepared in Toluene in ACN:TEA (99:1)	155
Table 12.21:	Quenching factors calculated for BMA/EDMA films prepared in Toluene in ACN:TEA (99:1)	156
Table 12.22:	Imprinting factors calculated for PenG pot BMA/EDMA films prepared in Toluene in ACN	158

v. List of Abbreviations

ABDV	Azobisdimethylvaleronitrile
AIBN	Azobisisobutyronitrile
α_Q	Separation factor Quenching
ATRP	Atom transfer radical polymerisation
BMA	Benzyl methacrylate
CIS	Complexiation induced shift
DAD	Diode-array Detector
DFG	Deutsche Forschungsgesellschaft
DVB	Divinyl benzoic acid
EA	Elemental analysis
EDMA	Ethylene glycol dimethacrylate
HEMA	(Hydroxyethyl)methacrylate
HPLC	High performance liquid chromatography
IC	Internal conversion
IF _Q	Imprinting factor calculated from fluorescence quenching
ISC	Intersystem crossing
IUPAC	International Union of Pure and Applied Chemistry
L-PA	L-Phenylalanine anilide
LASER	Light amplification by stimulated emission of radiation
MIP	Molecularly Imprinted Polymer
MMA	Methylmethacrylate
NIP	Non-Imprinted Polymer
NMR	Nuclear magnetic resonance
NMP	Nitroxide mediated polymerisation
PMP	1,2,2,6,6-Pentamethylpiperidine
PVB	Para-vinylbenzoic acid
RAFT	Reversible Addition-Fragmentation chain transfer
PenG Pot	Penicillin G potassium salt
PenG Proc	Penicillin G procaine salt

QF	Quenching Factor
Z-L-Glu	Z-L-Glutamic acid
Z-L-Phe	Z-L-Phenylalanine

ABSTRACT

The presented work is part of a DFG project. The goal of the project was the design, synthesis and evaluation of molecularly imprinted polymers (MIPs) with optical sensing properties, aimed at the selective detection of anionic guest-molecules.

The projects combines the rapidly growing field of anion-detection with molecular imprinting. Upon integration of tailor-made monomers with fluorogenic properties into MIPs, selective materials with the dual ability to bind a specific anionic analyte and simultaneously report the binding by a luminescence change were developed.

In order to meet this goal in a first step urea-based monomers containing a chromophoric π -system were designed and synthesised. Their affinity towards anionic guest-molecules and thus their applicability for the integration into MIPs was investigated. Furthermore, it was evaluated, if the binding event is transduced into a spectroscopically detectable signal.

Based on the monomers showing the desired properties, MIPs in different formats were developed and investigated. Monolithic bulk polymers were prepared in order to evaluate the separation properties of the polymers. For applications with the focus on sensory characteristics thin-film MIPs on glass-supports were synthesised.

The materials prepared for the presented work meet the goal of the project in an outstanding way. Upon chromatographic evaluation, MIPs prepared from the novel monomers showed pronounced discrimination between their template and structurally related analytes. Furthermore, the polymers were able to discriminate enantioselectively. Also the polymers in film-format revealed strong enantioselective discrimination and selectivity towards structurally related analytes. The binding of the template induces pronounced fluorescence quenching. This quenching is not, respectively less pronounced observed for the other enantiomer and other analytes.

In summary MIPs based on tailor-made monomers with fluorogenic properties were successfully prepared. These polymers detect their respective template selectively, leading to high imprinting factors in chromatographic evaluations and strong luminescence changes in spectroscopical tests.

ZUSAMMENFASSUNG

Ziel der vorliegenden, im Rahmen eines DFG Projektes erstellten Arbeit waren das Design, die Synthese und die Untersuchung molekular geprägter Polymere (MIPs) mit optischen Sensoreigenschaften zur selektiven Detektion anionischer Gastmoleküle.

Das Projekt verbindet das wachsende Feld der Anion-Detektion mit dem Bereich der molekularen Prägung. Durch den Einbau speziell entwickelter, funktioneller Monomere mit fluorogenen Eigenschaften in molekular geprägte Polymere wurden selektive Materialien hergestellt, die die Bindung eines spezifischen, anionischen Analyten durch eine einfach zu detektierende Änderung in der Lumineszenz anzeigen.

Im Zuge dessen wurden zunächst Harnstoff-basierte, ein chromophores π -System enthaltende, Monomere entwickelt. Um ihre Attraktivität für den Einbau in ein Sensor-MIP zu überprüfen, wurden die Affinität der Monomere zu anionischen Gastmolekülen überprüft und ermittelt, ob die Interaktion mit einer Änderung in den spektroskopischen Eigenschaften verbunden ist.

Die vielversprechendsten Monomere wurden für die Synthese von MIPs in verschiedenen Formaten ausgewählt. Zur Untersuchung der Trennungseigenschaften in chromatographischen Anwendungen wurden zunächst monolithische Polymere synthetisiert. Für Anwendungen, bei denen Sensoreigenschaften im Vordergrund stehen, wurden geprägte Filmsysteme auf Glassoberflächen entwickelt.

Die im Rahmen dieser Arbeit hergestellten Materialien erfüllen in herausragender Weise die Zielstellung des Projektes. MIPs basierend auf den neu entwickelten Monomeren zeigen sehr gute Diskriminierung zwischen ihrem Templat und strukturell verwandten Analyten in chromatographischen Untersuchungen und zeigen Enantioselektivität. Auch die Polymere in Filmformat zeigen starke enantioselektive Diskriminierung und Selektivität gegenüber anderen Analyten. Die Bindung des Templats wird in diesem Fall indiziert durch eine Verringerung der Fluoreszenz, die nicht oder wesentlich schwächer für das andere Enantiomer und andere Analyten beobachtet wird.

Zusammenfassend ist es gelungen, MIPs in verschiedenen Formaten basierend auf neu entwickelten, fluorogenen Monomeren herzustellen. Diese Polymere reagieren selektiv auf ihr jeweiliges Templat; resultierend in hohen Imprinting-Faktoren in chromatographischen Anwendungen und stark selektiver Fluoreszenzabnahme in spektroskopischen Tests.

THEORETICAL PART

1. Introduction

Due to the reason that molecular recognition of anions is omnipresent in biological systems, the field of anion sensing in general and the detection of small molecule anions in particular has gained rapidly growing attention during the last decades.

The examples of processes in biological systems based on molecular recognition via highly specific bindings are various, ranging from antibody-antigen binding over ligand-receptor interactions to enzyme catalysis.¹ The outstanding capability of these materials to selectively bind a target molecule results from combining several complementary weak interactions such as hydrogen bonding or van-der-Waals interactions.² Employing these biological recognition elements in big-scale technical applications is hindered by the characteristics of these materials e.g. their limited availability and poor resistance against chemical treatment. Thus, the need for artificially made materials with similar recognition properties but overcoming the limiting characteristics of naturally - occurring materials is constantly growing.

Molecular imprinting enables chemists to create polymer materials mimicking biological compounds in their molecular recognition properties, but overcoming their limiting characteristics. The design and synthesis of molecularly imprinted polymers (MIPs) is aiming at meeting this goal. MIPs are tailor-made receptors for a given target analyte. A perfectly fitting imprint is obtained via polymer preparation using the target molecule as a mould. The resulting polymers are of higher operational stability and robustness than their biological models, which increases their applicability in industrial processes also under harsher conditions³ such as high temperatures, acidic or basic media and organic solvents.

MIPs feature various favourable characteristics with regards to a wide range of end-user applications. Depending on the preparation technique and the amount of cross-linker employed, MIPs exhibit good thermal and mechanical stability. To date various examples of polymers with good recognition and separation properties have been published.

Nevertheless, these artificial receptors are still rather primitive compared to what nature offers. Sellergren presents a list of limitations for their application in real life.⁴ These are e.g.:

- Non-specific binding
- Slow mass transfer

- Poor recognition in aqueous solvents
- Non-applicability for important compound classes

The work presented in this thesis contributes to overcome some of these challenges. It is aimed at the design, development and synthesis of molecularly imprinted polymers for optical sensing applications, mainly of small molecule anions, in different formats. Apart from the well-established and commonly used monolithic approach, the molecularly imprinted polymers were transferred to other systems such as films and nanoparticles. Depending on the application, both formats offer distinct advantages over bulk materials. Nanoparticles offer e.g. a high surface area⁵ whereas film systems show faster mass transfer and are therefore well suited for sensing applications⁶.

Via integration of newly-designed fluorogenic or chromogenic sensing units into the backbone of a molecularly imprinted polymer, materials were developed that are able to simultaneously bind a given target molecule and indicate the binding event by spectroscopical means, namely a colour-change visible to naked-eye or a change in the fluorescence emission properties. Unlike anion sensors used in their molecular state in solution, sensory MIPs are able to discriminate not only specific compound groups, but also between specific molecules within a group.

Materials with this unique combination of characteristics can be of great interest for a broad range of real-life applications such as sensing and selective determination of trace compounds in e.g. food industry, biotechnology, environment and health care.⁷

2. Basic spectroscopy

2.1. Spectroscopy

To allow better understanding of the field of sensing applications a short introduction on spectroscopy is given here.

Spectroscopy investigates the interaction between matter and radiated energy and is an important field of instrumental analytics. Radiated energy, or light, is a small part of the spectrum of electromagnetic radiation. All kinds of electromagnetic radiation vary only in wavelength λ , respectively frequency ν . Optical radiation is subdivided into ultraviolet (UV, 400-10 nm), visible light (VIS, 780-380 nm) and near and far Infrared (IR).

Analysing e.g. emission and absorption allows quantitative and qualitative characterisation of a given substance. When matter is hit by radiation, the radiation might be absorbed, transmitted, scattered or reflected. Matter may absorb radiation of a distinct frequency; the energy of the frequency relates to the difference between two electron energy-levels. The relationship between absorbance, the concentration of the absorber and the path length is described by the Lambert-Beer Law:

$$A = \epsilon \cdot c \cdot l \qquad A = \log_{10} I_0/I \qquad (2.1)$$

A = Absorbance

ϵ = molar absorption coefficient

c = Concentration

l = absorption path length

I_0 = Incident light

I = Transmitted light

Figure 2.1: Lambert - Beer Law

UV/VIS spectroscopy is a technique commonly employed to gain information about a given sample and is based on the specific absorption of ultraviolet or visible radiation by chromophores. The resulting electromagnetic spectrum is referred to as absorption spectrum and is characteristic for a given sample. Depending on the sample the absorption spectra show

a more or less broad absorption band. Due to the validity of the Lambert-Beer law UV/VIS spectroscopy may be used not only for qualitative but also for quantitative analysis.

Also the **emission**, the electromagnetic spectrum emitted by matter when it returns from an excited to a lower energy state, can be evaluated. In case that the return is fast the emission is referred to as fluorescence; in case that the return is slow due to a spin-forbidden intersystem crossing the emission is referred to as phosphorescence.

For better understanding the Jablonski-diagram is displayed here.

The Jablonski-scheme is a visualisation of the energy states and transitions of a molecule. The energy of a molecule is defined by four kinds of energy:

- Translation energy
- Rotation energy
- Vibration energy
- Electron energy

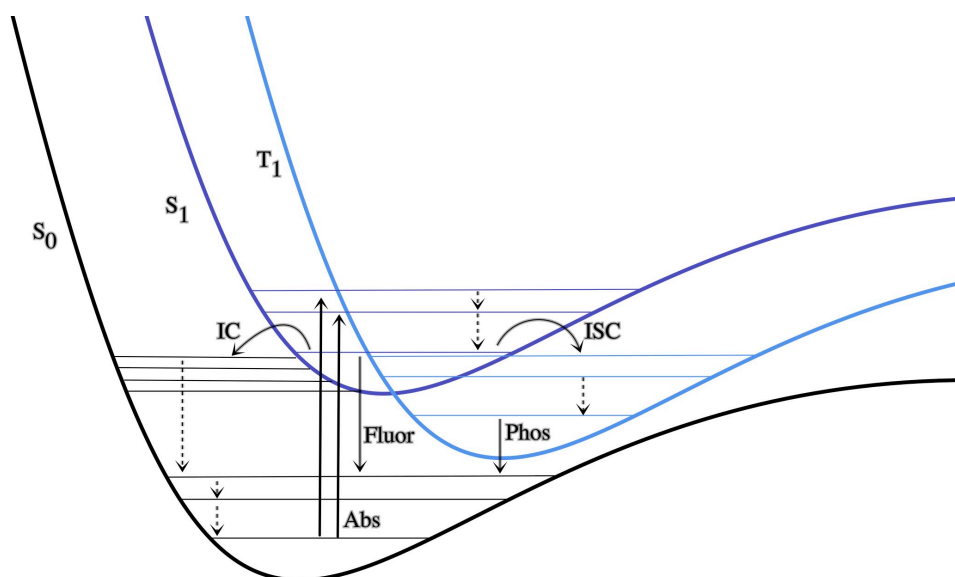


Figure 2.2: Jablonski diagram

The diagram displays the singlet ground state S_0 , one higher singlet excited state S_1 and the triplet state T_1 with parallel spins.

If a photon with appropriate energy is absorbed by a molecule, an electron is transferred from the ground state S_0 to a vibrational state of an excited singlet state e.g. S_1 . From here the energy can be dispersed of by radiative or non-radiative transitions. The fluorescence efficiency of a molecule is thus strongly dependent on the rate of the non-radiative deactivation of the fluorescent state.⁸

The molecule changes from a vibrational state of S_1 to the ground state of the excited state (non-radiative).

- *Fluorescence*: The molecule changes from the excited ground state to a vibrational state of S_0 (radiative transition)
- *Internal conversion (IC)*: The molecule changes from the excited ground state to a high vibrational state of S_0 and reaches the ground state by emitting heat (non-radiative transition)
- *Intersystem crossing (ISC)*: The molecule changes via spin-forbidden transition to the triplet state T_1 (parallel spins)
- *Phosphorescence*: From the triplet ground state the molecule changes to a vibrational state of S_0 (radiative transition)

Whether a molecule emits fluorescence or phosphorescence is predetermined by the position of the states and the transition probabilities defined by the Franck-Condon principle.

In photochemistry one distinguishes between chromophores and luminophores. IUPAC defines a *chromophore* as „The part (atom or group of atoms) of a molecular entity in which the electronic transition responsible for a given spectral band is approximately localized. The term arose in the dyestuff industry, referring originally to the groupings in the molecule that are responsible for the dye’s colour.“⁹ The terms chromophore or chromogenic are thus referring to absorption phenomena.

In case that an emission phenomena is referred to the term *luminophore* is the appropriate one. A luminophore is „A part of a molecular entity (or atom or group of atoms) in which electronic excitation associated with a given emission band is approximately localized.“¹⁰ A fluorophore is a molecular entity that emits fluorescence and hence a special type of luminophore.

2.2. Solvatochromism

The term *solvatochromism* describes the influence of a solvent on the colour of a dye molecule. Depending on the nature of the dye and the resulting behaviour it is commonly distinguished between positive and negative solvatochromism.

In the case of *positive solvatochromism* the dye-molecule is present in a non-polar structure in its ground state. Upon addition of a polar solvent the ground state is destabilised, resulting in a higher energy level and thus an absorption maximum located at a longer wavelength. Due to the fact that the energy difference between the ground state and the excited state is diminished, the absorption process needs less energy. The wavelength is anti-proportional to the energy content and thus a *barthochromic shift* in the absorption spectrum is observed (shift to longer wavelengths, red shift).

In the case of *negative solvatochromism* the dye molecule is mainly present in a polar structure in its ground state. Addition of a polar solvent stabilises the polar structure and the energy level is lowered. Due to the fact that the excited state is not influenced by the polar solvent the energy gap between the ground state and the excited state is growing. Thus, the absorption process needs more energy. More energy corresponds to shorter wavelength, resulting in a *hypsochromic shift* (shift to shorter wavelengths, blue shift).

3. Chromogenic and fluorogenic sensors for anions

Materials with the desired properties described in the introduction belong to the group of chemosensors, respectively chemical sensors. IUPAC defines a chemical sensor as: „...a device that transforms chemical information, ranging from the concentration of a specific sample component to total composition analysis, into an analytically useful signal.“¹¹

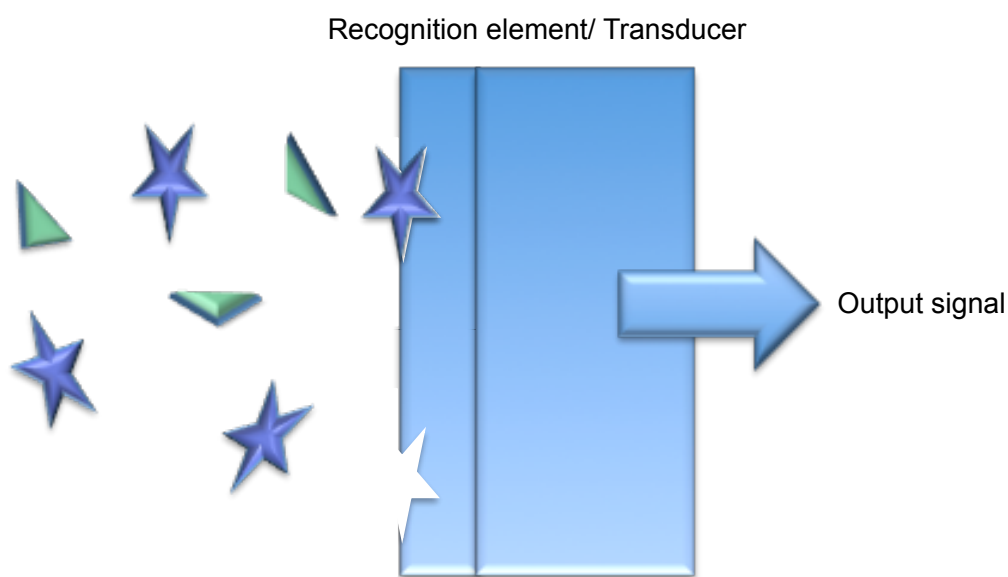


Figure 3.1: Built-up of a chemical sensor

As displayed in figure 3.1 a chemical sensor consists of a receptor part or recognition element and a transducer part. The transducer part transforms the interaction with an analyte into an electrical or optical signal.

Generally, the reception mode in a chemical sensor may be classified by the type of interaction taking place:¹²

1. *Physical receptors:* Without chemical reaction; detects changes in e.g. absorbance, temperature
2. *Chemical receptors:* The analytical signal is the result of a chemical reaction including the analyte
3. *Biochemical receptors:* The analytical signal is due to a biochemical process, e.g. immunosensors

In the sensing systems the presented work is dealing with, the interaction of the receptor with an analyte is transformed into an optical signal.

3.1. Approaches towards optical sensors

The ultimate goal in the development of anion sensors is the creation of a material that is able to detect and bind an anion and simultaneously indicate the presence of the analyte spectroscopically. Ideally, the reported change allows the quantification of the anion present.

Depending on the nature of the signalling unit the binding of an analyte leads to easily detectable changes in the spectroscopic properties of the monomer. In case of chromophores the detection is based on increased or decreased absorption intensity, or a shift of the absorption band, whereas in the case of fluorophores changes in the fluorescence emission are detected. Sensing based on fluorescence offers higher sensitivity than other spectroscopic methods. A fluorescence enhancement is usually preferred over fluorescence quenching, since the enhancement leads to a higher signal to noise ratio.¹³ Being less sensitive than fluorescence assays colourimetric sensing systems may offer the great advantage of naked-eye detection. Furthermore, it supersedes the usage of an internal standard.

As stated by Suksai and Tuntulani, chromogenic sensors can be sub-grouped into two categories according to the omission or presence of metals. In the latter case, the observed colour-change in presence of anions is based on the metal or metal-complexes.¹⁴ As an example for the first category Gunnlaugsson et al. presented charge-neutral receptors in 2005 exhibiting a colour-change from yellow to purple upon addition of anions in competitive solvents.¹⁵ (Critical) reviews have been published by Gale, presenting the advances in the development of anion receptors.^{16,17}

Various approaches towards optical sensors for anionic species have been developed during the last years. Depending on the nature of the analyte it can either be detected directly or needs to be detected indirectly. Due to the inherent need for special functionalities that have to be present in the target molecule, the applicability of the first case is rather limited. Thus, examples for the following two approaches are far more wide-spread.

3.1.1. Competitive or displacement approach

In this case the target molecule does not contain any chromophores or fluorophores, but a signalling analogue is employed. Upon addition of the target molecule to a solution or dispersion containing a molecular ensemble of the receptor or binding site and the signalling analogue, the target competes with the analogue for the binding site. Thus, the analogue is freed up from the complex and can be analysed spectroscopically in the supernatant.¹⁸

In 1997 Piletsky et al. presented the application of a fluorescent template analogue that competes with the template for the binding sites within the MIP. In these studies MIPs were incubated in presence of the fluorescent template analogue. Upon addition of the original template, the template analogue is replaced and its concentration can be determined from the supernatant.¹⁹ Drawbacks of this approach are the unfavourably slow equilibration time of the systems for sensing applications and the need of an additional synthesis step yielding a custom-made fluorescent template analogon.

3.1.2. Chromogenic and fluorogenic sensors via coupling of binding and signalling unit

This approach offers a straight-forward way towards a sensing system. In this approach the sensor consists of a binding site as well as a signalling unit.²⁰ These sub-structures are fused in a way that a binding event is transformed to a spectroscopically detectable signal (see *6.1 monomers*). Upon binding of an analyte either the geometrical organisation of the sensor is altered or the electron density in the π -conjugated sensing element is relocated.

The crucial step in this approach is the careful design of the sensor (here functional monomer) according to the nature of the analyte (here template). Given the weak interactions between the template and the binding unit of the host-monomer that is usually accomplished via hydrogen-bonding the induced relocation of electron density has to be strong enough to yield to a spectroscopic change and allow recognition also in competitive solvents.

Various examples have been published over the last years, following this approach and focussing either on *fluorogenic* or *chromogenic* examples of the sensing material. In 2003 Suksai and Tuntulani published a review on chromogenic anion sensors based on NH-hydrogen interactions.²¹ The presented materials proved to yield strong colour-changes visible to naked-eye in presence of anions. The work presented by Bissell et al. already in 1992 presents the application of PET systems in molecular fluorescent signaling.²²

3.2. Molecularly imprinted optical sensors

Upon closer investigation of the above-mentioned systems it is easily concluded that using the sensor in its molecular state is limited to the detection of functional groups. No further discrimination of molecules is possible, because the sensor is rather indifferent to the rest of the molecule apart from the functional group.

Sensors based on molecular imprinting may overcome this limitation. By polymerising a mixture of tailor-made signaling units with high affinity towards a respective analyte as described in section 3.1.2, co-monomer and cross-linker in presence of the analyte, materials containing cavities that are complementary in size and shape to the analyte of interest are generated. Thus, the recognition of the target relies not only on the complementarity of the functional groups, but also on the cavity matching the analyte like a complementary puzzle-piece.

As in case of the materials described in paragraph 3.1.2 careful design of the host molecule is crucial to the success of the recognition. In contrast to the application of the sensor in its molecular state a polymerisable sub-unit has to be introduced, in order to integrate the sensor into the backbone of a sensory molecularly imprinted polymer. Extensive research has been done, e.g. by our group in order to design monomers with high binding affinity to oxy-anionic guest molecules, yielding easily detectable spectral changes upon addition of the guest and have good polymerisation properties. Urea-monomers proved to be valuable candidates matching these demands. Already in 2004 and 2005 Manesiotis and Hall presented the successful composition of signaling MIPs of in-house made urea-based monomers.^{23,24}

3.3. Molecular imprinting and Molecularly Imprinted Polymers (MIPs)

The term „polymer“ sub-sums three classes of compounds. These are on one hand naturally occurring polymers such as cellulose, starch and modified naturally occurring polymers. On the other hand there is the group of synthetic polymers; sub-divided into inorganic compounds (e.g. silicone) and organic compounds (e.g. polyethylene, -propylene).

According to their properties polymers are distinguished into thermoplasts, elastomers or duromers. Based on the application polymers can be formed with numerous constitutions, e.g. homo-polymers, co-polymers (alternating, statistical, block, graft) and polymers of various more complicated architectures such as dendrimers or star polymers.

Molecular imprinting is a technique that combines various chemical disciplines, listed by Nicholls as polymer, organic, analytical, physical and bio-chemistries.²⁵ It emerged from the attempt to mimic the extraordinary characteristics of naturally occurring molecules such as enzymes and antibodies with custom-made materials.²⁶

The original idea for the creation of a molecularly imprinted polymer (MIP) is inspired by the lock and key theory. The template serves as miniature key in the imprinting process during which the monomers form the „lock“ complementarily matching the template in size and shape. More precisely, monomers with matching functional groups in respect to the template molecule are pre-arranged around the template and polymerised yielding a polymer that contains cavities specific for a given target that can discriminate between the template molecule and other analytes.

MIPs inherit various favourable characteristics with regard to a wide range of end-user applications. Depending on the preparation technique and the amount of cross-linker employed MIPs exhibit good thermal and mechanical stability and various examples of polymers with good recognition and separation properties have been published.

The lions share of polymers prepared up to now for imprinting purposes are macroporous systems with a high inner surface, good stability and accessibility of the binding sites.

3.4. Approaches for the preparation of MIPs

The pre-arrangement of the monomers and the template may be established employing covalent or non-covalent interactions. According to this differentiation the polymerisations are sub-grouped as covalent or non-covalent imprinting.

3.4.1. Covalent approach

Covalent imprinting was first reported by Wulff and co-workers in 1972 in the macromolecular colloquium²⁷ and published in 1973 as „Enzyme-analogue built polymers and their use for the resolution of racemates“.²⁸ They present the radical co-polymerisation of *D*-glyceric acid (p-vinylanilide)-2,3-0-(p-vinyl-phenylboranate) with a cross-linker that bound *D*-glyceric acid significantly better than the *L*-enantiomer in a competitive binding study. They observed that the non-swellability is crucial for the recognition properties of the material, because the resolution of racemic mixtures was impossible in solvents that swell the polymers.

In the covalent imprinting approach an assembly is formed between the template and a polymerisable functional monomer through reversible covalent linkages. The copolymerisation with a high amount of cross-linker leads to rigid polymers. The cleavage of the covalent bonds and thus removal of the template molecule leaves cavities within the polymer that are complementary in size, shape and functionality to the template. Upon rebinding of the guest the bonds can be reformed.

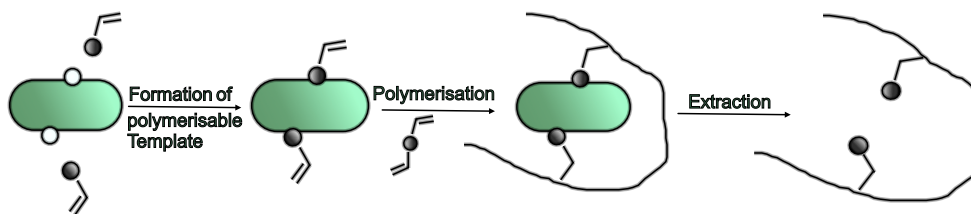


Figure 3.2: Schematic representation of the covalent imprinting approach

Covalent imprinting allows the stoichiometric employment of the functional monomers in respect to the template. Due to this reason as well as the high stability of the covalent bonds the resulting binding sites are relatively clear-cut. Furthermore, the high-stability complex allows

the utilisation of polar solvents. On the other hand, the stability leads to slow guest binding and release²⁹ and the harsh conditions necessary in the guest removal may influence the integrity of the cavities negatively.

Suitable covalent bonds for this purpose have to be stable during polymerisation but at the same time reversible. Possible covalent bonds are for instance the above mentioned boronic acid esters formed from boronic acids employed by Wulff, Schiff bases by imino bond formation or ketal formation from diketones.³⁰

3.4.2. Non-covalent approach

The non-covalent approach of imprinting was introduced by Dickey already in 1949.³¹ Mosbach et al. Andersson, Sellergren and Mosbach presented in 1984 the imprinting of phenylalanine-ethyl-ester via electrostatic interactions with para-vinylbenzoic acid (PVB) and co-polymerised with divinylbenzene (DVB). Substrate-selectivity was observed in this study and it was assigned to binding to substrate specific binding sites by the authors.³² Due to the versatility and straight forwardness of this approach it is nowadays the most widespread one.

The crucial factor for the success of the non-covalent imprinting process is the stability of the pre-polymerisation self-assembled complex between the guest-molecule and the functional monomer. Association between these molecules may be obtained via various non-covalent interactions e.g. hydrogen bonds, electrostatic interactions and coordination-bond formation. Hydrogen bonds are the interaction of choice, since they are highly dependent on distance and direction between template and monomer and thus lead to the highest definition of the binding sites.³³ In case that the binding between the functional groups of the monomers and the template are strong, only a few of them are needed to obtain sufficient complexation. The pre-polymerisation complex is subsequently co-polymerised with an excess of cross-linker leading to porous materials containing defined cavities.

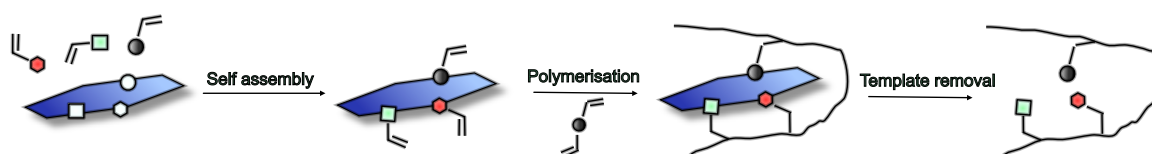


Figure 3.3: Schematic representation of the non-covalent imprinting approach

Being non-covalent and thus relatively weak, the bonds can be broken and reformed easily and fast upon guest rebinding (**Figure 3.3**). Commonly employed functional groups are e.g. carboxyl-, amino-, pyridine-, hydroxyl- and amide-functionalities.³⁴ Sufficient selectivity may be obtained even by using simple acrylic or methacrylic monomers.³⁵

Due to the rather weak interaction between template and monomers and the resulting need to use the functional monomer in large excess in respect to the template, the binding sites are less clear-cut in these materials and in-homogeneously distributed. This is especially valid for weaker binders. The non-covalent approach requires a more careful choice of the reaction conditions in order to favour the formation and stabilisation of the pre-polymerisation assembly.

The employment of specific functional monomers that bind strongly to certain template molecules (association constants $K_a = 10^2 - 10^7 \text{ M}^{-1}$) allows their usage in stoichiometric amounts in respect to the template molecule. This is referred to as the stoichiometric non-covalent approach. Materials prepared according to this technique imply rather clear-cut binding sites with functional groups that are exclusively located within the cavities.

A representative example for materials prepared according to this approach was presented by Wulff and Schönfeld in 1998.³⁶ The authors designed and synthesised novel polymerisable amidine monomers. These monomers show a strong affinity towards carboxylic groups ($K_a = 10^6 \text{ M}^{-1}$). Upon rebinding of dicarboxylic acids employed as template in the synthesis strong enantioselectivity could be observed.

4. MIP formats and formation

Molecularly imprinted polymers might be synthesised in various formats according to their final purpose e.g. as bulk polymers, as polymeric beads or as molecularly imprinted films.

The lions share of MIPs is prepared following free radical polymerisation.

4.1. Free radical polymerisation

Free radical polymerisation is a straight forward and versatile way of producing high-molecular weight polymers. Due to its various advantages it is nowadays often the method of choice for the commercial polymer production.

Moad lists the following characteristics as outstanding:³⁷

- relatively free choice of monomers
- tolerates oxygen and unprotected functionalities in monomers and solvents
- free choice of reaction conditions

On the down part this technique is difficult to control, resulting in e.g. broad weight distributions and varying macromolecular architecture.

Mechanistically a free-radical polymerisation procedure consists of three elementary reactions:

1. *Initiation*: The reaction is initiated by cleaving a thermally instable molecule (see *initiators*, 6.3) creating radicals. Furthermore, the reaction can be initiated via e.g. photolysis or redox reactions.
2. *Propagation*: The generated radicals react with monomers and produce the growing species, which is followed by fast chain growth until no monomer is available anymore or termination occurs
3. *Termination*: Chain termination may take place by radical disproportionation, combination of a chain with a initiator radical or with impurities. Instead of chain termination also chain transfer might occur.

Free-radical polymerisation may be performed in a homogenous or heterogeneous way. Homogeneous polymerisations are one-phase reactions, no matter how many components are involved. Prominent example for homogeneous polymerisations is the bulk polymerisation also employed in the presented work. Heterogeneous polymerisations take place in systems containing more than one phase. Of these especially suspension- and emulsion polymerisation are of great technical importance.

4.2. Monolithic MIP blocks by bulk polymerisation

Monolithic MIPs are prepared by free radical polymerisation. The bulk polymerisation is the easiest and thus most widespread approach for the preparation of MIPs. Depending on the cross-linking level applied it generates solid polymer materials with good thermal and mechanical stability.

The procedure is a straight forward mixing-polymerising process; functional monomer (optionally co-monomer, cross-linker and template are dissolved in a solvent/porogen. The polymerisation is subsequently initiated thermally or photochemically. The obtained polymer block is crushed to the desired particle size and the template and unreacted compounds are extracted by soxhlet-extraction.

Even though the simplicity of this approach is appealing it comprises crucial weak points. This refers mainly to the after-polymerisation work-up. The crushing process leads to irregularly shaped and sized particles, which is problematic in various applications e.g. producing back-pressure in HPLC columns upon application as stationary phase or light-scattering in optical applications. Furthermore, the main part of the material gets lost in this process. Template removal from the polymer is another difficult task. The highly-crosslinked polymer network may entrap template molecules that either bleed out upon usage and lead to false positive results in the analysis or are blocking binding sites irreversibly.

4.3. MIPs in thin-film format

Molecularly imprinted polymers in thin film format are especially suitable for sensing applications. These films tend to be of much higher sensitivity than bulk materials and the film format should allow the direct integration of the MIP concept into a sensing system.

MIP films of different thickness are commonly prepared by entrapping the pre-polymerisation mixture between a non-adhesive surface and a modified, reactive one such as RAFT modified. The polymer film is then subsequently grafted onto the reactive surface. Another method is to fill preexisting pores in other films or networks. By this method usually films of higher thickness might be obtained.³⁸

Significant drawbacks of these films are their relatively high fragility and the reproducibility regarding the synthesis, especially concerning the thickness. For this reason there are various examples of polymer films or nanoparticles synthesised by techniques formally known as „living polymerisation“.

4.3.1. Living Polymerisation

According to the International Union of Pure and Applied Chemistry (IUPAC) a living polymerisation is defined as „chain polymerization from which chain termination and irreversible chain transfer are absent“.³⁹ Strictly speaking only anionic polymerisation may be performed under conditions that fulfill these criteria. The „living“ mechanism for anionic polymerisations was already proposed in the early 1950s by Szwarc. IUPAC published a guideline in 2010 regarding the appropriate naming of reactions commonly referred to as „controlled“, „controlled/living“ or „living“. Instead of this terminology these reactions should now be referred to as „reversible-deactivation radical polymerisations“.⁴⁰ Applying the RAFT polymerisation technique it is possible to form particles with a very narrow size distribution, which is a step in the direction of monodispersity. The RAFT process was invented at CSIRO by the group of Rizzardo in the 1990s.⁴¹

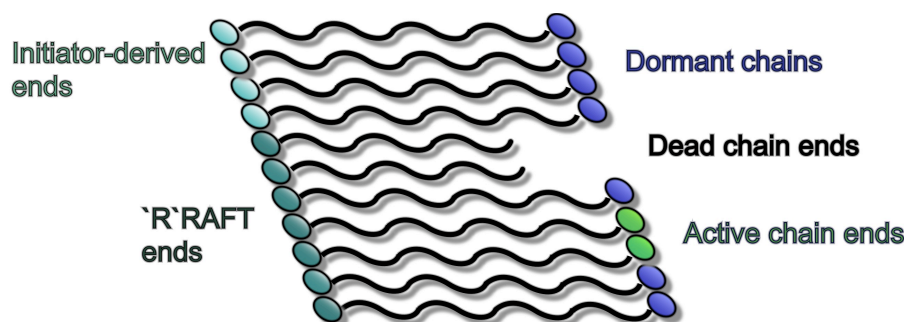


Figure 4.1: Schematic representation of RAFT polymerisation

Moad signifies RAFT polymerisation as the most versatile and effective representative of „living“ free radical polymerisation at that time.⁴² Rizzardo on the other hand criticises the limited range of monomers and the need for special reaction conditions.⁴³

Indeed, a special RAFT agent is employed in the synthesis to guarantee the „living“ character of the reaction. It guarantees a dynamic equilibrium between dormant chains and propagating radicals and thus the growth of all polymer chains at the same rate. Depending on the nature of the monomers chosen for polymerisation the appropriate RAFT agent should be chosen. The general built-up of a RAFT agent is displayed in **Figure 4.2**:

Figure 4.2: General structure of RAFT agents

Moad⁴⁴ names compounds as most effective with:

X = Sulfur

R = free radical leaving group

Z = Group that modifies the activity of the RAFT agent

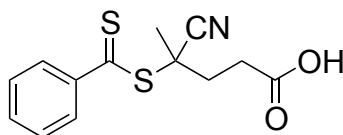
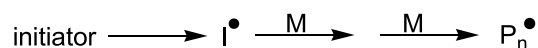


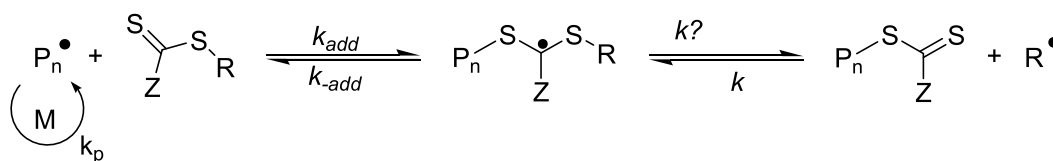
Figure 4.3: RAFT agent 4-Cyano-4-(phenylcarbonothioylthio)pentanoic acid

The RAFT procedure follows the path displayed in scheme 3.1:

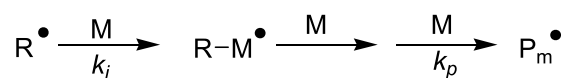
Initiation



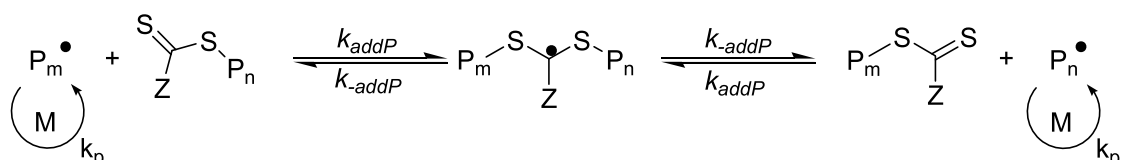
reversible chain transfer/ propagation



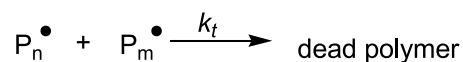
Reinitiation



Chain equilibration/ propagation



Termination

**Scheme 3.1:** Reaction scheme of RAFT polymerisation

(Scheme adapted from Moad, Accounts 2008)

In the initiating step a propagating radical (P_n) is generated by e.g. thermal or photochemical initiation. The propagating radical subsequently reacts with the RAFT agent turning it into a polymeric RAFT agent via addition-fragmentation. The radical formed in this process forms with the monomers present a new propagating radical (P_m). Due to this process the $S=C(Z)S$ part is transferred from active to dormant chains. For this reason all chains grow with the same rate, which guarantees the highly ordered systems.

4.4. Nanoparticles

Nanoparticles have drawn growing interest in the last years especially for e.g. drug delivery applications. The term refers to a wide array of particle sizes ranging from 10 - 1.000 nm.⁴⁵

Polymeric beads are commonly synthesised via biphasic or uniphasic heterogeneous polymerisation. The choice of system depends on the desired particle size. The particle size obtained by suspension polymerisation employing water as dispersing phase varies from 5 µm to 2 mm; employing fluorocarbons leads to particles of a size between 5 and 50 µm. Dispersion or precipitation polymerisation commonly leads to beads between 100 nm to 10 µm.

Imprinted nano-sized beads offer a relatively high surface area, in comparison to crushed bulk materials, a higher monodispersity and colloidal stability. Depending on the synthesis procedure particles with cavities only on the surface can be obtained or materials that contain binding sites distributed all over the polymer matrix.

In the preparation of imprinted beads a modified silica template can be employed as „carrier material“. This guarantees the formation of uniformly shaped, spherical beads. It is also possible to use porous silica particles and fill the pores with polymer. Removal of the silica then leaves behind a highly accessible polymer material that is complementary to the silica morphology. This technique is commonly used in the so-called „hierarchical imprinting“.⁴⁶

5. Applications

The possible applications for molecularly imprinted polymers are various, ranging from separation and purification procedures to catalysis and chemical sensing.

The most wide-spread and furthest developed application for MIPs nowadays is their usage as stationary phase in Solid Phase Extraction (SPE). Stationary-phase MIPs are commercialised as SupelMIP® by Supelco and serve in the purification of environmental and biological samples. Furthermore, MIPs are used in the separation of racemic mixtures or mixtures of enantiomers. The custom-made synthesis for the compound of interest leads to superior selectivity in respect to conventional chiral stationary phases.

One of existing challenges is the development of MIP systems that are on the one hand able to mimic the unique features of nature materials i.e. antibodies and enzymes and on the other hand overcome the drawbacks associated by being highly thermal-, chemical- and stress-tolerant.

The application related to the work presented here focuses on the application of MIPs for optical sensing purposes. The goal here is the design and synthesis of materials that are able to selectively determine and sense trace compounds. Optical sensors, especially based on luminescence, are of great analytical importance since it is possible to gain various information from the obtained signal, e.g. intensity, characteristics of the spectra and lifetimes.⁴⁷ This might be of use for e.g. food industry, environmental applications such as water purification and health care.⁴⁸

6. Sensory MIPs via the non-covalent approach

As stated in *chapter 3.2.* the non-covalent approach towards molecularly imprinted polymers was invented in the 1940s. Up to now, the most successful MIPs in terms of separation applications are composed of methacrylic acid (MAA) as monomer and ethyleneglycol-dimethacrylate (EDMA) as cross-linker.⁴⁹ Already in 1988 this system was extensively studied using L-phenylalanine anilide (L-PA) as template. In these studies presented by Sellergren, MIPs of this composition proved to be highly substrate selective and enantioselective.⁵⁰

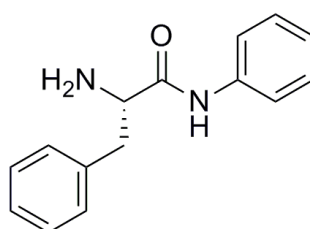


Fig. 6.1: L-Phenylalanine anilide

Due to the remarkable results obtained with this system it became the model system ever since and the reference for the performance of newly developed MIPs.

The success of a newly developed system is influenced by various factors that need to be considered in the design and fine-tuning of a molecularly imprinted polymer. Factors to be considered are the template molecule, the functional monomer, the co-monomer, the cross-linker, the solvent and the method of initiating the polymerisation.

6.1. Templates

There are various compounds that might be of interest for the area of molecular imprinting. The range of possible templates reaches from small molecules such as amino acids to large and complex molecules like peptides and proteins.

To serve as a template, the target molecule has to meet some criteria. The use and amount used is limited by the availability and the solubility of the molecule.⁵¹ Being of bio-

logical or environmental importance, some substances might be too dangerous or hazardous to be used as a template. In these cases the molecule is substituted by a structurally related analogue. Using a so-called „dummy - template“ avoids also the above mentioned problem of template bleeding. Template bleeding refers to the phenomena that template that has been entrapped in the polymer material is released in trace quantities upon evaluation of the polymer. This might lead to false positive results or mistakes in quantification.

Since the template molecule has to serve as mould for the organisation of the polymerisable monomers during polymerisation,⁵² it has to possess at least one functional group that might interact with the monomers. The interaction has to be sufficiently stable to stay intact during the polymerisation. For this reason, templates with multiple interaction sites are more likely to yield binding sites of higher selectivity and affinity with the specific template.⁵³ Hydrogen bonding groups are widely used but also electrostatic interactions are employed. E.g. templates carrying groups that can serve as Brønsted bases are suitable for the well-established methacrylic acid system.⁵⁴

The template should be immune to the polymerisation conditions⁵⁵, meaning it should not contain any polymerisable groups, which make its removal from the polymer difficult. Furthermore, no functionalities such as thiols or hydroquinones should be present, since they are able to inhibit or retard the polymerisation. The template has to be stable under initiation conditions, either heat or UV-irradiation, and should not react with the solvent.

All templates employed in the presented work are small-molecule anions.

6.1.1. Amino acids

Amino acids are organic compounds that contain at least one carboxylic group and one amino group. The amino acids are used as building blocks in the protein synthesis are designated as proteinogenic. Apart from this function some amino acids have regulatory functions in metabolism or are essential for the biosynthesis of other functional structures.

The amino acids *L*-Glutamic acid and *L*-Phenylalanine that are relevant for this thesis are both proteinogenic α -amino acids. α -amino acids are nonvolatile and thermally stable.

This results from their solid state dipolar structure (inner salt). Except from Glycine all natural amino acids are chiral. In human or animal metabolism they occur only as L-enantiomers. Their small size and them being chiral makes amino acids favourable as template molecules especially for the establishment of polymer systems. The employment of a chiral compound as template offers the opportunity to use the other enantiomer as cross-analyte. Since the enantiomers are almost identical non-specific interaction should affect them both in a similar way. Better affinity of a MIP towards the template molecule should thus be due to an imprinting effect.

The resolution of racemates is not only interesting from an analytical point of view but is also important for real life applications. Being almost identical, the two enantiomers of a compound can have significantly different properties, e.g. taste and smell. Dramatic and well known example is the case of Contergan, where one enantiomer serves as sleep-inducing drug and the other one caused severe abnormalities in babies.

Glutamic acid

Glutamic acid is a non-essential α -amino acid and present in almost all protein-containing foodstuffs.

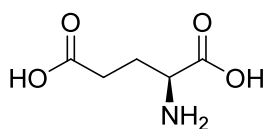


Fig. 6.2: *L*-Glutamic acid

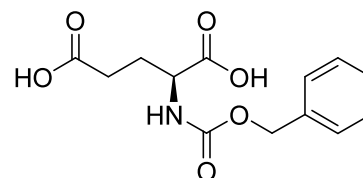


Fig. 6.3: *Z-L*-Glutamic acid

For human and animal organisms *L*-Glutamic acid is a proteinogenic amino acid. Furthermore, *L*-Glutamate is the most important excitatory neurotransmitter in the central nervous system of vertebrates.

L-Glutamic acid is commercially produced via fermentation. The by far biggest part of the produced Glutamic acid is used as its Sodium salt as taste enhancer in food production. The taste of this compound is known as Umami.

Phenylalanine

Phenylalanine is one of the eight essential α -amino acids. Unlike the case of many other amino acids the *D*-enantiomer of Phenylalanine has an application in the antidiabetic drug Nateglinide.

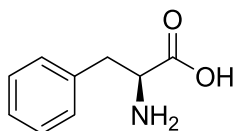


Fig. 6.4: *L*-Phenylalanine

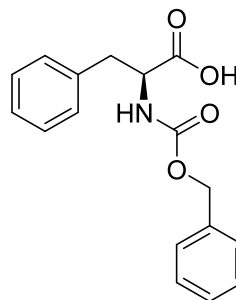


Fig. 6.5: *Z-L*-Phenylalanine

Phenylalanine for commercial purposes is produced by fermentation based on glucose-consuming *L*-Phenylalanine overproducing mutants of *E. coli* and coryneform strains.

The lion's share of the produced *L*-Phenylalanine is used in the synthesis of the sweetener Aspartame. Aspartame serves as a sugar substitute. Since it does not influence the insulin production it is compatible with diabetic products.

6.1.2. Penicillin G

Penicillin G or benzyl penicillin is the β -lactam antibiotic produced by the mould fungus *penicillium notatum*. It was discovered by coincidence in 1928 by Alexander Fleming, who discovered that the presence of the fungus destroyed a bacteria culture growing on an agar plate. Penicillin G is the parent substance for all other Penicillins; all following compounds were derived from it.

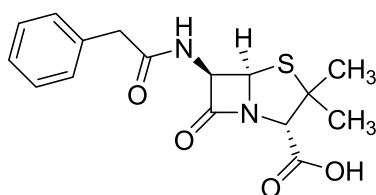


Fig. 6.6: Penicillin G

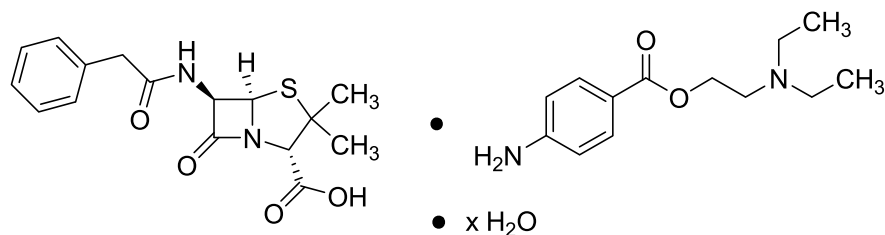


Fig. 6.7: Penicillin G procain

Penicillins hinder the cell wall synthesis of gram-positive bacteria.

Bacteria easily grow resistances against Penicillin derivatives, e.g. by producing β -lactamases. Antibiotic resistance is recognized as a growing health problem worldwide that might result e.g. from treatment of human diseases and usage in industrial livestock feeding. Antibiotics can reach the waste water system with human and animal excrement and thus trace amounts of the antibiotics are then present in nature.

The matter of antibiotic resistance is so severe that the EU has established projects like the European Surveillance of Antimicrobial Consumption (ESAC) and European Antimicrobial Resistance Surveillance System (EARSS) to collect data about the European antibiotic use.

Several studies have been published linking the higher rates of antibiotic resistance to high consumption.⁵⁶ Goossens shows a correlation between antibiotic resistance and outpatient use and strongly recommends guidelines for appropriate prescription of antibiotics and the prohibition of antibiotic usage in clinical situations in which they are unnecessary.

There are critical voices regarding these studies pointing out the complexity of resistance ecology.⁵⁷ Nevertheless, all authors agree on reconsidering the usage of antibiotics.

6.2. Cross-linker/ Commonly employed Co-monomer- cross-linker systems

The choice of type and amount of cross-linker is a crucial point to the success of molecular imprinting. Cross-linkers serve several purposes in a molecularly imprinted polymer.

The cross-linker „freezes“ the three-dimensional structure of the polymer. A high level of cross-linking ensures the formation of stable guest-binding sites in the polymers and provides sufficient porosity.⁵⁸ Due to this reason the kind and amount of cross-linker chosen is the key factor of influence for the selectivity of a MIP.⁵⁹ Furthermore, they provide mechanical stability to the polymeric matrices, making them insoluble in organic solvents and hence facilitate their use in practical applications.

The selection of the appropriate cross-linker is not only predicated on the target molecule but also on the used solvent system. Depending on the nature of the solvent different cross-linkers has proven useful. Favourable for usage in aqueous solvents is e.g. N,N'-methylenebisacrylamide.

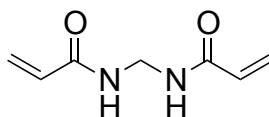


Figure 6.8: N,N'-methylenebisacrylamide

For organic applications cross-linkers like EDMA or DVB are commonly employed:

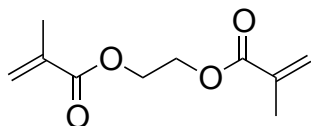


Fig. 6.9: EDMA

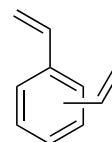


Fig. 6.10: DVB

The choice of the actual (co-)monomer/ cross-linker combination depends on various considerations. First of all the reactivity of the present double-bonds should be similar to al-

low homogeneous polymerisation. Furthermore, the polarity of the employed co-monomer/cross-linker system has to be adapted to the requirements for the pre-polymerisation complex. A relatively weak complex requires a less polar environment than a strong complex does.

Commonly employed systems in organic solvents are for example:

- HEMA/ EDMA
- MMA/ EDMA
- Styrene/ DVB

Hydroxyethylmethacrylate (HEMA)/ EDMA systems are suitable for usage in organic media. The reactivities of the present double-bonds are similar. Being relatively polar, the system might be used for monomer/template combinations that exhibit strong affinity. Since HEMA contains a hydrophilic OH-group the polymers tend to swell in aqueous media.

The MMA/EDMA system is a less polar alternative to the HEMA/ EDMA system. Being a di-ester consisting of methacrylic acid and ethylene glycol, the reactivity of the double bonds of EDMA is comparable to the ones in MMA. The MMA/EDMA system thus became the most commonly used one for this kind of material. Its main advantages are the mechanical and thermal stability. Furthermore it provides overall good wettability and fast mass transfer.⁶⁰

The Styrene/ DVB system is the least polar of the presented ones. This system is favourable for pre-polymerisation complexes exhibiting weak interactions.

The morphology of the polymer might be fine tuned by the relative amount of cross-linker used in respect to monomer. The resulting materials range from poorly solvated gel-like polymers (low amount of cross-linker) to stable macroporous materials (high amount of cross-linker). To avoid the predominant polymerisation of either cross-linker or monomer both components should be of similar reactivity to create uniformly distributed recognition sites.

6.3. Solvents

In molecular imprinting one distinguishes between solvents and porogens. Solvents solubilise the reactants for the polymerisation and disperse the occurring reaction heat, especially in bulk reactions. A good solvent leads to homogeneously distributed cross-links in solution polymerisation. In precipitation polymerisation the choice of solvent is more difficult, since the solvent has to solubilise all the reagents well but has to allow precipitation of the formed polymer.

A solvent with the ability to induce pore formation in the polymeric system is referred to as porogen. Pore formation is a crucial point in the polymer synthesis, since porosity ensures the accessibility of the cavities for the template.⁶¹ Even upon careful choice of the porogen most cross-linked network polymers have a wide distribution of pore sizes ranging from micro- over meso- to macro-sized pores.

Table 6.1: Properties of commonly-employed imprinting solvents
(own table after Sellergren⁶²)

	dispersive term δ_d	polar term δ_p	H-bond term δ_h	H-bond capacity
ACN	15.3	18.0	6.1	Poor
THF	16.8	5.7	8.0	Moderate
CHCl₃	17.8	3.1	5.7	Poor
Benzene	18.4	0	2.0	Poor
DMF	17.4	13.7	11.3	Moderate
CH₂Cl₂	18.2	6.3	6.1	Poor
Isopropanol	15.8	6.1	16.4	Strong
HOAc	14.5	8.0	13.5	Strong
MeOH	15.1	12.3	29.3	Strong
Toluene	18.0	1.4	2.0	Poor
H₂O	15.5	16.0	42.4	Strong
Cyclohex.	16.8	0	0.2	Poor

Table 6.1 gives an overview about the properties of solvents commonly employed in MIP synthesis. It is crucial to the success of imprinting that the choice of solvent favours or at least not hinders the pre-polymerisation assembly between the host monomer and the template. Depending on the mode of interaction a suitable solvent has to be chosen. Polar solvents may disrupt conjugates based on electrostatic interactions; also high dielectric constants can distract the interactions between two oppositely charged molecules. The commonly employed hydrogen bonds are sensitive to protic solvents. As can be extracted from the values displayed in table 6.1 water is an unfavorable solvent for imprinting, due to its high polarity and to its proneness to form hydrogen-bonds competing with the pre-polymerisation complex. This is also true for e.g. methanol. Favorable solvents are e.g. THF or chloroform, these being less polar and unable to form hydrogen bonds. Nevertheless, often the monomers might only be soluble in solvents of higher polarity, generating the need for highly stable pre-polymerisation complexes.

The nature of the porogenic solvent is known to have pronounced impact on the structure of the polymer.⁶³ Nevertheless, the influence of the solvent on the success of the imprinting process is controversial. Wulff constats that the influence of the porogenic solvent on the selectivity of the imprinted polymer is rather low.⁶⁴ This statement is in contrast to the observations presented below (films in optimised solvent).

The porous structure of a molecularly imprinted polymer is strongly dependent on the amount of cross-linker and the non-solvent. In order to describe the interplay between the amount of cross-linker and the volume of non-solvent a phase-diagram has been developed by Guyot in 1988. This diagram represents the nature of the resulting material depending on the above mentioned factors.

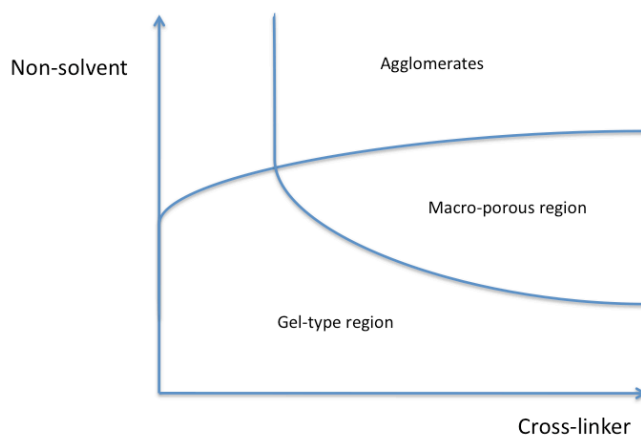


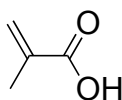
Figure 6.11: Phase diagram after Sellergren, following Guyot⁶⁵; the desired macro-porous morphology is only achieved using a narrow ratio-range between non-solvent and cross-linker, high amount of cross-linker results in smaller pore-sizes, high amount of non-solvent increases the number of large pores

6.4. Functional Monomers

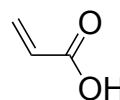
The success of molecular imprinting strongly depends on the stability of the pre-polymerisation complex between the template and the functional monomer. For this reason the careful choice and design of the monomer is crucial to the imprinting process.

Apart from structural requirements resulting from special applications, the monomers should contain functional groups that are complementary to those of the template in order to allow stable complex formation. Up to now a variety of monomers with different characteristics has been developed; figure 6.12 displays some of them:

Acidic monomers:

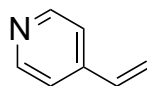


Methacrylic acid (MAA)



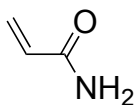
Acrylic acid (AA)

Basic monomers:

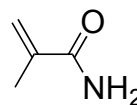


4-Vinylpyridine

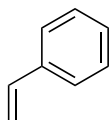
Neutral monomers



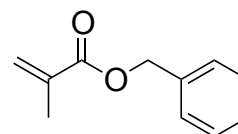
Acrylamide



Methacrylamide (MMA)



Styrene



Benzylmethacrylate (BMA)

Figure 6.12: Commonly employed monomers for molecular imprinting

In the case of the presented work, the commercially available monomers were only employed as co-monomers to a functional monomer due to several reasons.

Due to the fact that the system that was headed for is a polymer with sensing abilities the amount of the actual sensing monomer had to be kept relatively low. Experiments presented below supported the assumption that a high load of the functional monomer hinders the spectroscopic answer of the material to the presence of an analyte. For this reason the reduced amount of functional monomer in respect to the cross-linker was substituted by monomers that proved to be suitable for the imprinting process. The co-monomers employed in the sensing systems were chosen based on considerations concerning solubility, polarity and reactivity. The co-monomers should be in a polarity range that does not hinder the formation of the pre-polymerisation complex between the functional monomer and the template. At the same time the polymerisation rate should be similar to the one of the functional monomer and the employed cross-linker to ensure the homogeneous integration of the functional monomer and consequently the cavities into the polymer material.

6.4.1. Chromogenic and fluorogenic host monomers

The design of new polymerisable monomers mainly aims at the enhancement of the affinity of the monomer towards the template. Furthermore, secondary functions may be integrated into the monomer. In our case the goal was to design and synthesise monomers with high binding affinity and signalling properties.

The work presented in this thesis is based on the DFG project „Imprinted Chromogenic and fluorogenic receptors for biological and environmental target analytes“.

Since these receptors are meant to be selective materials that are able to indicate guest binding spectroscopically, a significant part of this work therefore aims at the design and synthesis of novel chromogenic or fluorogenic monomers that may serve as building blocks of the above mentioned materials.

To be suitable for this project the monomers have to meet the following criteria: The monomers should show a sufficiently high binding affinity towards oxyanionic functionalities that allows polymer formation according to the stoichiometric non-covalent approach. Furthermore, the monomers should contain a chromophoric or fluorophoric π -system. To enable prospective usage in real-life applications the system should absorb in a region compatible with commonly used laser sources and exhibit a lifetime range that does not require ultra-fast detection systems.

To guarantee the strong guest binding a urea-moiety was chosen as the binding unit in all cases. Urea-based monomers have been successfully employed in the imprinting of oxyanionic guests.⁶⁶ Hall et al. presented in 2005 an assortment of urea-based vinyl monomers.⁶⁷ They observed that the affinity of the monomers towards an oxyanionic guest depended on the substitution of the binding unit. These monomers served as building blocks upon imprinting of glutamic acid derivatives. The resulting polymers proved to recognise their template. Based on the above mentioned criteria for the signaling unit monomers from four different compound classes were chosen:

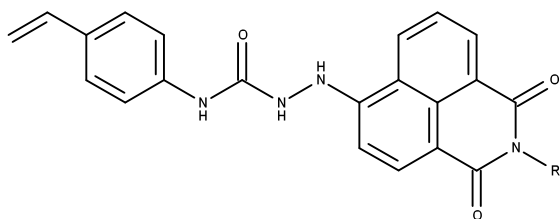


Fig. 6.13: Naphthalimides

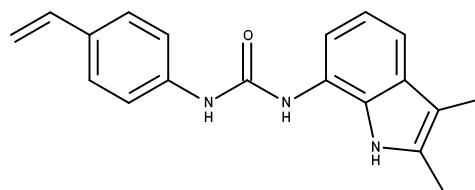
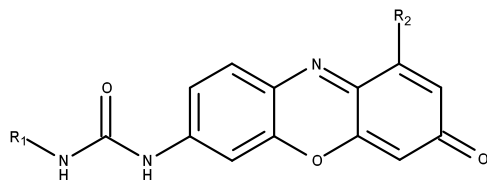
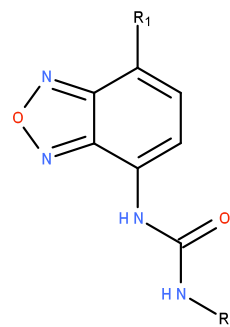


Fig. 6.14: Indoles



R₁ = Bu, pol. Group
R₂ = pol. Group, pol. Group

Fig. 6.15: Phenoxazinones



R₁ = F, Cl, ...
R₂ = pol. Group

Fig. 6.16: Benzoxadiazoles

The phenoxazinones and benzoxadiazoles employed in the DFG project were synthesized and evaluated in the laboratories of Dr. Knut Ruracks group for bioanalytical sensor materials in Berlin at the Federal Institute for Materials Research and Testing (BAM) and will be described elsewhere in detail.

Phenoxazinones proved to be suitable for the usage in optical sensors due to their highly fluorescent nature. For example, Descalzo et al. published in 2007 the successful implementation of highly fluorescent solvatochromic phenoxazinones in vapour sensing materials showing that the synthesized dyes exhibit pronounced positive solvatochromism and strong dependence of the fluorescence quantum yields on the polarity of the environment.⁶⁸ The high fluorescence of **benzoxadiazoles** was already reported in 1968 by Ghosh and Whitehouse⁶⁹ and their photophysical properties have been extensively studied (computationally).⁷⁰

Indoles have been employed as fluorescent sensors e.g. for the detection of metal ions.⁷¹ Being strongly fluorescent the position of the absorption spectra however are located outside the spectral range that was aimed for ($\lambda = 450 - 550$ nm). As stated by Yu et al.⁷² the fluorescence of indoles may be quenched via either solvent quenching or excited-state proton transfer. Both of these processes are temperature dependent. (Nevertheless, the synthesised indol-based monomers showed strong guest-binding in titrations with an oxyanionic guest.

Naphthalimide-based chromophores

Naphthalimide-based compounds are commonly used as dyes for various materials such as wool, polyamides or cellulose fibres. Some of them show exceptionally brilliant, greenish-yellow fluorescent colours.⁷³

Furthermore, they were already used successfully in anion sensing purposes.⁷⁴

The large Stokes shift and their considerable brightness turns naphthalimides into promising candidates for fluorescent devices. We hope to incorporate the fluorogenic properties of naphthalimide-based compounds into our polymerisable urea-based monomers, in order to gain a material having the ability to selectively bind an analyte and to report the success and quantity of the binding.

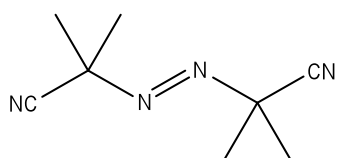
Grabchev et al. report on the synthesis of a polymerisable 1,8-naphthalimide dye that might serve as a PET sensor.⁷⁵

6.5. Initiators for free radical polymerisation

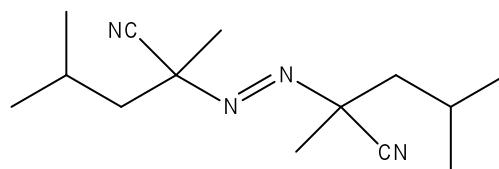
Depending on the nature of the employed compounds the polymerisation method may be chosen quite freely. Even though there are examples for MIPs prepared according to other techniques e.g. anionic polymerisation, radical polymerisation is the most wide-spread one due to versatility and experimental easiness.

There is a broad range of initiators that can be chosen from for initiating a radical polymerisation. A commonly used class are homolytically cleaving azo-initiators such as AIBN and ABDV:

Commonly used azo-initiators:



AIBN (Azobisisobutyronitrile)



ABDV (Azobisdimethylvaleronitrile)

Figure 6.16: Commonly employed azo-initiators for free-radical polymerisation

According to the nature of the initiator the decomposition may be started thermally at different temperatures (Decomposition temperature AIBN: 60 °C, ABDV: 45 °C) or photochemically.

7. Characterisation techniques

Depending on the information that one wants to gain about a molecular imprinted polymer, various characterisation techniques are available. Even though molecular imprinted polymers are difficult to characterise by chemical or morphological means, it is still worthwhile to gain insights about how useful properties of the material might depend on variables related to the preparation.

7.1. Elemental analysis (EA)

Elemental analysis (EA) is a technique to gain information about the qualitative and quantitative elemental composition of a material. A given sample is combusted in presence of an excess of oxygen and the composition may be calculated from the collected products.

With respect to molecular imprinted polymers conclusions may be drawn about the „success“ of the polymerisation and the integration of the functional monomer by comparing the obtained results with a theoretically calculated composition assuming a quantitative yield of polymerisation. An exact match between the theoretical values and the measured ones indicates, that all monomers have been incorporated into the polymer structure in high yield.⁷⁶

Nevertheless, the method may be not sufficiently sensitive to enable the detection of trace quantities of template remaining in the structure.⁷⁷

Calculation of theoretical mass-percentages:

- Calculation of the “molecular mass” of the “repeat unit”

This can be calculated from the molar ratio of the compounds (monomer, co- monomer, cross-linker) and their particular molecular weight.

$$M_{(repeat\ unit)} = \sum_i a_i \cdot M_{(compound)i} \quad (7.1)$$

a_i = relative amount of the compound i

M = molecular mass

- To calculate the percentages of a specific element in the polymer, all sources have to be

taken in account.

$$\%_{(element)} = 100 \cdot \frac{\sum_i N_i \cdot a_i \cdot M_{(element)}}{M_{(repeat\ unit)}} \quad (7.2)$$

N_i = number of atoms in compound i

7.2. Nuclear magnetic resonance (NMR) spectroscopy

NMR spectroscopy is often the method of choice for the identification of chemical structures. Main advantage of NMR spectroscopy over Elemental Analysis is that the sample does not need to be destroyed. Depending on the measurement it is possible to gain information about liquid as well as solid samples.

In terms of molecular imprinting NMR analysis is commonly used as technique to study the interaction between the monomer and the template. Upon addition of a guest molecule the urea protons of the monomers may shift (complexation induced shift, CIS). From the CIS titration curves can be constructed by plotting the CIS against the guest concentration. The data can then be fitted to a binding isotherm by non-linear regression and the affinity constant of the monomer towards the template in a given solvent can be calculated.

7.3. High performance liquid chromatography (HPLC)

High performance liquid chromatography is a method of analytical separation to obtain an effective peak-resolution in minimum time.

In the common flow chart of an HPLC a pump (continuous or discontinuous) pushes a constant flow of liquid mobile phase (against high pressure) together with an injected sample through a solid stationary phase. The stationary phase is connected to a detector, which transforms the measured characteristics of the liquid phase into an electronic signal.

HPLC detectors either detect parts per volume (concentration dependent) or are mass dependent. The Diode-array detector (DAD) utilised in our instruments belongs to the concentration dependent detectors. Just like UV/VIS detectors DAD-detectors measure the ab-

sorption of the sample but transform the signal using a diode array. DAD-detectors enable the recording of the full UV/VIS spectra and measurement at different wavelengths simultaneously and may display the obtained results in a 3D chromatogram containing information about the retention time, the wavelength and the absorption.

In general the separation is based on the different polarity of stationary and mobile phase. Systems employing a polar stationary phase and a non-polar mobile phase are referred to as „normal-phase“, whereas systems employing a non-polar stationary phase and a polar mobile phase are called „reversed phase.“

In our case the HPLC was not used serving its original purpose to separate a mixture of compounds but to evaluate the performance of the synthesised MIPs. For this purpose the imprinted material was slurry-packed into empty HPLC columns and used as stationary phase in the analysis. To define the dead volume of the columns non-retained void-marker is injected and the retention time is compared to the ones of the print molecule and structurally related compounds.

The heterogeneous population of binding sites, their affinities and accessibilities may lead to extensive peak broadening and tailing,⁷⁸ especially for the more retained components.

In case of successful imprinting the template molecule should be retained longer than all other injected components, because its binding should be selectively promoted.⁷⁹ The same evaluation is performed on the NIP. From the obtained data the capacity factor k , the imprinting factor IF and the separation factor α can be calculated.

Capacity factor:

$$k = (t_R - t_0) / t_0 \quad (7.3)$$

t_R = Retention time of the compound

t_0 = Retention time of the void marker (void volume of the column)

Imprinting factor:

$$IF = k_{MIP} / k_{NIP} \quad (7.4)$$

k_{MIP} = capacity factor of MIP for specific compound

k_{NIP} = capacity factor of NIP for specific compound

If a peak resolution upon injection of an analyte mixture is observed the separation factor α can be calculated.

Separation factor α :

$$\alpha = k_2 / k_1 \quad (7.5)$$

Given that the stationary phase is less variable than the mobile phase the choice of an appropriate mobile phase is crucial in terms of resolution and retention times. Organic solvents proved to be suitable for low to moderately polar template molecules⁸⁰ but retention might be improved with increasing amount of water, whereas polar analytes become less retained.⁸¹

7.4. Absorption and UV/Vis-spectrophotometric titrations/ Fluorescence spectra and titrations

These techniques are listed here only for the sake of completeness; for explanations of the basics of these techniques see above (see Spectroscopy, 2).

For the quenching results obtained in fluorescence studies a Imprinting Factor (IF_Q) was calculated in order to determine whether the quenching is more pronounced on the MIP than on the NIP.

$$IF_Q(n) = \frac{I_f^{MIP}(n) / I_f^{MIP}(0)}{I_f^{NIP}(n) / I_f^{NIP}(0)} \quad (7.6)$$

I_f = Fluorescence emission intensity

(0) = Reference signal in omission of analyte

(n) = Signal in presence of analyte

7.5. Time correlated single photon counting (Life time measurements)

Time correlated single photon counting is a technique that can be used in order to gain information about the life time of the fluorescence of a compound. The compound is excited with a pulsed light-source, e.g. a LASER at the maximum excitation wavelength. Subsequently, the photons emitted upon the return from the excited state to the ground state are counted and sorted into a histogram according to the decay-time (resolution 64.000 time channels, t in femto-second range).

In the presented case the measurements were performed with an in-house customised laser impulse fluorometer with picosecond time resolution equipped with Ti:sapphire laser pumped by a frequency doubled Nd:YVO Laser. The details of the measurement setup were described by Zhen in 2004 and already by Resch in 1997.^{82,83} The obtained fluorescence decays were analysed by global analysis yielding the life time distributions for the respective compound.

7.6. Scanning electron microscopy (SEM)

With scanning electron microscopy information about the topography and composition of a sample can be obtained with a resolution between 1 to 20 nm. The surface of the sample is scanned in a raster scan pattern applying an electron beam. Upon interaction of the electrons with the electrons within the sample, back-scattered electrons are produced that are combined with the position of the beam producing the SEM image.

7.7. Transmission electron microscopy (TEM)

Like the SEM the TEM is an electron microscope. With transmission electron microscopy resolutions down to 0.05 nm can be obtained. Unlike in scanning electron microscopy in TEM the electron beam is traveling through the sample. By traveling through the sample the electrons are scattered. Only electrons that are not scattered contribute to the image of the sample; positions in the sample where the electrons have been scattered appear black in the picture. Consequently, the most common technique in TEM is called „bright field“. In order to avoid

absorption within the sample and the electrons to be scattered repeatedly, the sample has to be very thin.

RESULTS AND DISCUSSION

A great part of the presented results is also accepted for publishing in JOCS.

8. Naphthalimide-based monomers

8.1. Design and synthesis

Based on the considerations mentioned above three naphthalimide-based urea-monomers were designed and synthesised.

The monomers are composed of a hydrazide obtained from naphthalic anhydride in a three-step synthesis and vinyl-isocyanate synthesised in a four-step path from para-bromomethylbenzoic acid.

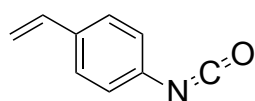
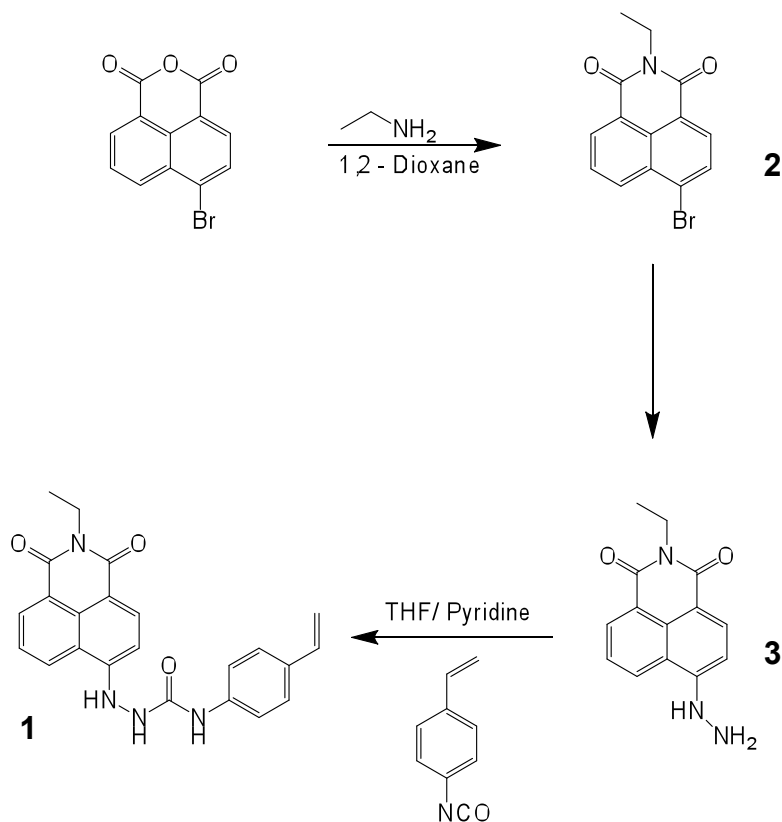


Figure 8.1: p- Vinylisocyanate

Depending on the desired imide substituent the appropriate synthesis path is chosen from scheme 8.1.



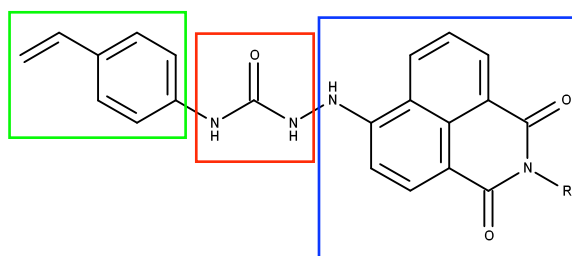
Scheme 8.1: Synthesis path of monomer 1

In a first step the imide is formed. In a second step the bromide is substituted via nucleophilic substitution and the hydrazide is formed. In a third step, the newly formed hydrazide moiety is reacted with the inhouse made vinyl-isocyanate to form the urea-based monomer.

Since the butyl-imide did not show the desired improvements concerning the solubility in commonly used imprinting solvents over the ethyl-imide and the substitution at this position has no effect on the photophysic properties, the rest of the work mainly focusses on the ethyl-imide.

N-Ethyl-4-(N-[4-vinylphenyl]hydrazinecarboxamidyl)-1,8- naphthalimide

Like all monomers from this family the novel urea-based monomer consists of three entities with different functionalities.



1. *The styrene entity (green)*: The vinyl group serves as polymerisable group for the integration of the monomer into the polymer network. Furthermore, the aryl-substitution of the urea-function proved to be favourable in terms of the affinity towards oxyanionic guests.
2. *The urea-moiety (red)*: The urea moiety is the actual binding unit of the monomer; it forms hydrogen bonds towards oxyanionic functionalities.
3. *N-ethyl-4-amino-1,8-naphthalimide moiety (blue)*: This moiety serves as the actual signalling unit. Since the urea-functionality and the chromophoric system are directly next to each other the binding should be transduced into a spectroscopic signal.

8.2. Evaluation

Before the monomer is integrated into a MIP network for signaling purposes it has to be evaluated whether the compound matches the above mentioned requirements.

8.2.1. Binding behaviour

The affinity of the monomer towards oxyanionic guest molecules can be assessed by different means.

The most wide-spread technique for the evaluation of complex stabilities is the ^1H -NMR titration in (competitive solvents) with an oxyanionic guest, namely TBA-Benzoate. DMSO mimics the polarity under polymerisation conditions for a polymer composed of e.g. MAA and EDMA. Here an increasing amount of TBA-Benzoate is added to a constant amount of monomer. From the complexation induced shift (CIS) the stoichiometry of the interaction can be determined via Job plot analysis and the association constant can be calculated from non-linear regression.

In this study an increasing amount of TBA-Benzoate was added to a constant amount of the monomer (0, 0.25, 0.5, 0.75, 1, 2, 6, 8, 10 equivalents).

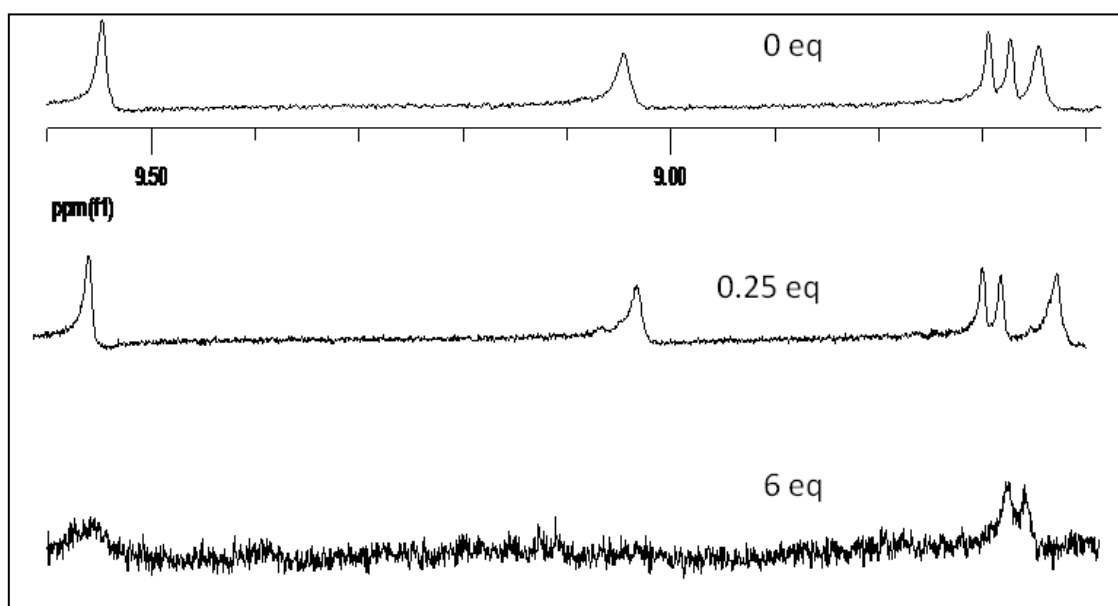


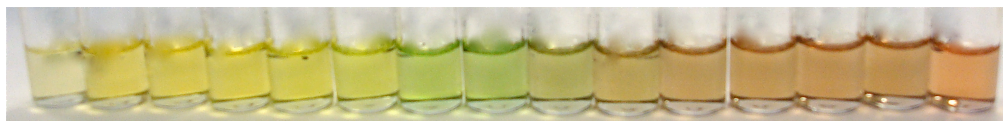
Figure 8.2: NMR Spectra of **1** upon addition of 0, 0.25 and 6 eq of TBAB in DMSO- d_6

From the spectra displayed in figure 8.2 it can be seen that the urea-protons as well as the hydrazide proton do not show a CIS but a severe peak broadening upon addition of the guest molecule. This behaviour indicates a deprotonation of the respective protons. Thus, the affinity cannot be evaluated by this method.

8.2.2. Spectroscopic evaluation

The response of the functional monomer towards oxyanionic guests was evaluated by spectroscopic means via different experiments.

Colourimetric test:



Picture 8.1: Induced colour-change of a solution of monomer **1** in DMSO in presence of increasing concentration of TBA benzoate

Picture 8.1 shows the induced colour-change of a solution of monomer **1** in DMSO upon addition of TBA benzoate. A colour-change visible to naked eye ranging from bright yellow over green to brownish can be observed.

Absorption spectra and UV/Vis spectrophotometric measurements

The absorption of monomer **1** was evaluated in different solvents; namely DMSO, ACN and THF. Figure 8.3 and 8.4 displays absorption titration spectra of monomer **1** against TBA Benzoate in the respective solvents:

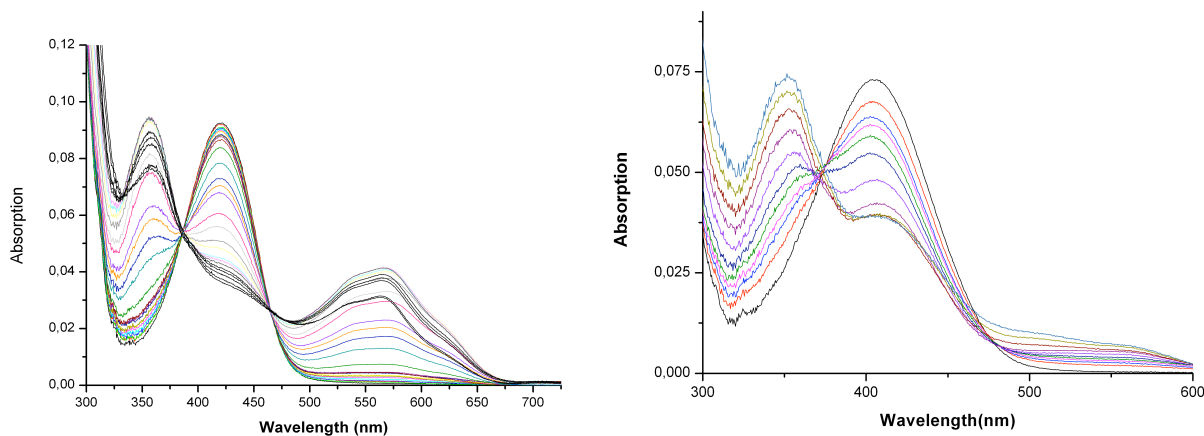


Figure 8.3: Absorption titration spectra of monomer **1** against TBA Benzoat, left: in DMSO, right: in ACN

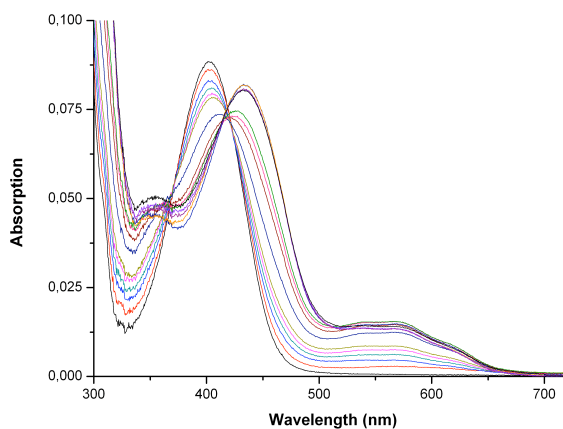


Figure 8.4: Absorption titration spectra of monomer **1** against TBA Benzoat in THF

The pure monomer shows a broad and non-structured absorption band at around 400 nm in all the solvents. This band is typical for 4-amino-naphthalimide-chromophores.⁸⁴

Monomer **1** is a solvatochromic compound. Thus, the position of the absorption and emission spectra strongly depend on the solvent polarity. Due to the different polarities of their ground state and excited state solvatochromic compounds exhibit a change in position of the UV/VIS absorption band or the emission wavelength depending on the polarity of the solvent. Depending on the nature of the ground state of the compound it can exhibit either positive or negative solvatochromism. Positive solvatochromism defines the shift of the bands to longer wavelength upon higher polarity of the solvent, while negative solvatochromism defines the opposite behaviour. The behaviour of the monomer was thus studied in solvents of different polarity and the results are listed in **table 8.1**.

Table 8.1: Maximum absorption and emission wavelengths of monomer **1** and precursor in different solvents

Solvent	Dielectricity constant	λ_{abs} /nm
DMSO	48	420
EtOH	24.55	412
ACN	37.50	404
THF	7.50	402
Dioxane	2.3	392
ACN (3)	37.50	425

Monomer **1** shows pronounced positive solvatochromism. The position of the the maximum absorption is located at 392 nm in the low-polar solvent Dioxane, whereas it is strongly red-shifted for the polar solvent DMSO ($\lambda_{\text{abs}} = 420$ nm). As comparison also the position of the maximum absorption wavelength of the hydrazide - precursor (compound **3**) in ACN is listed in table **8.1**. The maximum absorption of compound **3** is located about 20 nm red-shifted in respect to the one of monomer **1**. This observation supports the findings of Saha and Samanta. In 2002 they published a study on the photophysical behaviour of 4-amino-1,8-naphthalimides differing in the amino functionality in media of different polarity. They found out that the solvatochromic properties of the dyes depend on the nature of the amino-substituent and on the polarity of the media.⁸⁵

As displayed in **Figure 8.3** and **8.4** the absorption of monomer **1** was evaluated in presence of the model-compound TBA Benzoate in order to gain information about guest-induced spectroscopic changes.

In the two solvents of higher polarity DMSO and ACN the addition of increasing concentration of TBA Benzoate induces a decrease of the absorption band referred to above. The decrease is more pronounced in the solvent of higher polarity, namely DMSO. Simultane-

ously, a strongly red-shifted non-structured band arises with a maximum at around 570 nm. Also the occurrence of this new band is most pronounced in DMSO.

In contrast to the behaviour in solvents of high polarity, the absorption band of monomer **1** in THF exhibits a red-shift of about 30 nm upon addition of increasing concentration of TBA Benzoat. Also in THF the absorption band develops a shoulder at about 570 nm.

Pronounced bathochromic shifts as obtained in the case of monomer **1** upon addition of increasing concentration of the anionic guest TBA Benzoate are not common for mere coordination interactions. Thus, the observed behaviour indicates that hydrogen-bonding between the urea-functionality of monomer **1** and the guest-molecule is not the only event induced, but that the secondary 4-amino group is proceedingly deprotonated and, in case of DMSO, coordinated by the solvent. This assumption is supported by the findings of Harriman published in 2009, who observed deprotonation-induced red-shifts for naphthal-imide based compounds.⁸⁶

From the obtained titration data association constants in the different solvents were calculated and are displayed in **table 8.2**:

Table 8.2: Association constants for monomer **1** in THF, ACN and DMSO derived from titration data

	$\lambda_{\text{abs}} / \text{nm}$	k
THF	403	$1.5 \pm 0.1 \times 10^6$
	435	$5.6 \pm 0.2 \times 10^6$
	565	$3.0 \pm 0.1 \times 10^6$
ACN	400	$1.1 \pm 0.1 \times 10^5$
	555	$1.6 \pm 0.3 \times 10^5$
DMSO	430	$1.1 \pm 0.1 \times 10^4$
	560	$1.0 \pm 0.1 \times 10^4$

As expected upon taking into account the considerations displayed above, the derived association constants are strongly dependent on the employed solvent, namely its ability to stabilise the deprotonated form of the monomer and its ability to coordinate to the monomer and thus compete with the guest molecule. The least competitive solvent THF allows the strongest interaction between monomer **1** and TBA Benzoate.

In THF and ACN the affinity constant of the monomer towards the oxyanionic guest is strongly dependent on the spectral position used for the calculation. This indicates that more than only two species (unbound monomer and bound monomer) play a role in the titration. This assumption is supported by the observation that the isosbestic points in THF and ACN are less clear-cut than in DMSO. The titration spectra were subsequently submitted to non-linear regression that supported the assumption of de- and reprotonation in DMSO and the presence of more than two species in the other solvents.

Evaluation in presence of Z-L-Phe

The photophysics of monomer **1** were furthermore investigated in presence of a weaker base, namely Z-L-Phenylalanine deprotonated with the help of 1,2,2,6,6-pentamethylpiperidine (PMP) in ACN. The obtained spectra show no development of the broad band at around 570 nm that was obtained in presence of TBA Benzoate and sharp isosbestic points were obtained. Thus, it can be concluded that no deprotonation is induced in this case. A new absorption band arises at 412 nm belonging to the 1:1 complex between monomer **1** and the guest molecule. Upon addition of only Z-L-Phe no change in the spectra is observed, whereas the addition of only PMP induces the development of a strongly red-shifted band with a maximum at 570 nm implicating deprotonation. This phenomenon is reversible upon addition of Z-L-Phe.

Fluorescence emission and fluorescence titration:

The fluorescence emission properties of monomer **1** were evaluated in different solvents and in presence of increasing concentration of TBA Benzoat. The free monomer in solution shows a strongly Stokes-shifted broad emission band at around 500 nm. Upon addition of TBA Benzoat the monomer exhibits fluorescence quenching, which is in agreement with the assumption that deprotonation or anion binding should lead to reduced fluorescence.

Excitation at 570 nm (maximum absorption of deprotonated species) revealed that the deprotonated form of monomer **1** is non-emissive.

Table 8.3 displays the position of the maximum emission wavelength on monomer **1** and its precursor compound **3**:

Table 8.3: Maximum emission wavelengths of monomer **1** and precursor in different solvents

Solvent	Dielectricity constant	λ_{em} /nm
DMSO	48	542
EtOH	24.55	535
ACN	37.50	517
THF	7.50	512
Dioxane	2.3	500
ACN (3)	37.50	516

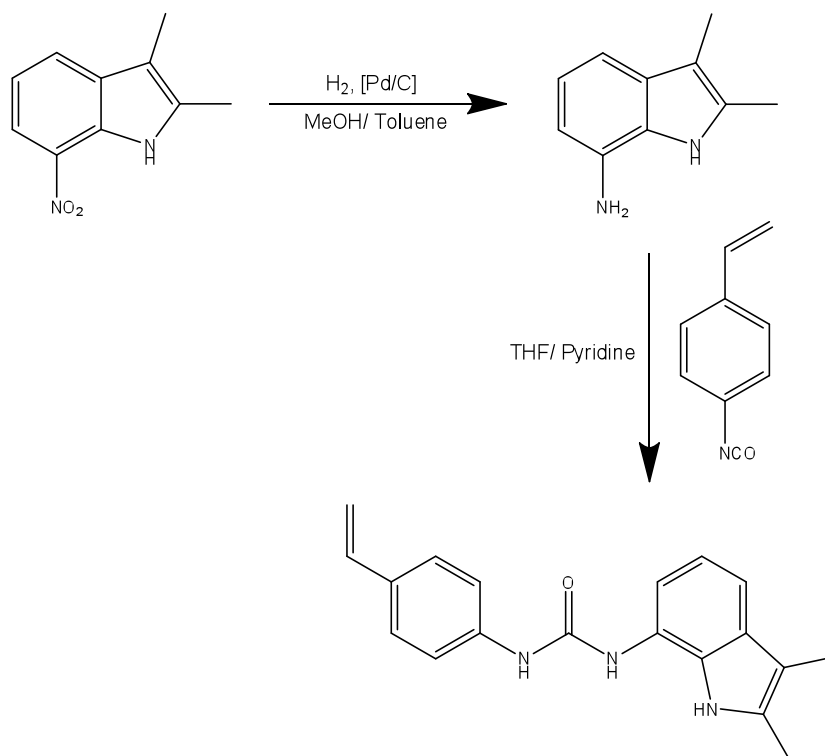
As in case of the absorption, the position of the maximum emission wavelength is strongly dependent on the solvent employed. With increasing polarity of the solvent the monomer exhibits positive solvatochromism.

Conclusion:

A polymerisable naphthalimide-based monomer was designed, synthesised and spectroscopically evaluated. The monomer shows broad and strongly Stokes' shifted absorption and emission bands. Evaluation in different solvents revealed positive solvatochromism in agreement with formally published findings for naphthalimides. Furthermore, titrations against oxyanionic guests show that the nature of the induced events (complex formation or deprotonation) is dependent on the employed solvent as well as the basicity of the guest molecule. Monomer **1** proved to be a promising candidate for the integration into molecularly imprinted polymers with signaling properties.

9. Indole-based monomers

The indole monomer was obtained from a two step synthesis in almost quantitative yield (94 %).



Scheme 9.1: Synthesis path of monomer 2

In a first step the starting material is hydrated to form the amin-functionality. Subsequently, the urea-moiety is obtained upon reaction with the in-house made para-vinylisocyanate.

9.1. Binding behaviour

A NMR titration employing monomer **2** as host and TBA-benzoate as guest was performed in deuterated DMSO according to the standard procedure. Figure 9.1 displays the dependency of the urea-proton shift on the concentration of TBA-benzoate.

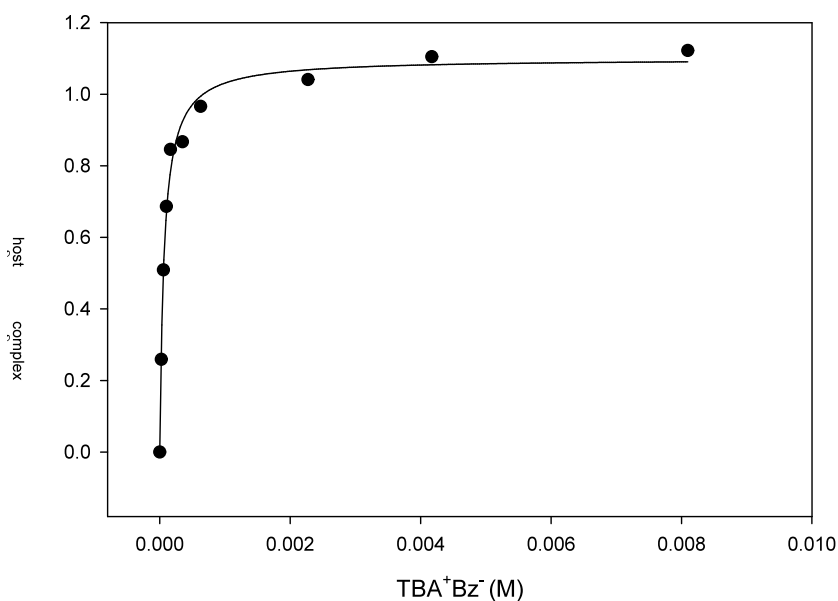


Figure 9.1: Complexation induced shift (CIS) as a function of the free concentration of TBA benzoate in DMSO-d₆

The CIS curve of the complex between monomer **2** and TBA benzoate yields a binding constant of 15084 M⁻¹ demonstrating high affinity for this model substrate.

9.2. Spectroscopic evaluation

The absorption and the fluorescence emission properties of monomer **2** were investigated in DMSO and its response towards oxyanionic guests was investigated in UV/VIS- and fluorescence titrations.

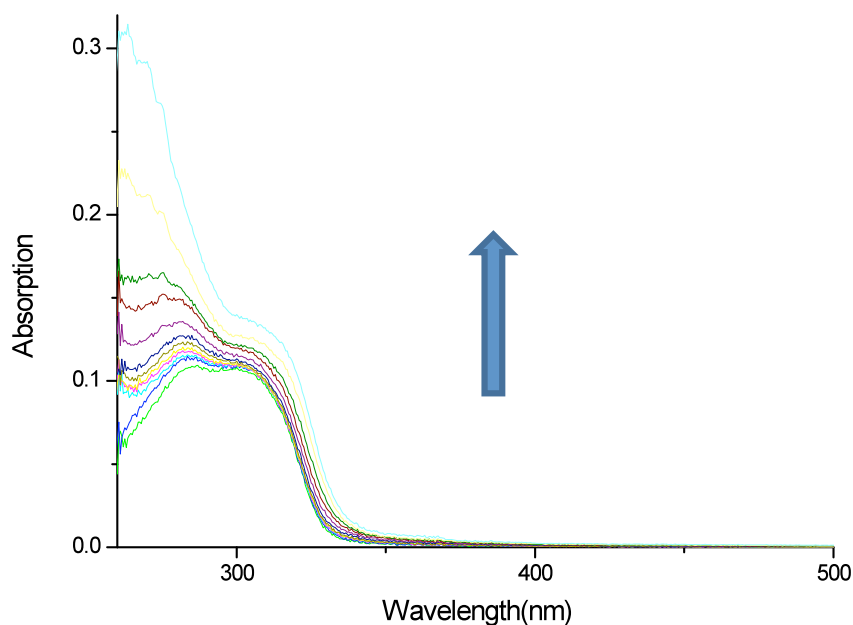


Figure 9.2: Absorption spectra of monomer **2** in DMSO in presence of increasing concentration of TBA-benzoate

Figure 9.2 represents the absorption spectra of monomer **2** collected in DMSO upon addition of increasing concentration of TBA-benzoate. The solution of the pure monomer shows a maximum in absorption at around 300 nm. Upon addition of TBA-benzoate the absorption increases and no shift of the band can be observed. Showing a high affinity towards oxyanionic guests (see NMR titration), monomer **2** is unfortunately of minor interest for optical applications due to the absorption band being located outside the easily applicable range. The binding constant derived from this experiment was calculated to 7586 M^{-1} .

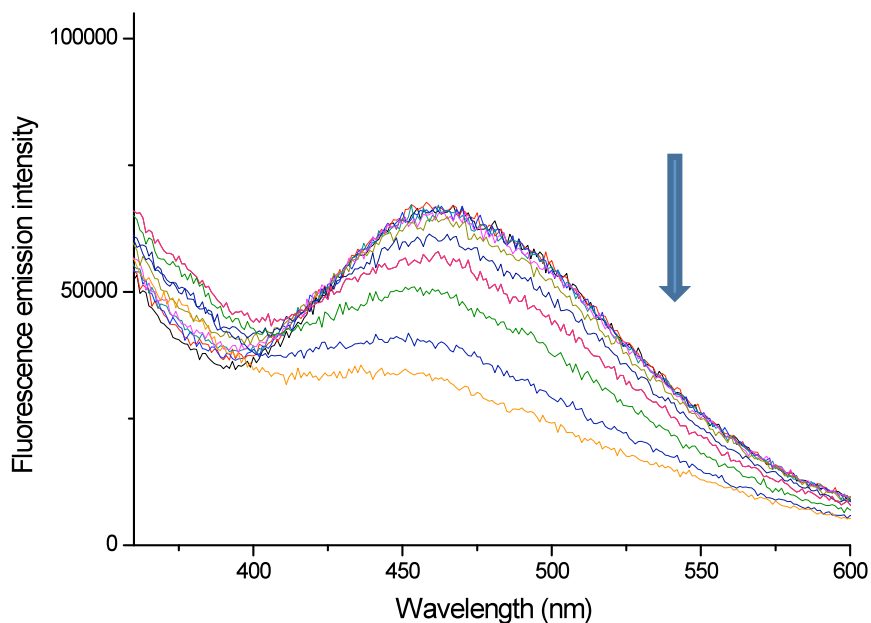
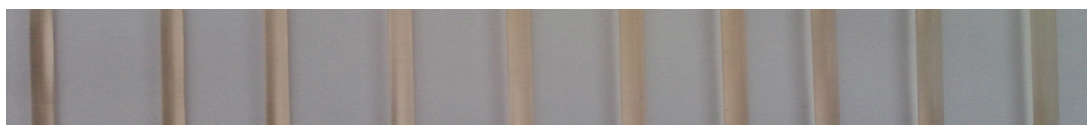


Figure 9.3: Fluorescence emission of monomer **2** in DMSO in presence of increasing concentration of TBA-benzoate

The solution of the pure monomer in DMSO shows a maximum intensity of fluorescence emission at ca. 470 nm. Upon addition of TBA-benzoate the fluorescence quenches.

Colourimetric evaluation:

Picture **9.1** shows the colours of solutions of monomer **2** in presence of increasing concentration of TBA-benzoate.



Picture 9.1: Colours of monomer **2** solutions in DMSO and in presence of increasing concentration of TBA-benzoate

Monomer **2** shows no colour-change induced by the presence of increasing concentration of the guest molecule TBA-Benzoate.

Conclusion

A new polymerisable indole-based monomer **2** was designed, synthesised and evaluated regarding its affinity towards oxyanionic guests, namely TBA-benzoate and its spectroscopical properties.

In the NMR titration monomer **2** showed high affinity towards TBA-benzoate. The absorption range of this monomer lies outside the spectral range suitable for sensing applications. Nevertheless, due to the high affinity towards oxyanions, monomer **2** can be of great value for separation applications and was thus included into the bulk synthesis for HPLC analysis.

10. Polymers

Polymers in different formats were prepared and evaluated. The range of possible formats is wide, each one having distinct advantages and disadvantages (see **3. MIP formats and formation**).

Bulk polymers were prepared due to the fact that this is the most commonly used format for molecularly imprinted polymers. This format is well-suited for the evaluation of the recognition and selectivity properties of the polymers by chromatographic experiments. The performance of the bulk polymers was evaluated upon employing them as stationary phase in HPLC analysis and in spectrophotometric experiments.

For optical sensing applications polymers in **film format** proved to be better suited than bulk materials. Films are known to be more sensitive and the occurrence of scattering phenomena resulting from the presence of (irregularly shaped) particles is avoided. Various approaches including different polymer compositions and immobilisation procedures were developed and tested regarding their reproducibility, the robustness of the obtained films and the recognition performance.

10.1. Monolithic polymers via bulk-polymerisation

The bulk polymers were prepared by free radical solution polymerisation via thermal initiation. Here thermal initiation employing an azo-initiator with low decomposition temperature was chosen over photochemical initiation to avoid photobleaching of the integrated dye.

10.1.1. Monomers for bulk synthesis

For the bulk synthesis three monomers were selected from the portfolio of the DFG project. These were namely monomer **1**, monomer **2**, and the phenoxazinone-based monomer **3**.

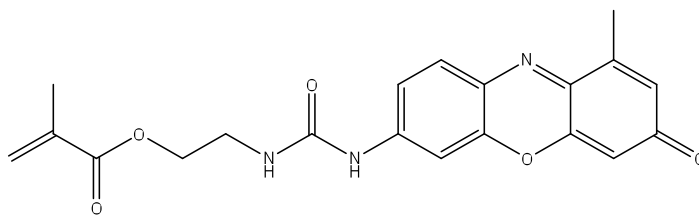


Figure 10.1: Monomer 3

This monomer showed a high affinity towards oxyanionic guests in the evaluation of the free monomer.

Apart from the monomers that are part of the project two other in-house made, urea-based monomers were chosen for bulk polymerisation as well. In earlier studies regarding the spectroscopical properties and binding affinities towards oxyanionic guest molecules performed in our group, these monomers proved valuable (lazraq thesis).

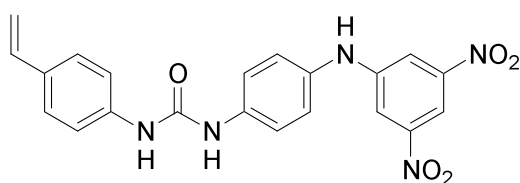


Figure 10.2: Monomer 4

The design of monomer 4 was based on the idea to develop a compound signalling via charge-transfer bands. The monomer showed an association constant of $K = 2085 (\pm 85) \text{ M}^{-1}$ towards TBA benzoate in the competitive solvent DMSO. It also proved to be UV active in the presence of the guest exhibiting a shift of λ_{max} from 275 nm to 290 nm in presence of the oxyanionic guest. Furthermore, a colour-change visible to naked-eye can be observed upon guest addition.

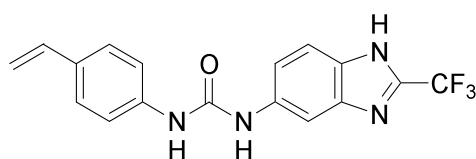
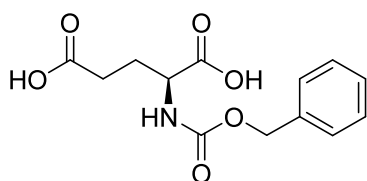


Figure 10.3: Monomer 5

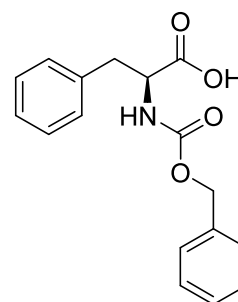
This monomer exhibits a moderate affinity towards TBA benzoate in DMSO (binding constant $534 (\pm 85) \text{ M}^{-1}$). Nevertheless, the fluorescence emission intensity of the monomer is quenched upon addition of the guest molecule.

10.1.2. Template molecules

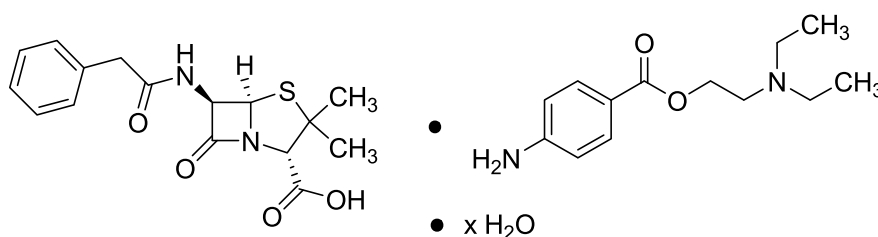
The template molecules were selected according to the above mentioned considerations (see template sections).



Z-L-Glutamic acid



Z-L-Phenylalanine



Penicillin G procain

Composition:

Table 10.1: Composition of the monolithic polymers NIP, P_{Glu}, P_{Phe}, P_{PenG}

Polymer	Z-L-Glu [mmol]	Z-L-Phe [mmol]	PenG Proc [mmol]	PMP [mmol]	Urea [mmol]	EDMA [mmol]
NIP	/	/	/	/	0.5	20
P _{Glu}	0.25	/	/	0.5	0.5	20
P _{Phe}	/	0.5	/	0.5	0.5	20
P _{PenG}	/	/	0.5	/	0.5	20

Being polar-aprotic turns DMF into a non-favourable solvent for imprinting. Nevertheless, the polymers had to be prepared in DMF due to poor solubility of the naphthalimide-based monomer in less polar solvents.

10.1.3. Evaluation

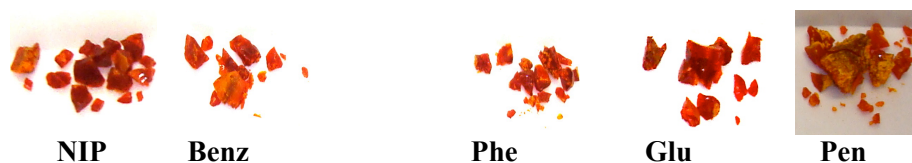
The following photos display the colours of the obtained bulk materials prior and after soxhlet extraction.

Polymers employing monomer 4:

Before extraction:



After extraction:



Picture 10.1: Colours of monomer 4 polymers prior and after extraction

In case of the polymers prepared employing monomer 4 as building block no colour difference of NIP and MIP could be observed. This observation agrees with the results of the UV/Vis spectrophotometric titration of the free monomer in solution against TBA benzoate, where no distinct shift upon addition of the template could be observed.

Polymers employing monomer **5**:

Before extraction:



After extraction:

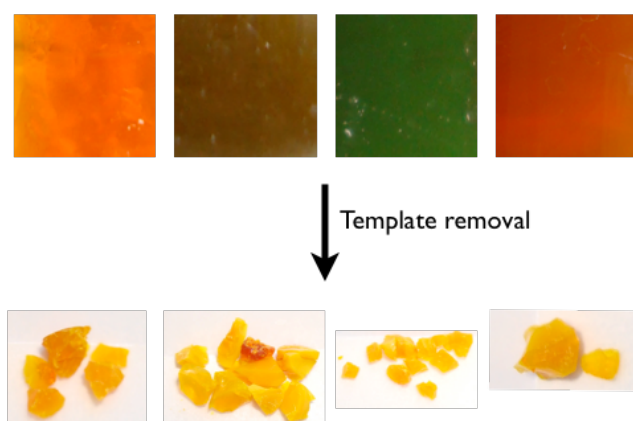


Picture 10.2: Colours of monomer **5** polymers prior and after extraction

Also in case of the polymers employing monomer **5** as building block no colour difference could be observed.

Polymers employing monomer **1**:

Before extraction:



Picture 10.3: Colours of monomer **1** polymers prior and after extraction

In case of the polymers prepared employing monomer **1** clear colour-differences are obtained imprinting on different templates. The NIP and *P_{IPenG}* are orange prior and after extraction. The closeness in colour between these two polymers indicates that hydrogen-bonding

is the main interaction in this case. The green colour of *P_{1Glu}* and the brownish colour of the polymer imprinted on Z-L-Phe hints at deprotonation of monomer **1** in the polymer. This indicates that the templates were successfully removed from the polymers. The template removal is confirmed via elemental analysis (see *experimental section, synthesis of bulk polymers*).

10.1.3.1. Chromatographic evaluation

As described in the analysis section under HPLC analysis, this technique may provide information about the recognition properties of the polymers. For this reason the polymers were evaluated employing different mobile phases consisting of acetonitrile and water and base-modified acetonitrile. The recognition of the respective template was evaluated and the success of the imprinting step was examined by analysing the cross-selectivity of the polymer upon injection of structurally related compounds to the template.

Results obtained for the Z-L-Glutamic acid columns

The polymers employing the different functional monomers and imprinted on Z-L-Glu were evaluated in four mobile phases. The following tables contain the obtained results:

Table **10.2** displays the results obtained for *P_{1Glu}* and *P_{1N}*.

Table 10.2: Retention times, capacity- and imprinting factors on P_{1Glu} and P_{1N}

	Analyte	ACN:H ₂ O (50:50)	ACN:H ₂ O (10:90)	ACN	ACN:TEA (99:1)
Retention time t_R (NIP) [min]	Z-L-Glu	n.r.*	n.r.*	1.40	1.39
	Z-D-Glu	n.r.*	n.r.*	1.38	1.39
	Z-L-Phe	2.10	n.r.*	/	1.32
Retention time t_R (MIP) [min]	Z-L-Glu	5.38	n.r.*	2.77	1.45
	Z-D-Glu	4.37	n.r.*	2.52	1.43
	Z-L-Phe	2.03	n.r.*	2.46	1.15
Capacity factor k (NIP)	Z-L-Glu	/	/	0.80	0.54
	Z-D-Glu	/	/	0.78	0.54
	Z-L-Phe	1.25	/	/	0.46
Capacity factor k (MIP)	Z-L-Glu	5.23	/	2.66	0.60
	Z-D-Glu	4.06	/	2.33	0.59
	Z-L-Phe	1.30	/	2.25	0.27
Imprinting factor IF	Z-L-Glu	/	/	3.02	1.11
	Z-D-Glu	/	/	2.99	1.09
	Z-L-Phe	1.04	/	/	1.70

* n.r. = no retention (Retention time lower or comparable to retention time of void marker)

** Imprinting factors calculated from $k < 1$ unreliable; only listed for the sake of completeness

In mobile phase ACN: H₂O (50:50) P_{1Glu} retains both enantiomers of Z-Glutamic acid better than P_{1N} , whereas the retention time for the cross-analyte Z-L-Phenylalanine is comparable on NIP and MIP. Furthermore, P_{1Glu} is clearly able to discriminate between its template and the D-enantiomer of the template. In pure ACN the retention time on P_{1Glu} is higher than on the corresponding NIP. Nevertheless, the MIP is not discriminating between its template and the other injected compounds. In the mobile phase containing a high water content of 90 % no retention of any of the analytes was obtained. The presence of the water seems to

hinder the interaction between the polymer and the analytes. Using TEA as a base-modifier leads to shorter retention times compared to in pure ACN. This observation supports the assumption made in the monomer section (see section **8**) that strongly basic conditions deprotonate the rather acidic secondary-amin functionality.

Table 10.3: Retention times, capacity- and imprinting factors on P_{4Glu} and P_{4N}

	Analyte	ACN:H ₂ O (50:50)	ACN:H ₂ O (10:90)	ACN	ACN:TEA (99:1)
Retention time t_R (NIP) [min]	Z-L-Glu	n.r.*	n.r.*	1.40	1.37
	Z-D-Glu	n.r.*	n.r.*	1.38	1.35
	Z-L-Phe	/	3.16	1.79	2.75
Retention time t_R (MIP) [min]	Z-L-Glu	n.r.*	n.r.*	2.77	2.33
	Z-D-Glu	n.r.*	n.r.*	2.52	2.33
	Z-L-Phe	/	n.r.*	n.r.*	3.05
Capacity factor k (NIP)	Z-L-Glu	/	/	0.80	0.66
	Z-D-Glu	/	/	0.78	0.64
	Z-L-Phe	/	0.99	0.14	0.75
Capacity factor k (MIP)	Z-L-Glu	/	/	2.66	2.15
	Z-D-Glu	/	/	2.33	2.15
	Z-L-Phe	/	/	/	2.50
Imprinting factor IF	Z-L-Glu	/	/	3.02	3.26
	Z-D-Glu	/	/	2.99	3.36
	Z-L-Phe	/	/	/	3.33

* n.r. = no retention (Retention time lower or comparable to retention time of void marker)

* Imprinting factors calculated from $k < 1$ unreliable; only listed for the sake of completeness

P_{4Glu} as well as its corresponding NIP P_{4N} are not retaining any of the analytes in aqueous mobile phases. The water containing mobile phases hinder the interaction between the polymer and the analytes, even with monomer **4** showing a higher association constant towards oxyanionic guests in the competitive solvent DMSO. In pure ACN the retention times for the template and its D-enantiomer on the MIP are higher than on the NIP, whereas it is not retaining Z-L-Phenylalanine. Also in the TEA- modified mobile phase the retention on P_{4Glu} is better than on the NIP, but no discrimination between the two enantiomers could be ob-

tained. Also in this case, the base modification lowers the retention times on the MIP, indicating deprotonation.

Table 10.4: Retention times, capacity- and imprinting factors on P_{5Glu} and P_{5N}

	Analyte	ACN:H ₂ O (50:50)	ACN:H ₂ O (10:90)	ACN	ACN:TEA (99:1)
Retention time t_R (NIP) [min]	Z-L-Glu	1.66	n.r.*	1.59	3.44
	Z-D-Glu	0.98	n.r.*	1.50	3.40
	Z-L-Phe	1.61	n.r.*	1.61	2.36
Retention time t_R (MIP) [min]	Z-L-Glu	1.86	1.82	1.72	3.52
	Z-D-Glu	1.11	1.81	1.70	3.55
	Z-L-Phe	1.88	2.40	1.71	2.47
Capacity factor k (NIP)	Z-L-Glu	0.71	/	0.02	1.07
	Z-D-Glu	0.02	/	/	1.05
	Z-L-Phe	0.66	/	0.07	0.42
Capacity factor k (MIP)	Z-L-Glu	0.91	0.19	0.12	1.18
	Z-D-Glu	0.14	0.19	0.11	1.20
	Z-L-Phe	0.94	0.58	0.12	0.53
Imprinting factor IF	Z-L-Glu	1.29	/	6.00	1.10
	Z-D-Glu	7.15	/	/	1.14
	Z-L-Phe	1.41	/	1.71	1.26

*n.r. = no retention (Retention time lower or comparable to retention time of void marker)

* Imprinting factors calculated from $k < 1$ unreliable, only listed for the sake of completeness

P_{5Glu} shows a pronounced difference in retention times of NIP and MIP only in the mobile phase with 90 % water content. Slight enantio-selective discrimination could be obtained in mobile phase containing 50 % water and 50 % ACN. In case of monomer **5** the base-modification with TEA leads to higher retention times. This indicates a lower acidity of the urea-protons compared to monomer **1** and monomer **4**.

Table 10.5: Retention times, capacity- and imprinting factors on P_{3Glu} and P_{3N}

	Analyte	ACN:H ₂ O (50:50)	ACN:H ₂ O (10:90)	ACN	ACN:TEA (99:1)
Retention time t_R (NIP) [min]	Z-L-Glu	n.r.*	n.r.*	n.r.*	n.r.*
	Z-D-Glu	n.r.*	n.r.*	n.r.*	n.r.*
	Z-L-Phe	n.r.*	n.r.*	n.r.*	n.r.*
Retention time t_R (MIP) [min]	Z-L-Glu	n.r.*	n.r.*	0.97	n.r.*
	Z-D-Glu	n.r.*	n.r.*	0.91	n.r.*
	Z-L-Phe	n.r.*	n.r.*	0.91	n.r.*
Capacity factor k (NIP)	Z-L-Glu	/	/	/	/
	Z-D-Glu	/	/	/	/
	Z-L-Phe	/	/	/	/
Capacity factor k (MIP)	Z-L-Glu	/	/	0.10	/
	Z-D-Glu	/	/	0.03	/
	Z-L-Phe	/	/	0.02	/
Imprinting factor IF	Z-L-Glu	/	/	/	/
	Z-D-Glu	/	/	/	/
	Z-L-Phe	/	/	/	/

* n.r. = no retention (Retention time lower or comparable to retention time of void marker)

* Imprinting factors calculated from $k < 1$ unreliable; only listed for the sake of completeness

P_{3Glu} and its corresponding NIP P_{3N} show are retaining none of the analytes in any of the mobile phases. It seems that the imprinting step was rather unsuccessful in this case. This might be due to the poor solubility of the monomer.

Table 10.6: Retention times, capacity- and imprinting factors on P_{2Glu} and P_{2N}

	Analyte	ACN:H ₂ O (50:50)	ACN:H ₂ O (10:90)	ACN	ACN:TEA (99:1)
Retention time t_R (NIP) [min]	Z-L-Glu	n.r.*	n.r.*	1.80	0.77
	Z-D-Glu	n.r.*	n.r.*	1.76	0.76
	Z-L-Phe	n.r.*	n.r.*	n.r.*	0.78
Retention time t_R (MIP) [min]	Z-L-Glu	n.r.*	n.r.*	2.38	4.49
	Z-D-Glu	n.r.*	n.r.*	2.32	4.53
	Z-L-Phe	n.r.*	n.r.*	2.20	3.36
Capacity factor k (NIP)	Z-L-Glu	/	/	0.75	0.18
	Z-D-Glu	/	/	0.71	0.18
	Z-L-Phe	/	/	/	0.19
Capacity factor k (MIP)	Z-L-Glu	/	/	1.63	3.48
	Z-D-Glu	/	/	1.57	3.40
	Z-L-Phe	/	/	1.40	2.35
Imprinting factor IF	Z-L-Glu	/	/	2.16	18.73
	Z-D-Glu	/	/	2.22	18.30
	Z-L-Phe	/	/	/	12.34

* n.r. = no retention (Retention time lower or comparable to retention time of void marker)

* * Imprinting factors calculated from $k < 1$ unreliable; only listed for the sake of completeness

In mobile phase ACN: Hepes (50:50) and ACN:Hepes (10:90) **P_{2Glu}** and the corresponding NIP retain neither the template nor the cross-analytes. In ACN the retention time for all analytes is higher in the MIP than in the NIP. The base modification of ACN by 1 % of TEA yields in a more pronounced retention on the MIP. Nevertheless, the MIP is not discriminating between its template and the D-enantiomer.

Results obtained for the Z-L-Phenylalanine columns

Table 10.7: Retention times, capacity- and imprinting factors on P_{1Phe} and P_{1N}

	Analyte	ACN:H ₂ O (50:50)	ACN:H ₂ O (10:90)	ACN	ACN:TEA (99:1)
Retention time t_R (NIP) [min]	Z-L-Phe	0.97	2.34	1.35	2.75
	Z-D-Phe	0.95	2.36	1.29	2.76
	Z-L-Glu	n.r.*	n.r.*	n.r.*	1.37
Retention time t_R (MIP) [min]	Z-L-Phe	1.79	2.49	7.48	2.95
	Z-D-Phe	1.78	2.42	1.32	2.95
	Z-L-Glu	1.26	n.r.*	n.r.*	n.r.*
Capacity factor k (NIP)	Z-L-Phe	0.07	1.29	0.79	0.95
	Z-D-Phe	0.05	1.31	0.50	0.96
	Z-L-Glu	/	/	/	/
Capacity factor k (MIP)	Z-L-Phe	1.00	1.44	7.78	1.92
	Z-D-Phe	1.01	1.36	0.55	1.92
	Z-L-Glu	0.42	/	/	/
Imprinting factor IF	Z-L-Phe	14.28	1.12	9.85	2.02
	Z-D-Phe	20.20	1.04	1.1	2.00
	Z-L-Glu	/	/	/	/

P_{1Phe} shows no enantioselective discrimination in the water containing mobile phases. In ACN the MIP shows a remarkably higher retention time upon injection of the template Z-L-Phe than upon injection of the D-enantiomer and Z-L-Glutamic acid, whereas the NIP shows no enantioselective discrimination. The base modification of the ACN leads to lower retention of the template. For this reason and the low retention time on the NIP it can be concluded that the imprinting step was successful. Apart from the hydrogen-bonding also the interactions between the aromatic monomer and the aromatic rest of the amino-acid can play a

role in the binding. This might explain the significantly better retention of *Z-L-Phe* in comparison to glutamic acid.

Table 10.8: Retention times, capacity- and imprinting factors on P_{4Phe} and P_{4N}

	Analyte	ACN:H ₂ O (50:50)	ACN:H ₂ O (10:90)	ACN	ACN:TEA (99:1)
Retention time t_R (NIP) [min]	Z-L-Phe	n.r.*	3.16	1.79	2.74
	Z-D-Phe	n.r.*	3.15	1.73	2.76
	Z-L-Glu	n.r.*	n.r.*	1.40	1.37
Retention time t_R (MIP) [min]	Z-L-Phe	2.51	4.28	1.56	3.05
	Z-D-Phe	2.51	4.08	1.57	2.90
	Z-L-Glu	1.48	1.43	2.77	2.33
Capacity factor k (NIP)	Z-L-Phe	/	0.99	0.39	0.75
	Z-D-Phe	/	0.99	0.10	0.75
	Z-L-Glu	/	/	0.80	0.66
Capacity factor k (MIP)	Z-L-Phe	0.71	2.06	0.01	2.50
	Z-D-Phe	0.71	1.92	0.01	2.29
	Z-L-Glu	/	0.02	2.66	2.15
Imprinting factor IF	Z-L-Phe	/	2.08	0.02	3.33
	Z-D-Phe	/	1.93	0.10	3.05
	Z-L-Glu	/	/	3.32	3.25

P_{4Phe} shows higher retention times upon injection of *Z-L-Phenylalanine* than its corresponding NIP in all the mobile phases but ACN. There is no remarkable enantioselective discrimination detectable. Nevertheless, like in case of the polymers employing monomer **1** the recognition of the aromatic acid phenylalanine is better than for the non-aromatic one glutamic acid. Also in this case, interactions between the aromatic monomer and the template seem to play a role.

Table 10.9: Retention times, capacity- and imprinting factors on P_{5Phe} and P_{5N}

	Analyte	ACN:H ₂ O (50:50)	ACN:H ₂ O (10:90)	ACN	ACN:TEA (99:1)
Retention time t_R (NIP) [min]	Z-L-Phe	1.61	n.r.*	1.61	2.36
	Z-D-Phe	1.60	n.r.*	1.61	2.36
	Z-L-Glu	1.66	n.r.*	1.59	3.44
Retention time t_R (MIP) [min]	Z-L-Phe	1.88	2.40	1.71	2.47
	Z-D-Phe	1.85	2.48	1.70	2.40
	Z-L-Glu	1.86	1.82	1.72	2.52
Capacity factor k (NIP)	Z-L-Phe	0.07	/	0.39	0.70
	Z-D-Phe	0.07	/	0.10	0.70
	Z-L-Glu	0.10	/	0.80	1.07
Capacity factor k (MIP)	Z-L-Phe	0.17	0.58	0.01	0.53
	Z-D-Phe	0.15	0.63	0.01	0.49
	Z-L-Glu	0.16	0.19	2.66	0.56
Imprinting factor IF	Z-L-Phe	2.42	/	0.02	0.75
	Z-D-Phe	2.14	/	0.10	0.70
	Z-L-Glu	1.60	/	3.32	0.52

P_{5Phe} shows higher retention times upon injection of the template and the D-enantiomer than the corresponding NIP. Nevertheless, the MIP does not discriminate between the two enantiomers. Also the polymers prepared from monomer **5** retain the aromatic amino acid phenylalanine better than the aliphatic glutamic acid.

Results obtained for the Penicillin G procain columns

Table 10.10: Retention times, capacity- and imprinting factors on P_{1PenG} and P_{1N}

	Analyte	ACN:H ₂ O (50:50)	ACN:H ₂ O (10:90)	ACN	ACN:TEA (99:1)
Retention time t_R (NIP) [min]	PenG Pot	n.e.*	n.e.*	1.52	n.r.*
	Benzoic acid	n.r.*	n.r.*	1.55	1.69
Retention time t_R (MIP) [min]	PenG Pot	n.e.*	n.e.*	1.43	n.r.*
	Benzoic acid	n.r.*	n.r.*	1.83	n.r.*
Capacity factor k (NIP)	PenG Pot	/	/	0.05	/
	Benzoic acid	/	/	0.07	0.01
Capacity factor k (MIP)	PenG Pot	/	/	0.02	/
	Benzoic acid	/	/	0.39	/
Imprinting factor IF	PenG Pot	/	/	0.40	/
	Benzoic acid	/	/	5.57	/

Due to solubility reasons the potassium salt of Penicillin G was employed as analyte. In the mobile phases with high water content the MIP is not eluting the template, whereas it is not retaining the cross-analyte benzoic acid. In ACN and ACN: TEA (99:1) the template as well as Benzoic acid are eluting fast.

Table 10.11: Retention times, capacity- and imprinting factors on P_{4PenG} and P_{4N}

	Analyte	ACN:H ₂ O (50:50)	ACN:H ₂ O (10:90)	ACN	ACN:TEA (99:1)
Retention time t_R (NIP) [min]	PenG Pot	n.r.*	1.60	1.52	n.r.*
	Benzoic acid	n.r.*	n.r.*	1.55	n.r.*
Retention time t_R (MIP) [min]	PenG Pot	n.r.*	1.48	1.43	1.49
	Benzoic acid	n.r.*	n.r.*	1.83	n.r.*
Capacity factor k (NIP)	PenG Pot	/	0.07	0.05	0.12
	Benzoic acid	/	/	0.07	/
Capacity factor k (MIP)	PenG Pot	/	0.09	0.02	/
	Benzoic acid	/	/	0.39	/
Imprinting factor IF	PenG Pot	/	1.28	0.40	/
	Benzoic acid	/	/	5.57	/

The polymers employing monomer **4** do not show any remarkable behaviour.

Table 10.12: Retention times, capacity- and imprinting factors on P_{5PenG} and P_{5N}

	Analyte	ACN:H ₂ O (50:50)	ACN:H ₂ O (10:90)	ACN	ACN:TEA (99:1)
Retention time t_R (NIP) [min]	PenG Pot	0.90	1.06	n.r.*	n.r.*
	Benzoic acid	n.r.*	n.r.*	0.94	n.r.*
Retention time t_R (MIP) [min]	PenG Pot	2.38	1.71	1.17	1.38
	Benzoic acid	n.r.*	n.r.*	0.79	0.89
Capacity factor k (NIP)	PenG Pot	/	0.02	/	/
	Benzoic acid	/	/	0.02	/
Capacity factor k (MIP)	PenG Pot	2.72	0.50	0.52	0.73
	Benzoic acid	/	/	0.03	0.12
Imprinting factor IF	PenG Pot	/	25	/	/
	Benzoic acid	/	/	1.50	/

In all mobile phases the retention time on the MIP is higher than on the NIP. Furthermore the Penicillin G is retained better than the Benzoic acid on the MIP. This implies that the imprinting step was successful.

Conclusion

Polymers according to the ratios displayed in **table 10.1** were prepared employing different aromatic urea-based monomers.

Polymers prepared with monomer 1

The results of the polymers employing monomer **1** as building block show that the imprinting was successful. They show good retention of the respective template and the polymers imprinted on *Z-L-Glu* and *Z-L-Phe* revealed remarkable enantioselective discrimination properties between their template and its *D*-enantiomer. Base modification of the mobile phase leads to reduced retention, supporting the assumption that the rather acidic secondary amine of the urea- monomer exhibits gradual deprotonation under basic conditions.

Polymers prepared with monomer 4 and 5

The polymers employing monomer **4** and monomer **5** as building block show higher retention times on the MIP than on the corresponding NIP in some of the mobile phases, but no enantioselective discrimination.

Polymers prepared with monomer 2 and 3

The polymers prepared using monomer **2** as well as monomer **3** do not meet the expectations resulting from the high affinity obtained for the monomer titrations against TBA-benzoate. Nevertheless, a nitrobenzoxadiazole fluorophore-based monomer has been successfully integrated into molecularly imprinted silica core nanoparticles, showing reasonable enantiomeric discrimination towards its template *Z-L-Phe*. These results obtained by Wei Wan at the BAM, Berlin are to be published elsewhere.

1. Spectroscopic evaluation of the bulk polymers containing monomer 1

According to the measurements on the free monomer in solution the spectroscopic properties of the bulk polymers were investigated in order to gain information whether the promising spectral characteristics of monomer **1** were preserved also upon integration into the bulk polymers. With the bulk polymers being unsuitable for spectroscopic studies they were crushed to small particles.

It was assumed that strong interaction between the polymer and the template displayed in high retention times in HPLC analysis should lead to strong effects also in the photo-physics of the polymers. The first evaluation was thus performed in the solvent that gave the best retention of the template or respectively the best imprinting factor in the HPLC analysis.

P_{1Glu} was thus first evaluated in a mixture of ACN: H₂O (50:50, v/v). The polymer did not show a significant change in fluorescence emission intensity upon addition of increasing concentration of the guest molecule *Z-L-Glu* or a shift in the position of the emission wavelength. As displayed in picture **10.4** and **10.5** no colour-change visible to naked-eye can be observed for both NIP and MIP.



Picture 10.4: left: NIP in solvent, right: NIP in 2 mM *Z-L-Glu*
MIP in 2 mM *Z-L-Glu*



Picture 10.5: left: MIP in solvent, right:

P_{1Phe} was first evaluated in pure acetonitrile. Since it showed pronounced enantio-selective discrimination in chromatographic analysis the fluorescence emission intensity was evaluated in presence of the template and the cross-analytes *Z-D-Phe* and *Z-L-Glu*. Also polymer *P_{1Phe}* shows no fluorescence quenching or a shift in the position of the emission spectrum as a result of the addition of increasing concentrations of the template and other cross-analytes in ACN.

The same observation was obtained for *P_{IPenG}* upon addition of Penicillin G potassium salt and benzoic acid.



Picture 10.6: left: NIP in solvent, right: NIP in 2 mM PenG



Picture 10.7: left: MIP in solvent, right: MIP in 2 mM PenG

For the NIP and the polymer imprinted on Penicillin G no colour-change visible to naked eye was induced by the addition of the analytes.

Conclusion

The bulk polymers tested previously in the HPLC were investigated spectroscopically in solvent system that gave the best results being employed as mobile phase. In all cases no quenching of the fluorescence emission intensity could be observed in the respective best-performing mobile phase upon addition of increasing concentration of the analytes.

In order to gain information if the non-responsiveness is a matter of concentration higher concentrated analyte/PMP solutions (10 mM) were added as Hepes-buffered solutions. Also in this case, no change in the fluorescence emission and no colour-change visible to naked eye was observed.

All tested bulk polymers *P_{IGlu}*, *P_{IPhe}* and *P_{IPenG}* did not show the expected quenching upon addition of the analytes in the best-performing mobile phases from the HPLC analysis also employing higher concentration. This could be due to the following reasons:

- Morphology of the polymer:

The dye-monomer **1** is shielded by the polymer backbone and not accessible to solvents of different polarity or analytes

- Nature of the solvent system

The buffered systems might inhibit the interaction between the polymers and the analytes.

Solvatochromism of the bulk polymers

In order to confirm the accessibility of the dye-monomer within the polymer-backbone solvatochromic studies of the bulk polymers were performed in solvents of increasing polarity.

The urea-based monomer **1** employed as building block in the synthesis of the polymer blocks is a solvatochromic dye (see section **8**). Due to the different polarities of their ground state and excited state, solvatochromic compounds exhibit a change in position of the UV/VIS absorption band or the emission wavelength depending on the polarity of the solvent. This effect may be used to evaluate the accessibility of the monomer that was built into the polymer by monitoring its behaviour in different solvents. Depending on the properties of the solvent and the polymer, the spectra of the solvatochromic dye should exhibit a hypsochromic or bathochromic shift upon analysis in solvents of increasing polarity. Properties of the solvent that influence the solvation of the polymer are the dipolarity and its hydrogen bonding abilities.

It is expected that high solvation and thus good accessibility of monomer **1** in the polymers should lead to emission properties similar to the ones of the free monomer in the respective solvent, whereas poor solvation should lead to properties similar to the ones of the dry polymer.⁸⁷

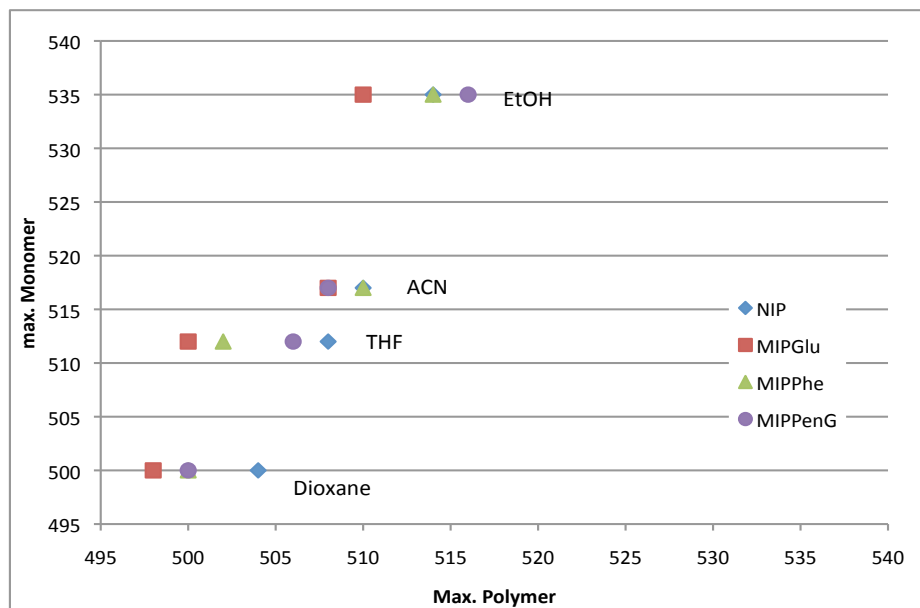


Figure 10.4: Maximum emission wavelength of P_{IN} , P_{IGlu} , P_{IPhe} and P_{IPenG} plotted against maximum emission wavelength of monomer **1** in Dioxane, THF, ACN, EtOH

Table 10.13 lists the values for the polymers, of which no corresponding data for the monomer exists.

Table 10.13: Maximum emission wavelength of P_{IN} , P_{IGlu} , P_{IPhe} and P_{IPenG} in water and dry state

λ_{em} / nm				
	P_{IN}	P_{IGlu}	P_{IPhe}	P_{IPenG}
Water	531	526	526	522
Dry	529	521	525	520

The investigation of the bulk polymers in solvents of different polarity revealed that the dye-monomer **1** exhibits positive solvatochromism also being built-in into the polymer. Thus, the accessibility of the monomer should not be the cause of the irresponsiveness of the polymers towards the analytes. Nevertheless, the bathochromic shift of the maximum emission wavelength is less pronounced than for the free monomer **1** in solution. The created micro-environment that the monomer exhibits depends on the template used during synthesis. P_{IN} and P_{IGlu} show a shift of 12 nm, whereas P_{IPenG} shows the strongest shift of 16 nm.

Solvent test

In order to investigate the influence of the solvent on the response of the polymers towards the analytes the experiment was repeated using P_{1Glu} in solvents of different polarity. The following diagrams display the change in the fluorescence emission intensity of the polymers upon addition of increasing concentration of the template molecule.

For P_{1Glu} no fluorescence quenching was observed upon evaluation in DMSO and ACN. In water on the other hand, pronounced quenching was induced by the presence of increasing concentration of Z-L-Glu.

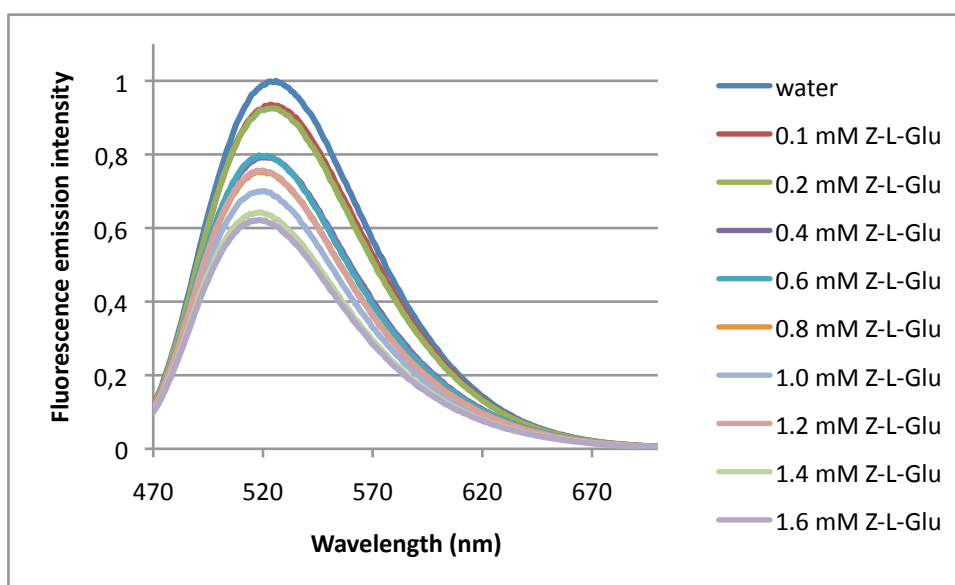


Figure 10.5: Fluorescence emission intensity of P_{1Glu} in water in presence of increasing concentration of Z-L-Glu

In order to allow better comparability the fluorescence quenching results obtained upon analysis of P_{1Glu} they are compiled in **figure 10.6:**

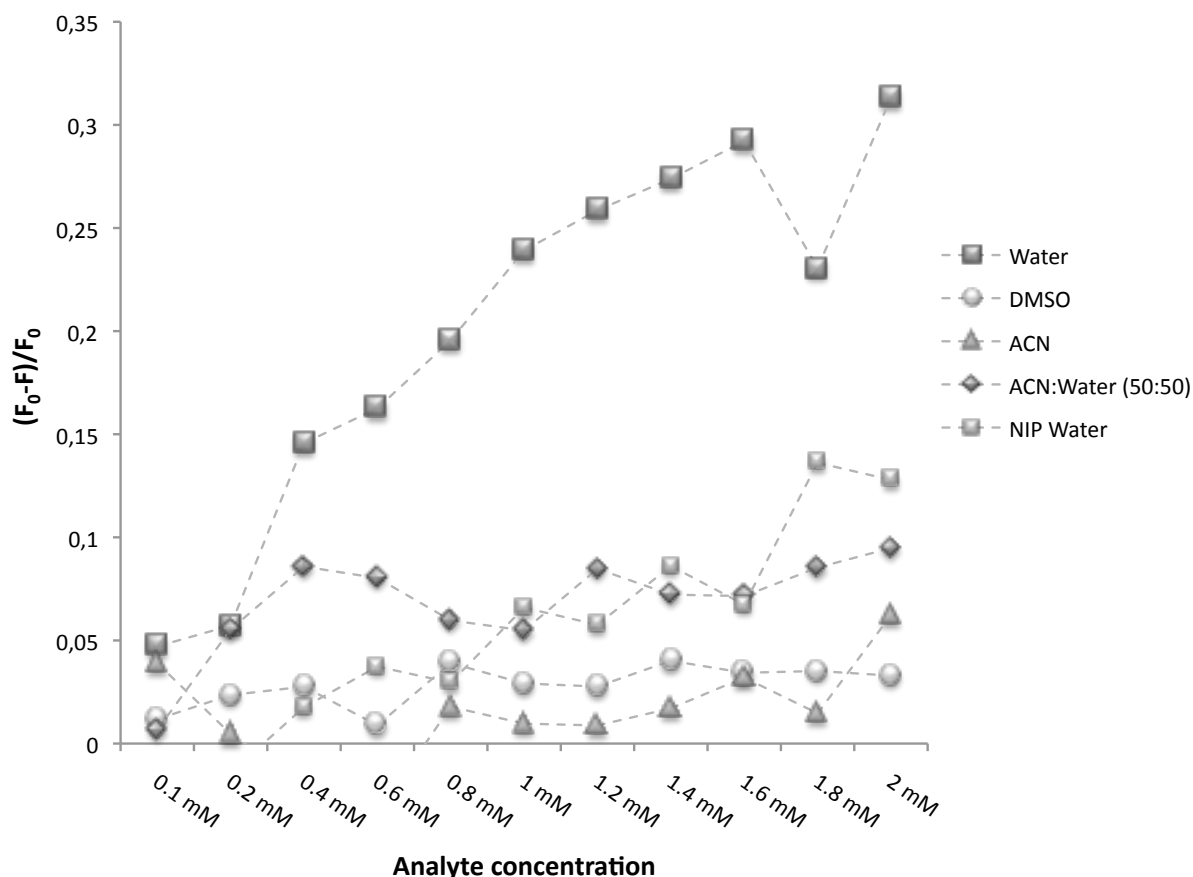


Figure 10.6: Comparison of fluorescence emission intensities of *P1Glu* in different solvents in presence of increasing concentration of Z-L-Glu

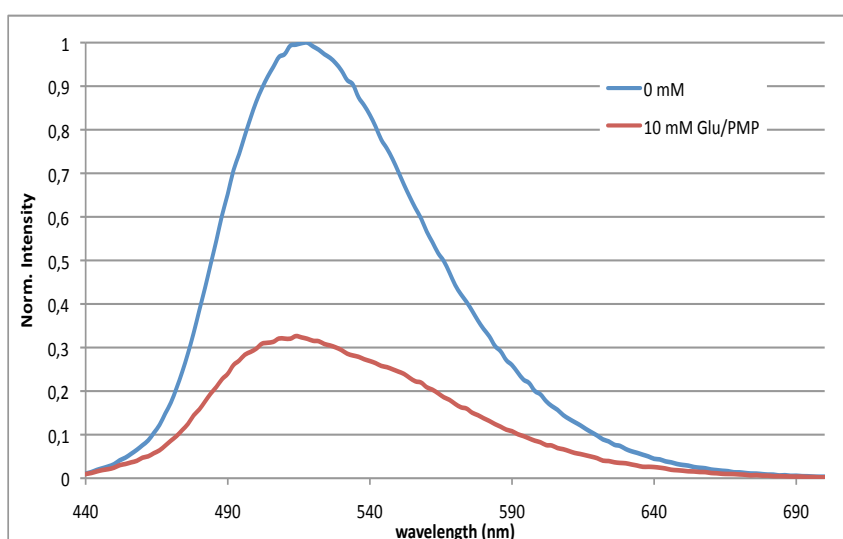
The diagram 10.6 gives an overview of the fluorescence emission intensities of *P1Glu* in different media obtained upon increasing concentration of a Z-L-Glutamic acid/ PMP mixture. Pronounced quenching of one third of the original fluorescence intensity is observed in pure water. In a 50:50 mixture of water and ACN quenching up to 10 % can be observed. Also the quenching observed upon addition of Z-L-Glu to the NIP, the quenching was much less pronounced than on the MIP. Using a HEPES buffer instead of water no quenching was observed in presence of the analyte on the NIP as well as the MIP.

The imprinting factors calculated from the quenching results for the NIP and *P1Glu* in water confirm that the quenching is more pronounced on the MIP than on the NIP. It can thus be assumed that the imprinting step was successful.

Table 10.14: IF_Q for *P1Glu* in presence of increasing concentration of Z-L-Glu/PMP

	IF _Q
0.2 mM Z-L-Glu	0.948
0.4 mM Z-L-Glu	0.957
0.6 mM Z-L-Glu	0.853
0.8 mM Z-L-Glu	0.893
1 mM Z-L-Glu	0.879
1.2 mM Z-L-Glu	0.792
1.4 mM Z-L-Glu	0.948
1.6 mM Z-L-Glu	0.743
1.8 mM Z-L-Glu	0.861

In order to gain information about the dynamic range of the experiment the response of the MIP towards a high concentrated Z-L-Glu/PMP solution in water (10 mM) was evaluated. As observed for the 2 mM solution, the fluorescence emission of *P1Glu* quenches to 1/3 with respect to the original intensity.

**Figure 10.7:** Normalised fluorescence emission intensity of *P1Glu* in water and in presence of 10 mM Z-L-Glu/PMP



Picture 10.8: Colours of **P₁Glu** in water and 10 mM Z-L-Glu/PMP

A pronounced fluorescence quenching and a colour-change from yellow to reddish can be observed for **P₁Glu** upon addition of high concentration of the template and base. This big difference in colour indicates that the observed quenching is, at least partially, due to deprotonation of monomer **1**. The fluorescence emission intensity of **P₁N** and the polymers imprinted on Phenylalanine and Penicillin were investigated in water as well. All the polymers show the same behaviour in water. Nevertheless, the quenching is less pronounced on the NIP than observed for the imprinted polymers.

Conclusion

The fluorescence emission intensity of the bulk polymers was investigated in different solvents including the mobile phase that resulted in the best retention/imprinting in HPLC analysis. The results show that chromatographic and spectroscopic analysis require different conditions. The best-performing mobile phase in HPLC analysis yielded in no significant change in the fluorescence emission intensity in spectroscopic analysis. A reason may be that in the HPLC the equilibration of the system is forced by pressure whereas this is not the case in the plate reader.

Also the buffer seems to interfere with the system. The fluorescence emission intensity of the polymers in buffered solutions does not change significantly, whereas the same polymers show pronounced quenching upon addition of the template solutions in presence of PMP in water.

Base-responsive test

In order to evaluate whether the polymers show quenching upon interaction with the deprotonated form of the analyte or if the quenching of the fluorescence emission intensity

is due to deprotonation of the urea protons the fluorescence properties of the polymers was investigated in water and in presence of PMP as a base.

Figure 10.8 shows the fluorescence emission of **P₁Phe** as a representative.

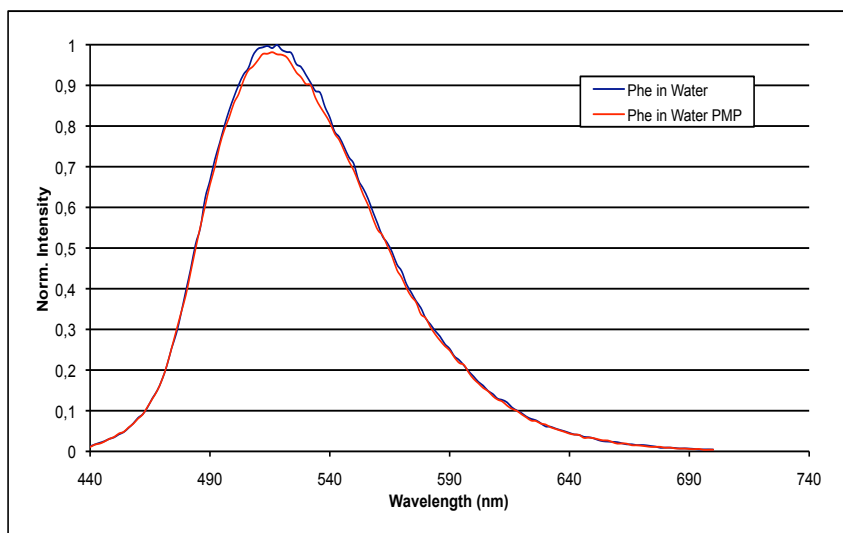


Fig. 10.8: Normalised fluorescence emission intensity of **P₁Phe** in presence of water and PMP in water plotted against wavelength

No change in the emission intensity of the polymer can be observed upon addition of the base. Furthermore, no colour-change visible to naked-eye occurs.



Picture 10.9: left: **P₁Phe** in water, right: **P₁Phe** in PMP in water

Thus, the observed colour-change and the quenching of the fluorescence emission intensity must be a consequence of the contemporaneous presence of the analyte and the base, respectively the formed salt.

Selectivity test

Based on the results displayed above the polymer **P₁Phe** was chosen for a selectivity test because it showed the most pronounced quenching in presence of its template and PMP in water. The fluorescence emission intensity was investigated in pure water, in presence of the template Z-L-Phe, the D-enantiomer and Penicillin G potassium salt in presence of PMP.

Showing equal quenching of the fluorescence emission intensity in all cases, the polymer P_{1Phe} is not discriminating between the template and the cross-analytes. The same behaviour was observed for the polymers imprinted on glutamic acid and penicillin G.

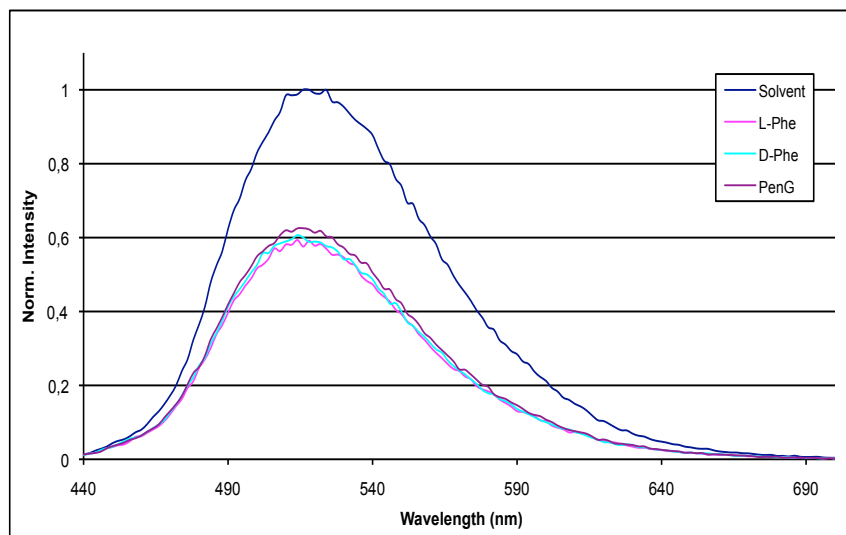


Figure 10.9: Normalised fluorescence emission intensity of P_{1Phe} in presence of water upon addition of Z-L-Phenylalanine/PMP, Z-D-Phenylalanine/PMP, Penicillin G potassium salt/PMP plotted against wavelength

1. Swelling test of the bulk polymers

All investigated bulk polymers show fluorescence quenching only in water. In order to gain information whether the quenching is due to a swelling phenomenon the swelling of the polymers was evaluated in five different solvents (ACN, ACN:H₂O (10:90), ACN:H₂O (50:50), ACN:TEA (99:1) and water).

Table 10.15: Swelling ratios of the bulk polymers in different solvents

	Swelling ratio P _{1N}	Swelling ratio P _{1Glu}	Swelling ratio P _{1Phe}	Swelling ratio P _{1PenG}
ACN	1.25	2.00	1.50	2.00
ACN:H₂O (10:90)	2.14	1.70	2.00	1.60
ACN:H₂O (50:50)	2.17	2.30	1.89	2.5
ACN:TEA (99:1)	1.30	1.30	1.60	1.70
Water	1.57	1.60	1.67	1.80

The swelling ratios displayed in **table 10.14** confirm that the fluorescence quenching in water cannot be only due to massive swelling.

Conclusion of the spectroscopic analysis of the bulk polymers

The bulk polymers with a 99 % cross-linking level employing monomer **1** as functional monomer and EDMA as cross-linker were spectroscopically evaluated regarding their fluorescence emission properties in varying solvents. The response towards their template, basic conditions and cross-analytes was investigated.

The polymers show no change in fluorescence emission intensity in organic solvents. Nevertheless, the accessibility of the dye-monomer **1** was confirmed by solvatochromic tests employing solvents of different polarity. In water a remarkable quenching can be observed upon addition of the analyte and PMP. No quenching was observed when only PMP was

added. It can thus be concluded that the quenching of the fluorescence emission intensity is not due to mere deprotonation of the urea-based monomer. In order to exclude swelling phenomena as a reason for the fluorescence quenching in water swelling tests were performed.

Upon addition of cross-analytes the same degree of quenching was observed as for the addition of the template. In this experiment, no selectivity can be observed even when the HPLC analysis proofed that the polymers were successfully imprinted.

Comparison of the results from the chromatographic analysis and the spectroscopic evaluation clearly show that a polymer aiming at separation applications has to be designed differently than a polymer suitable for sensing purposes. The fact that the sensing abilities of the free monomer in solution were not preserved in the bulk polymers can be a result of the changed microenvironment that the monomer encounters upon polymerisation. Due to the high dye content in the bulks they might also suffer from self-quenching phenomena.

11. Polymers with increasing cross-linking level

The intention of these measurements was to evaluate, to what extent the micro-environment of the monomer created by the polymerisation influences the chromogenic and fluorogenic response of the monomer to the template. The polymerisation strongly alters the micro-environment of the monomer; depending on the employed co-monomer and cross-linker and the cross-linking level the polarity in the polymer can be significantly different than for the free monomer in solution. It is assumed that the polymer backbone can built up a shielding effect for the monomer and prevent its interaction with solvents of higher polarity and the guest molecules. In order to investigate this, polymers with increasing cross-linking level were prepared and subsequently evaluated by a fluorescence titration employing the model template TBA-benzoate as guest-molecule.

Evaluated polymers

Polymers with increasing cross-linking level employing monomer **1** as functional monomer in two different loadings, Methylenemethacrylate (MMA) as co-monomer and EDMA as cross-linker were prepared and evaluated spectroscopically.

11.1. High load polymers

Polymers with a dye-load of 0.5 mmol were according to the ratios displayed in **Table 11.1**. This load is equal to the one employed in the synthesis of the bulk polymers.

Table 11.1: Polymer composition

	CL-Level [%]	n _{Urea} [mmol]	n _{MMA} [mmol]	n _{EDMA} [mmol]
Polymer 1	0	0.5	20	0
Polymer 2	8	0.5	18	2
Polymer 3	30	0.5	14	6
Polymer 4	50	0.5	10	10

	CL-Level [%]	n _{Urea} [mmol]	n _{MMA} [mmol]	n _{EDMA} [mmol]
Polymer 5	81	0.5	6	14
Polymer 6	99	0.5	0	20

11.1.1. Evaluation

11.1.1.1. Response towards TBA Benzoat

For better comparability with the monomer behaviour the measurements were performed in DMSO. 200 μL of the solutions were transferred to a 96 well plate. Subsequently, emission scans were performed in absence respectively presence of increasing concentration of guest molecule. **Table 11.2** displays the resulting ratios.

Table 11.2: Monomer to Template ratios

	Ratio Monomer/Template
Measurement 1	1: 0
Measurement 2	1: 0.1
Measurement 3	1: 0.3
Measurement 4	1: 0.6
Measurement 5	1: 1
Measurement 6	1: 10

Furthermore, the changes in colour were monitored.

The following diagrams display the fluorescence emission intensity obtained upon these additions. on the different polymers and the corresponding colour change.

Polymer 1:

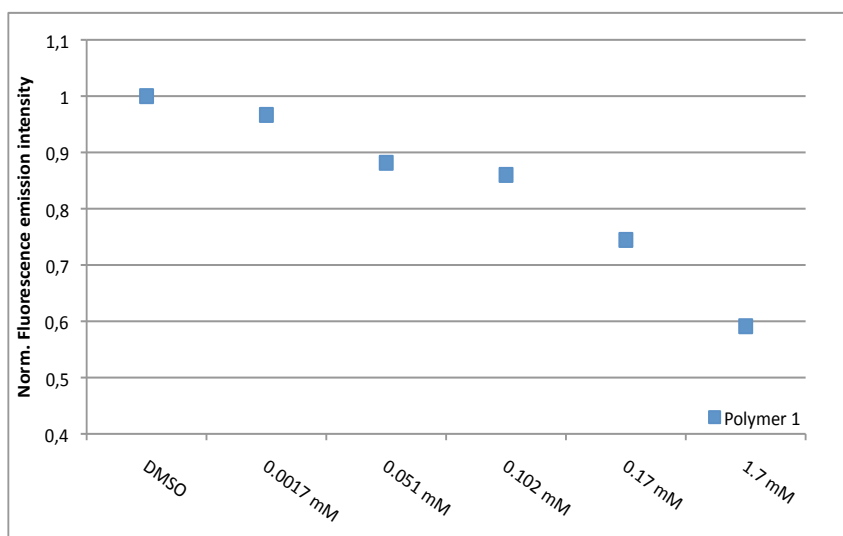
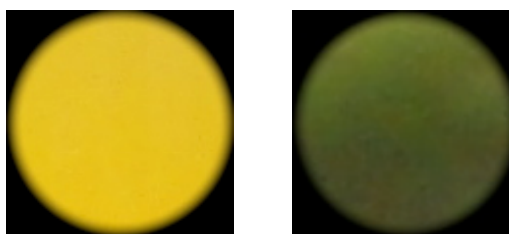


Figure 11.1: Normalised and background corrected fluorescence emission intensity of Polymer 1 upon increasing concentration of TBA Benzoat

In agreement with the behaviour with the free monomer **1** in solution, the fluorescence emission intensity of polymer 1 (cross-linking level 0 %) quenches upon addition of increasing concentration of TBA Benzoat to 60 %.

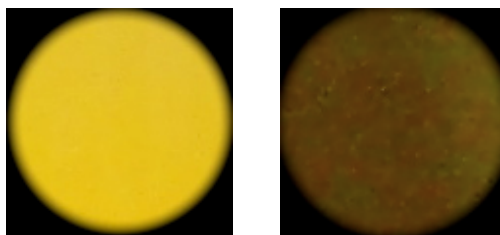
Also the colour-change visible to naked eye corresponds to the one observed for the free monomer in absence of template and in presence of about 1 eq TBA Benzoat.



Picture 11.1: Colour of polymer 1 in absence and in presence of 10 eq of TBA Benzoat

The change of colour from yellow to green indicates at least partial deprotonation of the integrated dye-monomer **1**.

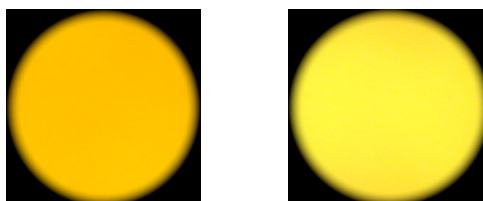
Polymer 2 (cross-linking level 9 %) shows fluorescence quenching to 78 % only for high concentration of TBA Benzoat.



Picture 11.2: Colour of polymer 2 in absence and in presence of 10 eq of TBA Benzoat

Also in case of polymer two the colour of the polymer in absence of guest is yellow. In presence of 10 eq of guest the colour turns into a brown-green, hinting at deprotonation of monomer **1**.

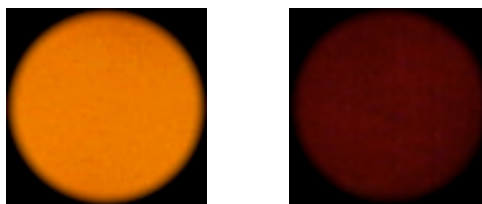
Polymer 3 (cross-linking level 30 %) shows enhanced fluorescence emission for low concentration of TBA Benzoat. For the highest concentration a slight quenching of 10 % can be observed.



Picture 11.3: Colour of polymer 3 in absence and in presence of 10 eq TBA Benzoat.

No colour change can be observed for polymer 3 in presence of TBA Benzoat. This fact together with the weak quenching observed in presence of the oxyanionic guest suggests that the microenvironment of the dye-monomer either stabilises the protonated form of **1** reduces the accessibility.

Polymer 4 (cross-linking level 49 %) shows a quenching of fluorescence emission intensity to 85 % upon addition of increasing concentration of guest.

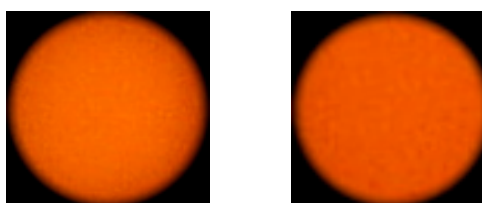


Picture 11.4: Colour of polymer 4 in absence and in presence of increasing concentration of guest

Polymer 4 is reddish-orange in absence of guest. In presence of the guest the colour darkens significantly, hinting at deprotonation taking place in the polymer. This behaviour is inconsistent with the assumption based on the results of polymer 3 and the observations made for polymer 5 and 6 indicating, that this cross-linking level hinders the homogeneous integration of monomer **1**.

Polymer 5 (CL 69 %) shows fluorescence quenching to 55 % upon addition of increasing concentration of TBA Benzoat. Only a slight darkening of the polymer colour could be observed upon addition of the guest molecule. It is thus concluded that the fluorescence quenching is mainly due to hydrogen-bonding interaction between TBA Benzoat and monomer **1**.

The fluorescence emission intensity of **polymer 6** (CL 98 %) does not change upon addition of TBA Benzoat. This observation is in agreement with the results obtained from the spectroscopical investigation of the bulk polymers.



Picture 11.5: Colour of polymer 6 in absence and in presence of increasing concentration of guest

The polymer shows no effect in colour upon addition of increasing concentration of guest.

11.1.1.2. Solvatochromism

The solvatochromism of the polymers with increasing cross-linking level was investigated in order to gain information about how the network composition influences the response of the dye-monomer **1**.

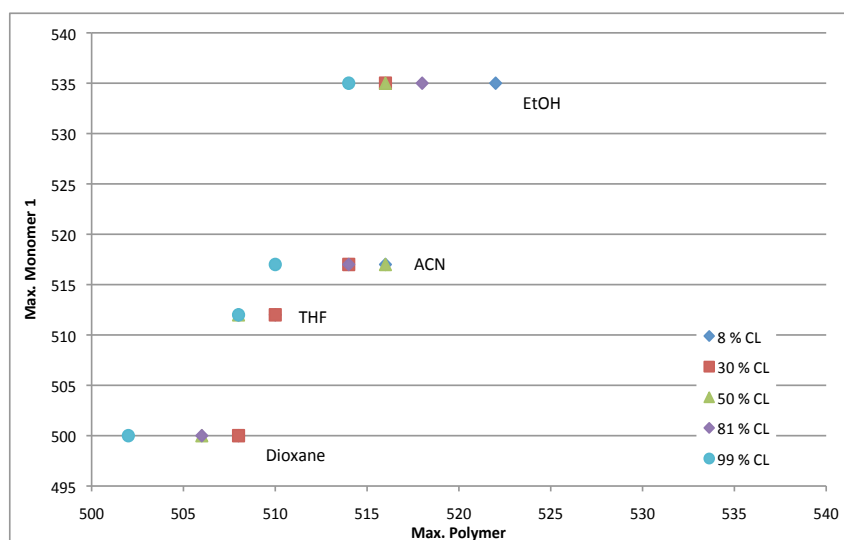


Figure 11.2: Solvatochromic behaviour of polymers of increasing cross-linking level

The obtained results of the evaluation of the solvatochromic behaviour of the polymers with increasing cross-linking level agree with the expectations. The polymer with the lowest cross-linking level (8 %) shows the strongest bathochromic shift with increasing polarity of the media. Furthermore, the position of the maximum emission wavelength is correlated to the cross-linking level of the polymer. The higher the cross-linking level the more red-shifted is the position of the maximum emission wavelength, indicating a lower polarity of the micro-environment.

Conclusion

Polymers employing monomer **1** as signalling unit, MMA as co-monomer to adjust the cross-linking level and EDMA as cross-linker were prepared with different cross-linking levels and evaluated spectroscopically. The response towards an oxyanionic guest was investigated in presence of increasing concentration of TBA Benzoate. All polymers apart from polymer 6 (98 % cross-linking level) showed fluorescence quenching in presence of (high concentration) of TBA Benzoate. The strongest fluorescence quenching was observed for polymer 1 (0 % CL)

and polymer 5 (69 % CL). The colour changes observed for the polymers without cross-linker and with low cross-linking level indicates that at least partial deprotonation of monomer **1** takes place in these polymers. It is assumed that the altered microenvironment in the polymers with higher cross-linking level (> 30 %) stabilises the protonated form of monomer **1**. This result is supported by the evaluation of the solvatochromism. Polymers with a very low cross-linking level and a high one seem to guarantee the best accessibility of monomer **1** for polar substances, whereas the very high cross-linking level of 99 % seems to prevent the interaction.

11.2. Low load polymers

The intention of these measurements was to investigate, if the amount of monomer **1** built into the polymer influences the chromogenic and fluorogenic response of the monomer to the template. Thus, another series of polymers with increasing cross-linking level were prepared with a 5-fold reduced monomer load. The polymers were subsequently evaluated by a fluorescence titration employing the model template TBA Benzoat as guest-molecule.

Table 11.3: NIP compositions with increasing cross-linking level

	CL-Level [%]	n_{Urea} [mmol]	n_{MMA} [mmol]	n_{EDMA} [mmol]
Polymer N1	0	0.1	20	0
Polymer N2	8	0.1	18.3	1.7
Polymer N3	11	0.1	17.7	2.3
Polymer N4	30	0.1	14	6
Polymer N5	50	0.1	10	10
Polymer N6	81	0.1	6	14
Polymer N7	99	0.1	0	20

For comparison polymers imprinted on the model template TBA-Benzoate were prepared according to the ratios in **table 11.3** and **table 11.4** and evaluated spectroscopically.

Table 11.4: MIP compositions with increasing cross-linking level

	CL-Level [%]	n _{Urea} [mmol]	n _{Benzoat} [mmol]	n _{MMA} [mmol]	n _{EDMA} [mmol]
Polymer M1	20	0.1	0.1	16	4
Polymer M2	45	0.1	0.1	11	9
Polymer M3	56	0.1	0.1	8.7	11.3
Polymer M4	81	0.1	0.1	6	14

11.2.1. Evaluation

11.2.1.1. Response towards TBA Benzoate

The respective amount of polymer was weighted into a 96 well plate. Subsequently, emission scans were performed in presence of 200 μ L of DMSO and increasing concentration of guest-molecule TBA-Benzoate.

It was observed that in all cases the polymers are rather non-responsive to the presence of TBA Benzoat. All polymers show fluorescence quenching of about 5 % upon addition of the guest molecule and no colour change visible to naked-eye could be observed. This indicates that the degree on non-specific interaction is low with the reduced dye-load and that no deprotonation is induced by the presence of the oxyanionic guest.

Also in case of the MIPs no significant change in fluorescence emission could be observed upon addition of TBA Benzoat.

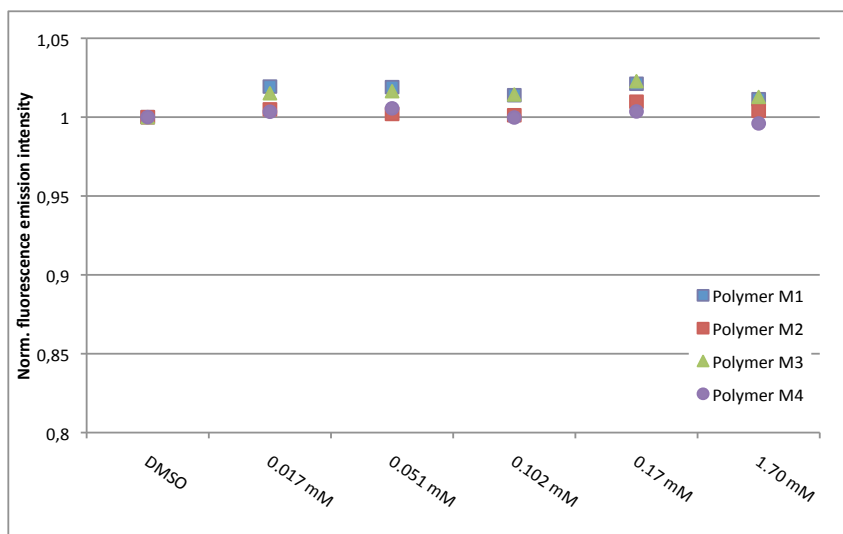
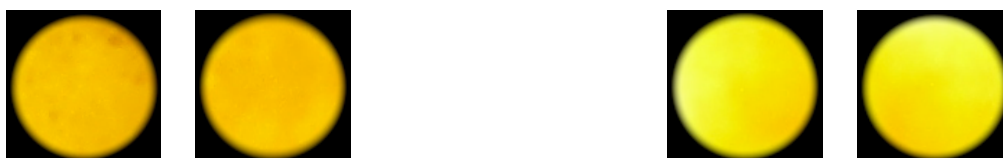


Figure 11.3: Fluorescence emission upon addition of increasing concentration of guest on M1, M2, M3 and M4

Furthermore, no colour-changes could be observed.



Picture 11.6: Colour in omission and upon addition of guest on left: M1, right: M2



Picture 11.7: Colour in omission and upon addition of guest on left: M3, right: M4

11.2.1.2. Solvatochromism

The solvatochromic behaviour of polymers with increasing cross-linking level was evaluated in solvents of different polarity in order to confirm the accessibility of monomer **1** in the polymers.

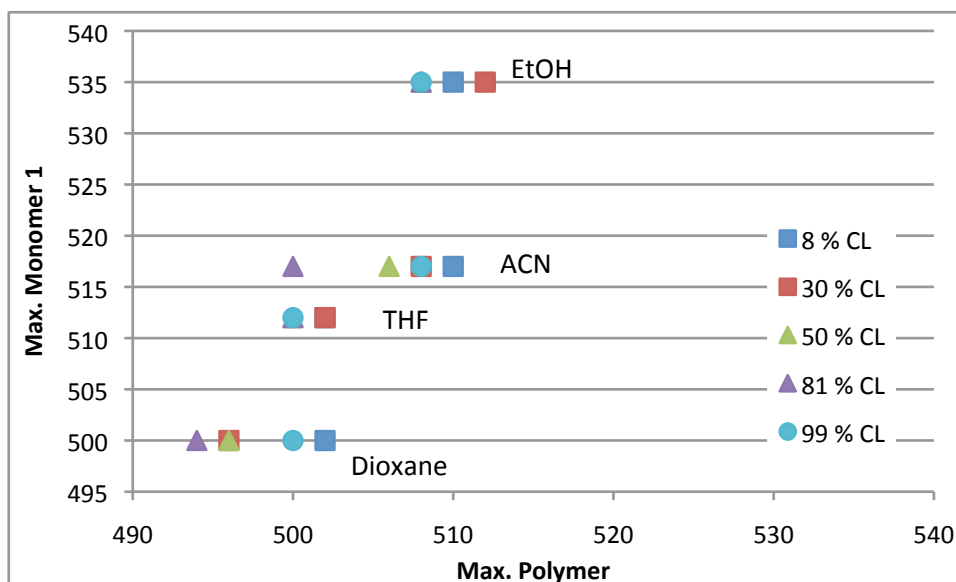


Figure 11.4: Solvatochromic behaviour of polymers of increasing cross-linking level (NIPs)

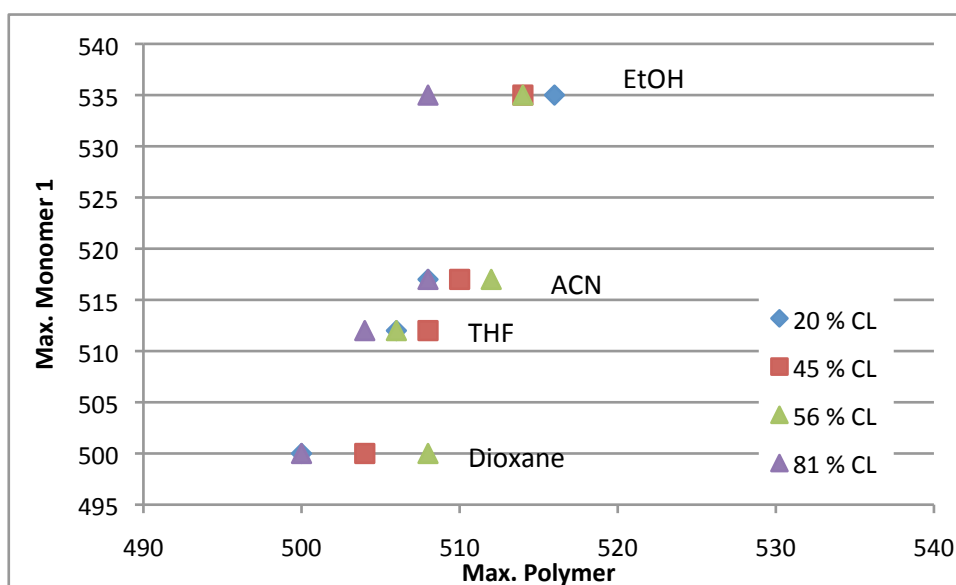


Figure 11.5: Solvatochromic behaviour of polymers of increasing cross-linking level (MIPs)

As in the case of the high-load polymers, the solvatochromic effect is more pronounced on the polymers with lower cross-linking level. The results from the solvatochromic tests confirm the assumption that the morphology of NIPs and MIPs is not the identical.

Compared to the NIPs the positions of the maximum emission wavelength are red-shifted for the MIPs indicating a better accessibility of the dye-monomer **1**.

Conclusion

Polymers employing monomer **1** as signalling unit, MMA as co-monomer to adjust the cross-linking level and EDMA as cross-linker were prepared with different cross-linking levels and different dye-monomer loads and evaluated spectroscopically.

The response towards an oxyanionic guest was investigated in presence of increasing concentration of TBA Benzoat. All polymers employing the high dye-monomer load apart from polymer 6 (98 % cross-linking level) showed fluorescence quenching in presence of (high concentration) of TBA Benzoat. The strongest fluorescence quenching was observed for polymer 1 (0 % CL) and polymer 5 (69 % CL). This result is supported by the evaluation of the solvatochromism. Polymers with a very low cross-linking level and a high one seem to guarantee the best accessibility of monomer **1** for polar substances, whereas the very high cross-linking level of 99 % seems to prevent the interaction. The colour changes observed for the polymers without cross-linker and with low cross-linking level indicates that at least partial deprotonation of monomer **1** takes place in these polymers. It is assumed that the altered microenvironment in the polymers with higher cross-linking level (> 30 %) stabilises the protonated form of monomer **1**.

The polymers in the low-load study are rather non-responsive regarding fluorescence quenching and colour-change visible to naked-eye towards TBA Benzoat. This might be due to the fact that in the high-load polymers five times more dye-monomer contributes to the fluorescence emission intensity.

12. Molecularly imprinted polymers in thin-film format

Optical sensing applications require transparent, homogeneous polymer materials. For this reason, thin - layer polymer-film systems were developed in order to allow straightforward anion sensing.

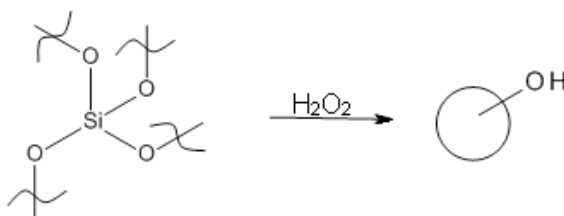
The spectroscopic properties of the incorporated monomer **1** allowed the usage of inexpensive, common cover-glass coverslips instead of quartz glass since the monomer absorbs in a region where glass is not interfering.

12.1. Films via RAFT polymerisation technique

The first attempts to form thin-layer molecularly imprinted polymers on glass via grafting-from were performed applying the RAFT technique. As explained in detail in **Chapter 3** this technique enables the formation of highly ordered systems of homogeneous polymers with low polydispersity.

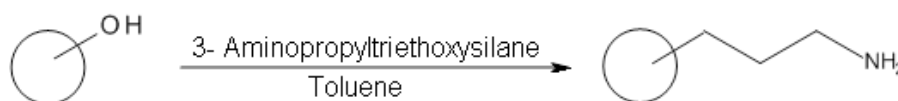
The films were obtained following the approach shown below:

1. Activation of the glass surface



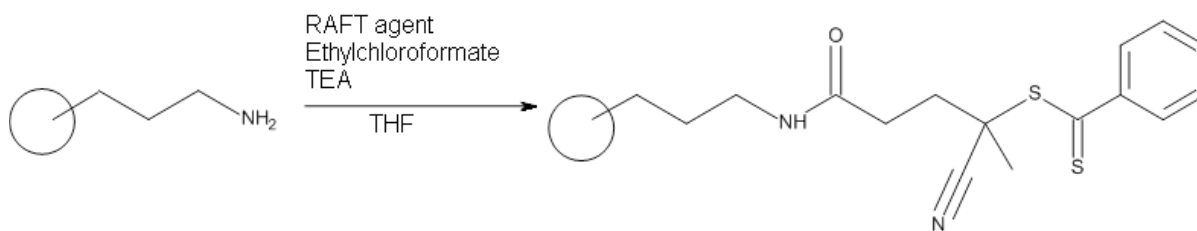
In a first step the surface of the glass slides was activated by treatment with H_2O_2 .

2. Amino-functionalisation with 3- Aminopropyl-triethoxysilane



In the second step the amino-linker 3-aminopropyl-triethoxysilane was introduced.

3. Immobilisation of the RAFT agent 4-Cyano-4-(phenylcarbonothioylthio)pentanoic acid



The RAFT agent 4-Cyano-4-(phenylcarbonothioylthio)pentanoic acid was immobilised on the glass surface by coupling it to the amino - linker via nucleophilic substitution.

12.1.1. Polymerisation of thin-layer films

For the formation of thin-layer polymer films on the glass-surface two different approaches were tested in order to establish a reliable system to prepare stable, homogeneous films.

Drop method

In this approach a small amount of the pre-polymerisation mixture was dropped onto the RAFT modified glass cover-slips and subsequently covered by unmodified glass cover-slips. The polymerisation was then initiated thermally in an inert atmosphere to form polymer-films growing from the modified glass cover-slip.

Dip method

In this approach the glass slides were kept completely covered in the pre-polymerisation mixture during the whole reaction time. It was assumed, that the polymerisation under these conditions leads to increased homogeneity of the formed films, since the cover-slip is well accessible to the monomer and no evaporation of the solvent may occur. Obvious drawback of this method is the risk of macrogelation. Macrogelation would entrap the cover-slip in the polymer matrix counteracting with the organised polymerisation obtained by using the RAFT method. Thus, four different methods were tested in order to avoid macrogelation:

- Dilution of the system by increasing the amount of solvent
- Reduction of the amount of added initiator
- Addition of soluble RAFT agent in 1/1 ratio with respect to the initiator
- Quench polymerisation reaction at low conversion

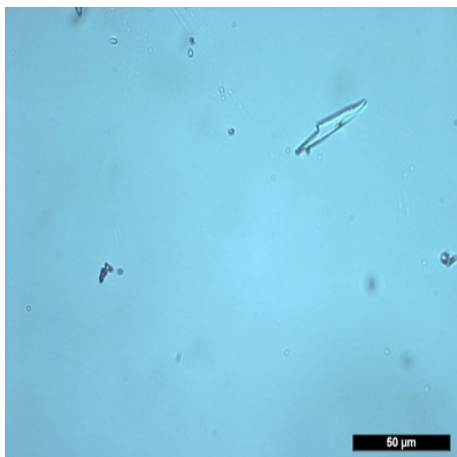
The pre-polymerisation mixture follows the recipe displayed in **Table 12.1**.

Table 12.1: Recipes for thin-film polymers

	Z-L-Phe [mmol]	PMP [mmol]	ABDV/RAFT [mg]	Monomer 1 [mmol]	MMA [mmol]	EDMA [mmol]
Dilution 1x						
NIP I*	/	/	8/0	0.022	4.663	20
MIP I*	0.022	0.022	8/0	0.022	4.663	20
NIP II*	/	/	8/8	0.022	4.663	20
MIP II*	0.022	0.022	8/8	0.022	4.663	20
NIP III**	/	/	0.8/0	0.022	4.663	20
MIP III**	0.022	0.022	0.8/0	0.022	4.663	20
NIP 30 I**	/	/	8/0	0.022	4.663	20
MIP 30 I**	0.022	0.022	8/0	0.022	4.663	20
Dilution 2x						
NIP IV*	/	/	8/0	0.022	4.663	20
MIP IV*	0.022	0.022	8/0	0.022	4.663	20
NIP V*	/	/	8/8	0.022	4.663	20
MIP V*	0.022	0.022	8/8	0.022	4.663	20
NIP VI**	/	/	0.8/0	0.022	4.663	20
MIP VI**	0.022	0.022	0.8/0	0.022	4.663	20
NIP 30 II**	/	/	8/0	0.022	4.663	20
MIP 30 II**	0.022	0.022	8/0	0.022	4.663	20

Evaluation of the success of the glass-surface modification

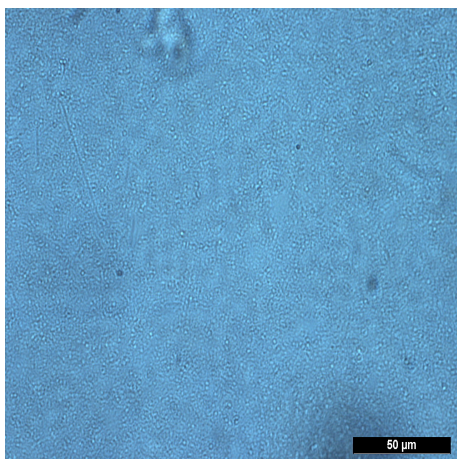
The success of the glass-surface modification was evaluated by monitoring each step by microscopy. The following pictures display images of the glass slides after each modification step.



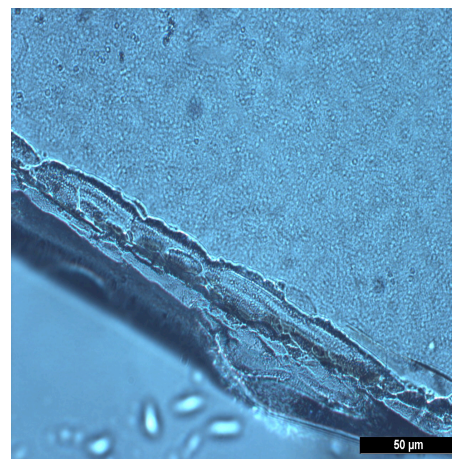
Picture 12.1: Unmodified glass cover-slip



Picture 12.2: Activated glass cover-slip



Picture 12.3: Amino- funct. glass cover-slip



Picture 12.4: Cover-slip with immobilised RAFT agent

The pictures show clearly that the glass surface was modified. **Picture 12.1** shows the unmodified surface of the cover-slip. The texture of the surface is smooth. **Picture 12.2** shows the activated surface after treatment with hydrogen-peroxide. The roughness of the surface is increased to a degree visible to naked eye. In **picture 12.3** the cover-slip with amino-linker is displayed. **Picture 12.4** shows the final cover-slip with the immobilised RAFT agent. The down-left corner shows the activated cover-slip whereas the rest of the slip was modified with the RAFT agent. This comparison proves that the surface of the cover-slip was successfully modified.

Microscopic evaluation of the films prepared by drop method

Polymer films were grown on the glass surface according to the ratios displayed in **table 12.2** in different solvents (ACN; ACN: Toluene (50:50, v/v), CHCl_3 and DMF) to find the most

suitable solvent in terms of film formation. The choice of the appropriate solvent is a challenging task in the case of film-polymerisation.

The solvent does not only have to solubilise the all reagents, it also has to allow stable formation of the pre-polymerisation complex. Additionally, the solvent may not evaporate during film formation. Thus, the volatility needs to be relatively low.

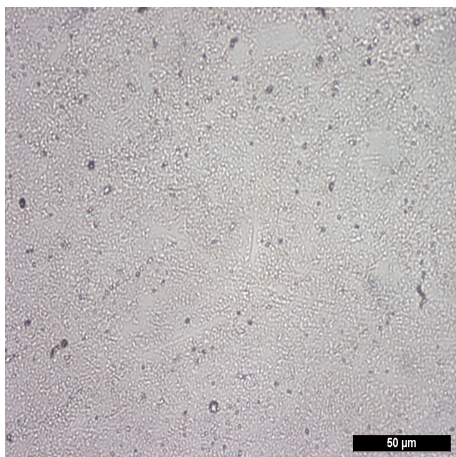
Table 12.2: Polymer composition of drop method films

	Z-L-Glu [mmol]	PMP [mmol]	n_{Urea} [mmol]	n_{MMA} [mmol]	n_{EDMA} [mmol]
NIP	-	-	0.022	4.663	20
MIP	0.011	0.022	0.022	4.663	20

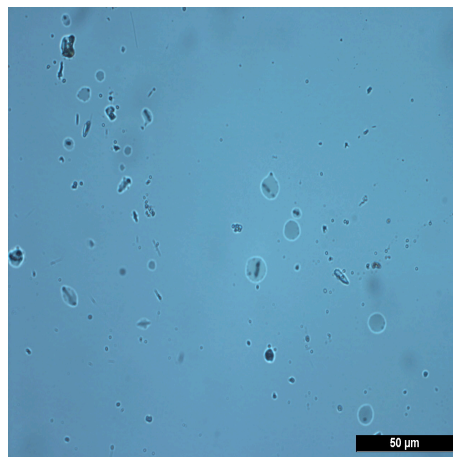
The ratios displayed in **Table 12.2** result in a cross-linking level of 81 %. This cross-linking level proved to yield good imprinting factors in HPLC analysis (see chapter 10) and showed the most significant change in the lifetime of the bulk polymers upon addition of increasing concentration of the guest TBA Benzoat.

The polymerisation was initiated thermally and polymerisation times of 30, 60, 90 and 180 minutes were compared. The desired film formation was obtained for the cover-slips that were kept for 3 h at 45 °C showed the desired film formation.

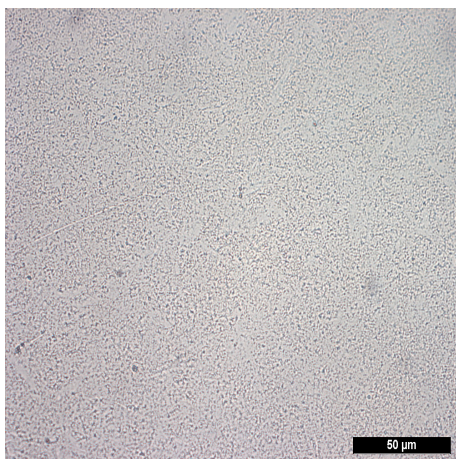
The quality of the formed polymer films in the different solvents ACN, ACN: Toluene (50:50, v/v), DMF and CHCl₃ was evaluated by optical microscopy.



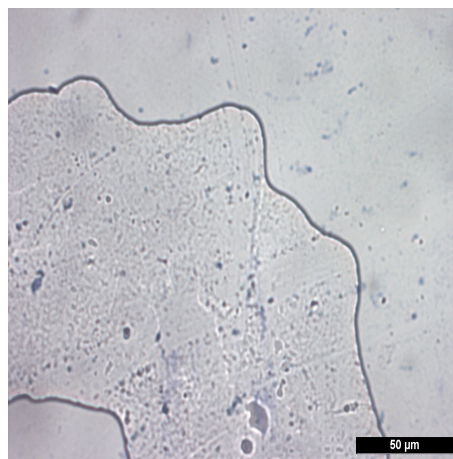
Picture 12.5: *Polymer film (ACN)*



Picture 12.6: *Polymer film (ACN:Toluene, 50:50)*



Picture 12.7: *Polymer film (DMF)*



Picture 12.8: *Polymer film (CHCl₃)*

The optical microscopy images show distinct differences upon employment of the solvents. The usage of DMF resulted in the most homogeneous films. This might be due to two reasons.

- **Solubility:** The employed naphthalimide-based monomer shows the best solubility in DMF. Thus, the pre-polymerisation mixture is most homogeneous in DMF.
- **Volatility:** Of all employed solvents DMF is the least volatile. It enables homogeneous film formation without drying out the pre-polymerisation mixture.

The employment of CHCl_3 resulted in the most inhomogeneous film formation. This is due to the rather poor solubility of the monomer in CHCl_3 and the high volatility of this solvent.

The pictures show, that polymer films can be successfully grown from glass coverslips via grafting-from employing a RAFT agent. The goodness of the obtained polymer films is strongly dependent on the choice of the employed solvent.

12.1.2. Response of drop method films

As a first test of the success of the imprinting process the fluorescence emission of the films was evaluated in water and in presence of the template Z-L-Glutamic acid and Z-L-Glutamic acid and PMP. Water was chosen here for the evaluation, because a remarkable fluorescence quenching could be observed in the evaluation of the bulk polymers upon addition of the template (see chapter 10).

The NIP polymer film employing **ACN** as porogen shows a slight increase in fluorescence emission intensity upon addition. The MIP polymer film employing **ACN** as porogen shows an increase in fluorescence emission intensity upon addition of the template.

The comparison of the normalised, background-corrected fluorescence emission intensity of the NIP film and the MIP film in presence of the template and the template + base shows in both cases an enhancement of the emission intensity. This observation does not correspond to the behaviour of the free monomer in solution.

The MIP film employing **ACN:Toluene (50:50, v/v)** as porogen shows a slight enhancement of fluorescence emission intensity upon addition of the template, whereas the intensity of the NIP is slightly quenched.

The polymer-films prepared in **DMF** show a quenching of fluorescence emission intensity upon addition of the template and the mixture of the template and the base. This behaviour is in agreement with the observations for the free monomer in solution. The quenching is more pronounced on the MIP than on the NIP.

Also in case of the films prepared in **chloroform** the fluorescence emission intensity quenches upon addition of the analytes. The quenching is more pronounced on the NIP than on the MIP. This might be due to the inhomogeneous films formed due to the evaporation of the volatile solvent chloroform.

Conclusion

The results displayed in the diagrams show that the signaling monomer was successfully integrated in the polymer films. In all cases at least the MIP changes the fluorescence emission intensity and in some cases a hypsochromic shift of the emission maximum can be observed. Nevertheless, the results do not correspond to the expected behaviour based on the studies of monomer **1**.

12.1.3. Response of dip method films

The films were prepared according to table **12.1** displayed above. Since this approach turned out to be the more promising one the spectroscopic properties of the obtained polymer films were extensively studied. Being very thin and the amount of built-in signaling monomer very low, the absorption of the films could not be evaluated, because it was below the detection limit of the instrument. The solvatochromism and the response towards Z-L-Phe and Z-D-Phe in ACN was evaluated in all cases.

Solvatochromism

The fluorescence emission intensity of the polymer films was evaluated in dry state and four different solvents. However, since the changes in the absorption are too small to be detected with the 96- well plate reader the change in the position of the maximum emission wavelength was evaluated.

Table 12.3 contains the dielectricity constants for the four solvents as a measure for the polarity.

Table 12.3: Dielectricity constants of the evaluated solvents

	1,4 Dioxane	THF	EtOH	ACN	DMSO
ϵ	2.3	7.50	24.55	37.50	48

The results obtained for the polymer films are compared to the values of the free monomer in solution.

Table 12.4 displays the position of the maximum of the fluorescence emission intensity for NIP IV and MIP IV:

	NIP IV	MIP IV
washed	497	499
1,4 Dioxane	499	495
THF	495	499
EtOH	505	503
ACN	505	501

The numbers displayed in **Table 12.4** show that NIP IV and MIP IV both show minor positive solvatochromism (bathochromic shift with increased solvent polarity).

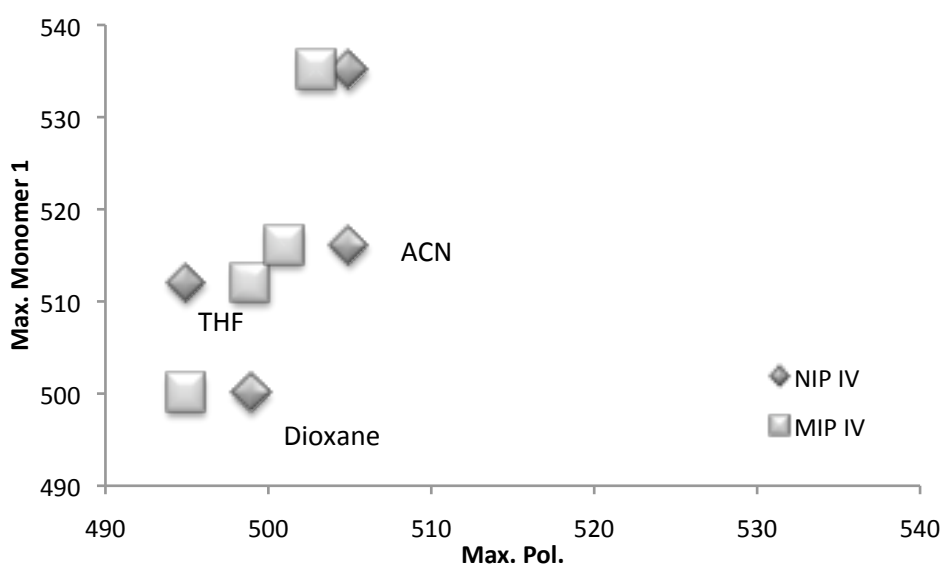


Figure 12.1: Maximum emission wavelength of NIP IV and MIP IV in presence of 1,4 Dioxane, THF, EtOH and ACN plotted against maximum emission wavelength of monomer 1

The positions of the maximum emission wavelength of the polymer films are located at shorter wavelengths than the ones of the monomer and the solvatochromism is less pronounced. This indicates that the polymer microenvironment is shielding the monomer from the polar solvents. It should thus be rather unreactive in rebinding tests.

Table 12.5 displays the position of the maximum of the fluorescence emission intensity for NIP II and MIP II:

Table 12.5: Maximum emission wavelength of NIP II and MIP II in solvents of different polarity

	NIP II	MIP II
washed	491	491
1,4 Dioxane	495	495
THF	495	495
EtOH	495	505
ACN	499	505

The numbers displayed in **Table 12.5** show that NIP II and MIP II both show positive solvatochromism. The effect is more pronounced in the MIP than in the NIP.

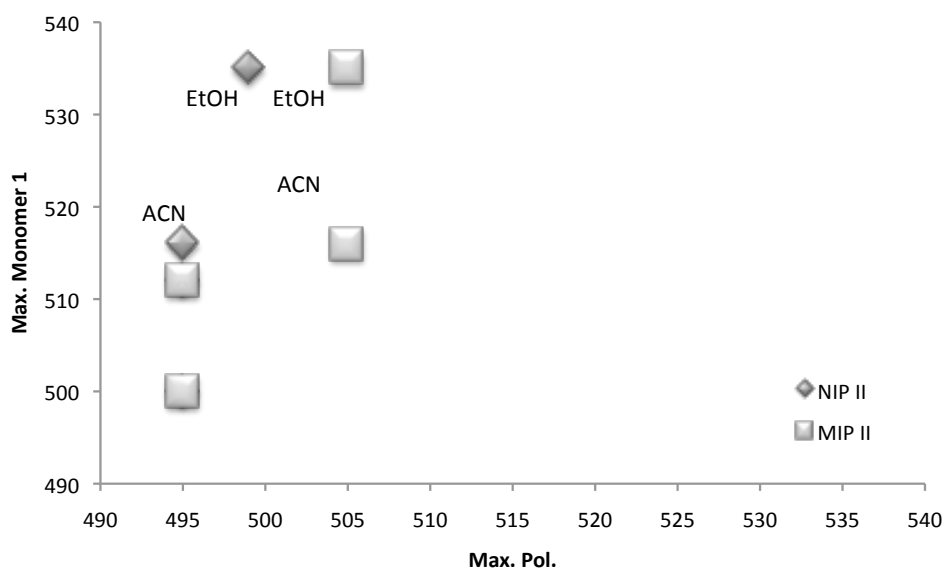


Figure 12.2: Maximum emission wavelength of NIP II and MIP II in presence of 1,4 Dioxane, THF, EtOH and ACN plotted against maximum emission wavelength of monomer 1

Both, NIP and MIP exhibit positive solvatochromism. The effect is stronger on the MIP than on the NIP. This could be due to the more open pore structure of the MIP as a result of the presence of the template during the polymerisation process.

Table 12.6 displays the position of the maximum of the fluorescence emission intensity for NIP V and MIP V:

Table 12.6: Maximum emission wavelength of NIP V and MIP V in solvents of different polarity

	NIP V	MIP V
washed	491	503
1,4 Dioxane	490	503
THF	499	505
EtOH	499	515
ACN	505	509

The numbers displayed in **Table 12.6** show that NIP V and MIP V both show positive solvatochromism. The effect is more pronounced in the MIP than in the NIP. Furthermore, the dilution seems to have an influence on the accessibility of the monomer. NIP and MIP V follow the same recipe as NIP and MIP II, except from double amount of porogen was used in the synthesis.

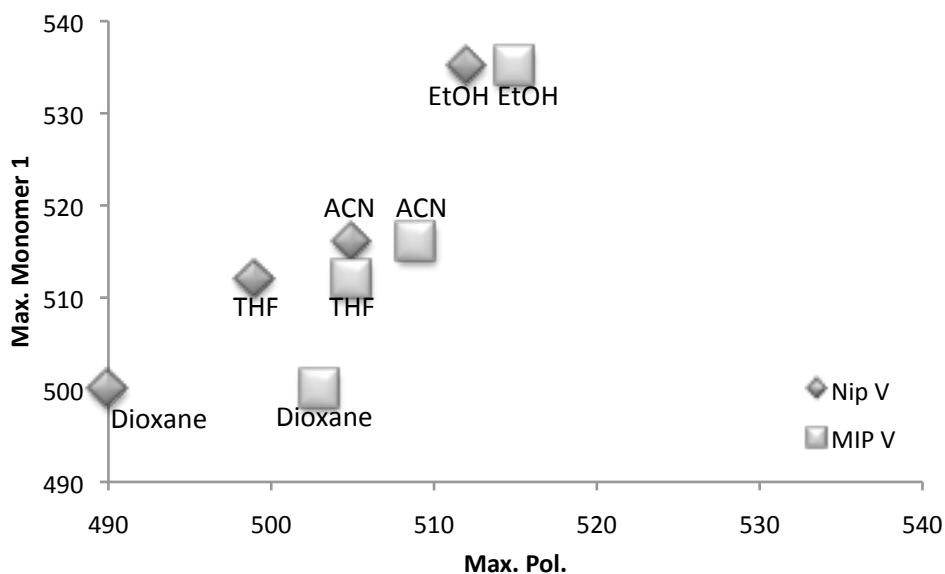


Figure 12.3: Maximum emission wavelength of NIP V and MIP V in presence of 1,4 Dioxane, THF, EtOH and ACN plotted against maximum emission wavelength of monomer 1

This results in a more pronounced bathochromic shift in NIP V and MIP V in comparison to NIP II and MIP II. MIP V follows the trend of the free monomer in solution.

Table 12.7 displays the position of the maximum of the fluorescence emission intensity for NIP VI and MIP VI:

Table 12.7: Maximum emission wavelength of NIP VI and MIP VI in solvents of different polarity

	NIP VI	MIP VI
washed	503	509
1,4 Dioxane	503	509
THF	509	509
EtOH	501	514
ACN	503	513

The numbers displayed in **Table 12.7** show that MIP VI shows positive solvatochromism. For the NIP the maximum emission wavelength is not changing with increasing polarity of the solvent.

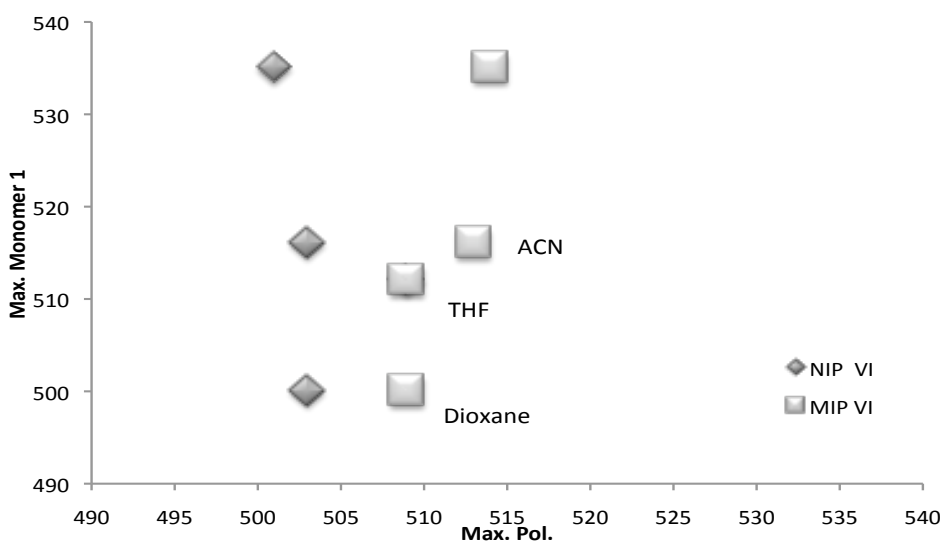


Figure 12.4: Maximum emission wavelength of NIP VI and MIP VI in presence of 1,4 Dioxane, THF, EtOH and ACN plotted against maximum emission wavelength of monomer 1

Table 12.8 displays the position of the maximum of the fluorescence emission intensity for NIP 30I and MIP 30I:

Table 12.8: Maximum emission wavelength of NIP 30I and MIP 30I in solvents of different polarity

	NIP 30I	MIP 30I
washed	515	521
1,4 Dioxane	513	509
THF	515	515
EtOH	525	529
ACN	525	529

The numbers displayed in **Table 12.8** show that NIP 30I and MIP 30I both show positive solvatochromism. The effect is more pronounced in the MIP than in the NIP.

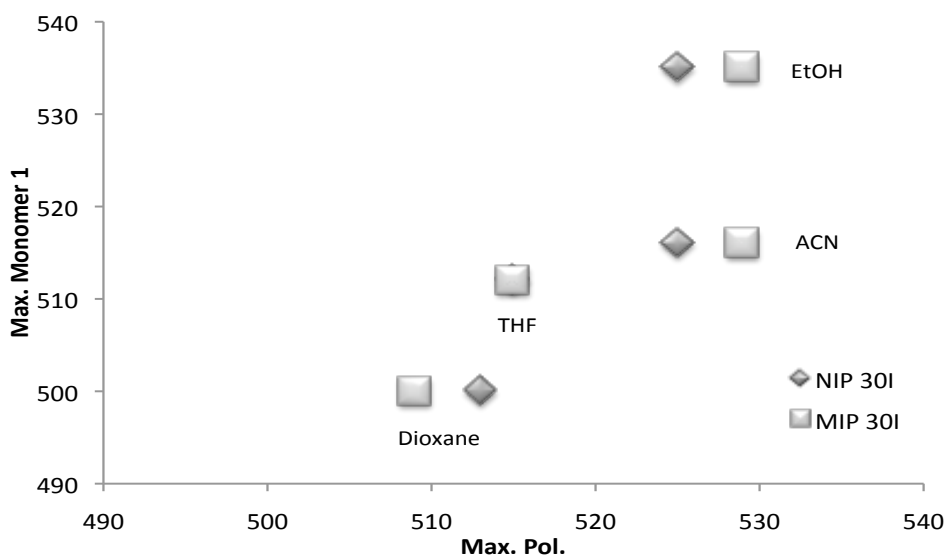


Figure 12.5: Maximum emission wavelength of NIP 30I and MIP 30I in presence of 1,4 Dioxane, THF, EtOH and ACN plotted against maximum emission wavelength of monomer 1

The monomer is more accessible to the polar solvents in the polymers where the polymerisation was quenched after 30 minutes.

Table 12.9 displays the position of the maximum of the fluorescence emission intensity for NIP 30II and MIP 30II:

Table 12.9: Maximum emission wavelength of NIP 30II and MIP 30II in solvents of different polarity

	NIP 30II	MIP 30II
washed	530	511
1,4 Dioxane	505	505
THF	517	513
EtOH	539	513
ACN	525	511

The numbers displayed in Table 10 show that NIP 30II and MIP 30II both show positive solvatochromism, except from in ACN. The effect is more pronounced in the NIP than in the MIP. The NIP follows the trend of the free monomer.

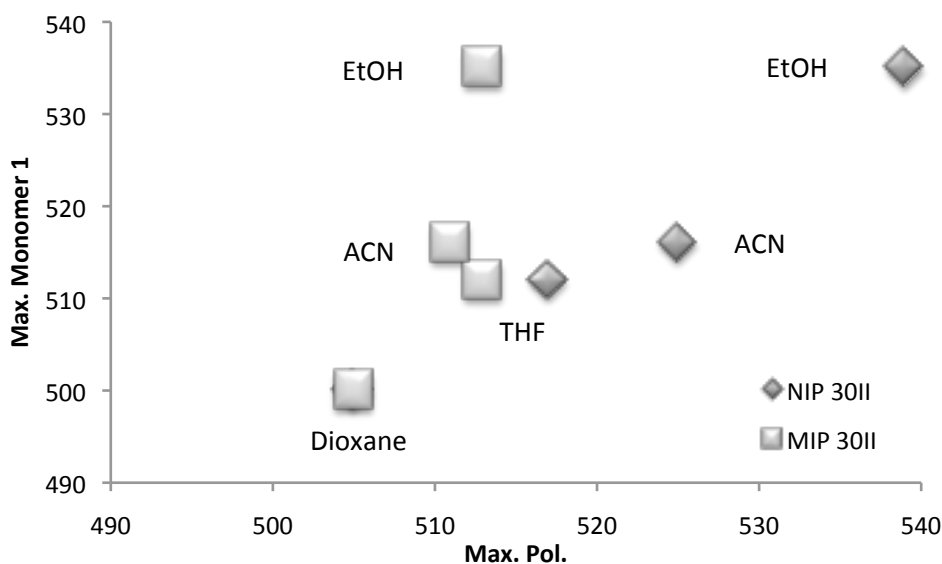


Figure 12.6: Maximum emission wavelength of NIP 30II and MIP 30II in presence of 1,4 Dioxane, THF, EtOH and ACN plotted against maximum emission wavelength of monomer 1

Conclusion

Polymer films composed according to the values presented in **Table 12.1** were synthesised and evaluated spectroscopically.

The obtained results show that all slides exhibit a positive solvatochromism, which is -in most cases- more pronounced in the MIP than in the NIP.

The solvation of the polymer seems to be influenced by the amount of porogen used in the synthesis and by the polymerisation time. Higher dilution of the system during polymerisation leads to a stronger bathochromic shift, which is an indication for better solvation. This observation is in agreement with the expectations, because a higher dilution should lead to a better accessibility of the built-in monomer.

The polymerisation time influences the position of the maximum emission wavelength. In the cases when the polymerisation was quenched after 30 minutes, the maximum emission is obtained at longer wavelengths than in the cases where the polymerisation was

quenched after 2 h. The values obtained after 30 minutes are closer to the ones obtained for the free monomer in solution.

Response of the films towards various analytes

The response of the obtained polymer films towards guest molecules, namely *Z-L-Phe*, *Z-D-Phe* and *Z-L-Glu* was evaluated in ACN. In all cases the measurement error was of 2 %.

Polymer I and **polymer II** show no significant change in fluorescence emission intensity and the position of the maximum emission wavelength upon addition of the analytes *Z-L-Phe*, *Z-D-Phe*, Benzoic acid and *Z-L-Glu*.

Polymer III:

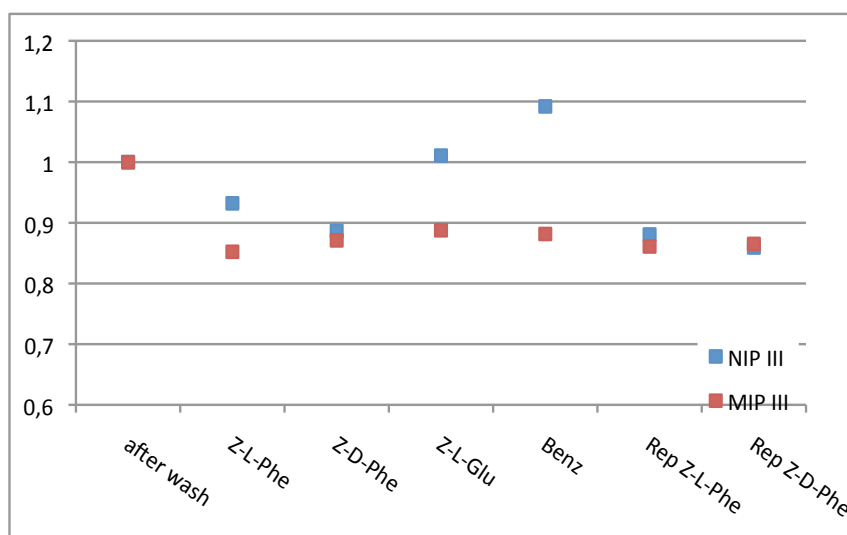


Figure 12.7: Normalised emission intensity of NIP III and MIP III slides recorded after polymerisation, washing and incubation with *Z-L-Phe*, *Z-D-Phe*, Benz and *Z-L-Glu* in dry state

The emission intensity of **NIP III** shows quenching in presence of the two enantiomers of phenylalanine. Upon addition of benzoic acid the fluorescence is enhanced. Glutamic acid induces no change in fluorescence emission intensity.

The fluorescence of **MIP III** is quenched in presence of all tested analytes. The position of the maximum emission wavelength of both polymers is not changing upon addition of the guest molecules.

The reproducibility of the results obtained with the polymers **NIPVI**, **MIPIV** and **NIPV**, **MIPV** is low. This indicates that the films are not stable and lose their integrity upon washing and reuse. Another reason can be the relatively poor accessibility of the signaling monomer in the film due to shielding effects of the polymer backbone, confirmed by the evaluation of the solvatochromism.

The position of the maximum emission wavelength shows no systematic dependence on the presence of guest molecules.

The position of the maximum emission wavelength does not exhibit a shift induced by the presence of the analytes.

Polymer 6:

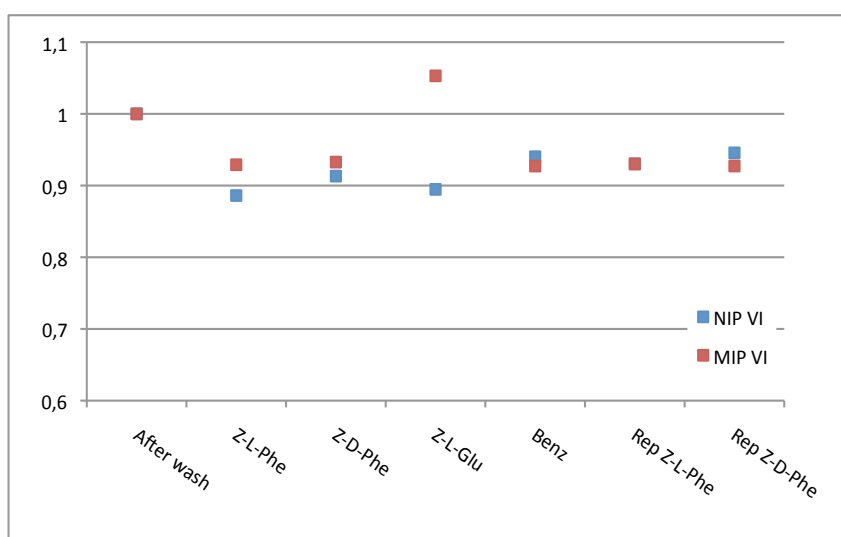


Figure 12.8: Normalised emission intensity of NIPVI and MIPVI slides recorded after polymerisation, washing and incubation with Z-L-Phe, Z-D-Phe, Benz and Z-L-Glu in dry state

The fluorescence emission intensity of both polymer-films quenches upon addition of the analytes. Only in the case of **MIPVI** in presence of glutamic acid the emission is enhanced. The results obtained in the test of the solvatochromic behaviour confirm the accessibility of the monomer to polar solvents and compounds.

Table 12.10: Maximum emission wavelength and intensity of the NIPVI and MIPVI at maximum emission wavelength after incubation with Z-L-Phe, Z-D-Phe, Benz and Z-L-Glu in dry state

	NIP VI	MIP VI

After Wash	503	501
Z-L-Phe	505	494
Z-D-Phe	504	501
Z-L-Glu	503	497
Benz	505	505

Based on the observation that **MIPVI** shows positive solvatochromism and **NIPVI** and the **MIP** show fluorescence quenching upon addition of the template, they were chosen for further evaluation. The polymers were submitted to a titration experiment employing the template *Z-L-Phe* and its *D*-enantiomer in **ACN**. **Figure 12.9** and **Figure 12.10** display the obtained results:

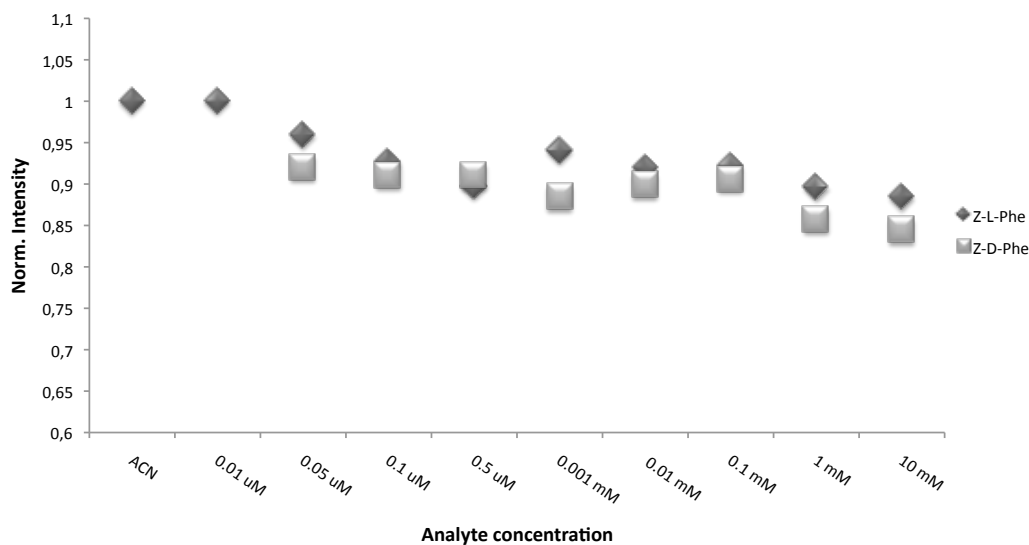


Figure 12.9: Background corrected intensity normalised emission intensity of NIPVI in ACN and increasing concentration of *Z-L-Phe* and *Z-D-Phe*

NIPVI exhibits fluorescence quenching upon addition of increasing concentration of the two enantiomers of phenylalanine.

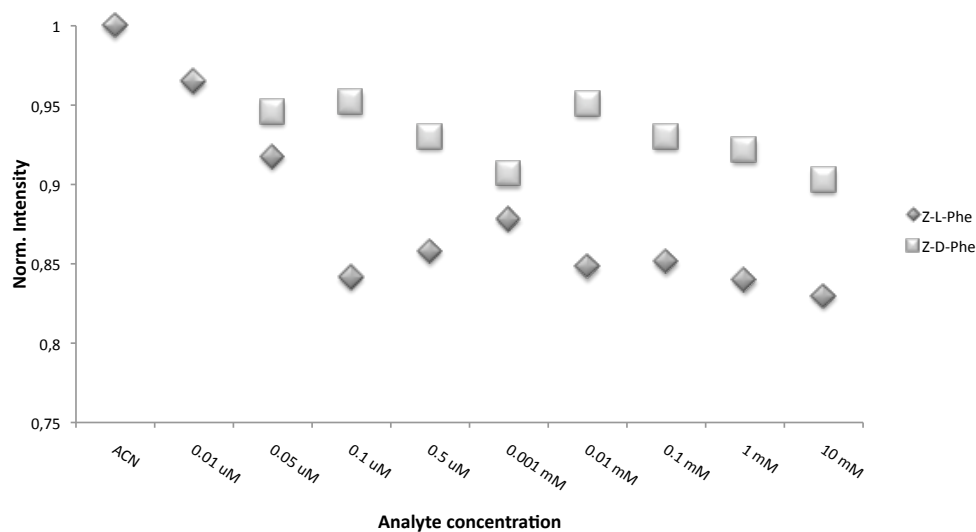


Figure 12.10: Background corrected intensity normalised emission intensity of MIPVI in ACN and increasing concentration of Z-L-Phe and Z-D-Phe

Also **MIPVI** exhibits fluorescence quenching upon addition of increasing concentration of the two enantiomers of phenylalanine. The quenching upon addition of the template *Z-L-Phe* is more pronounced (16 % at highest concentration) than for the *D*-enantiomer (10 %).

Table **12.11** the imprinting factors obtained from the fluorescence titration (IF_F) are listed. Unlike in the case of the imprinting factors calculated for the chromatographic evaluation the result is better the smaller the value is, because the quenching should be more pronounced on the MIP.

$$IF_Q = Q_{MIP}/Q_{NIP} \quad (12.1)$$

Q_{MIP} = Normalised background-corrected fluorescence intensity of MIP

Q_{NIP} = Normalised background-corrected fluorescence intensity of NIP

Table 12.11: Imprinting factors calculated from fluorescence titration of NIPVI and MIPVI in presence of *Z-L-Phe* and *Z-D-Phe*

	Z-L-Phe	Z-D-Phe
0.01 µM	0.964	/
0.05 µM	0.965	1.028
0.1 µM	0.908	1.046

	Z-L-Phe	Z-D-Phe
0.5 μM	0.956	1.022
0.001 mM	0.934	1.026
0.01 mM	0.921	1.056
0.1 mM	0.923	1.026
1 mM	0.937	1.074
10 mM	0.938	1.070

In case of all concentrations the calculated values are smaller for Z-L-Phe than for the D-enantiomer. Even with the difference being rather small the result indicates that the imprinting step was successful.

Furthermore, a quenching factor (QF) was calculated for NIP and MIP. This factor correlates the quenching obtained upon addition of the template with the quenching obtained for the D-enantiomer. **Table 12.12** compiles the calculated values for each concentration:

Table 12.12: Quenching factors calculated from fluorescence titration of NIPVI and MIPVI in presence of Z-L-Phe and Z-D-Phe

	QF NIP	QF MIP
0.05 μM	1.043	1.013
0.1 μM	1.018	0.884
0.5 μM	0.985	0.922
0.001 mM	1.064	0.968
0.01 mM	1.024	0.892
0.1 mM	1.018	0.915
1 mM	1.045	0.911
10 mM	1.048	0.919

The comparison of the quenching factors for NIP and MIP reveals that the NIP is not discriminating between *Z-L-Phe* and *Z-D-Phe* whereas the fluorescence quenching of the MIP is more pronounced in case of the template.

Conclusion:

Polymer films employing monomer **1** as functional monomer were successfully prepared via RAFT polymerisation. The success of the film formation and the integration of the functional monomer was proven by spectroscopical means. For the most promising polymer composition **VI** extensive titration experiments were performed revealing that the imprinting step in the preparation of the MIPs was successful. Furthermore, the results displayed in figure 12.10 and table 12.12 show that the MIP discriminates enantioselectively between its template *Z-L-Phe* and the *D*-enantiomer.

12.2. Films via grafting

In parallel to the RAFT-approach, also thin-film formation without the help of an additional agent was tested. In order to design this approach as rational as possible, the possible pre-polymerisation mixtures and the influence of different solvents were carefully studied with regard to the complex stability and the deprotonation of monomer **1**. The goal was to limit down the amount of trial-and-error and to predict the goodness of a film system with regard to stability and selectivity.

12.2.1. Solution studies of pre-polymerisation mixtures

The outstanding advantage of integrating spectroscopically active functional monomers into polymers is that they allow to follow the complex-formation between template and monomer by spectroscopical means.

If the pure functional monomer in solution absorbs or emits at another wavelength than the complex between functional monomer and the template molecule, conclusions regarding the complex-stability and presence of deprotonated monomer **1** can be drawn from the position of the bands.

For this reason, pre-polymerisation mixtures of different composition were prepared and evaluated regarding their absorption in solvents of different polarity. It is assumed that solvents of low polarity should allow higher complex stability. This also applies to the co-monomer/cross-linker system. The polar system HEMA/EDMA should destabilise the pre-polymerisation complex the most, whereas the low-polar Styrene/DVB system should keep the complex intact.

12.2.1.1. Monomer 1 in pentachloroethane

Pentachloroethane was chosen as solvent based on its high boiling point (BP = 160°C) favourable for film polymerisation. The co-monomer/ cross-linker systems MMA/EDMA and HEMA/EDMA are both well studied and have been successfully employed in MIP synthesis.

The pre-polymerisation mixtures of the following films were evaluated at different temperatures:

Table 12.13: Pre-polymerisation compositions tested in pentachloroethane

Functional Monomer	Template	Co-monomer	Cross-linker
1	TBA-Z-L-Phe	MMA	EDMA
1	TBA-Z-L-Phe	HEMA	EDMA

Figure 12.11 represents the obtained absorption spectra of monomer **1** in pentachloroethane and in presence of co-monomer and cross-linker:

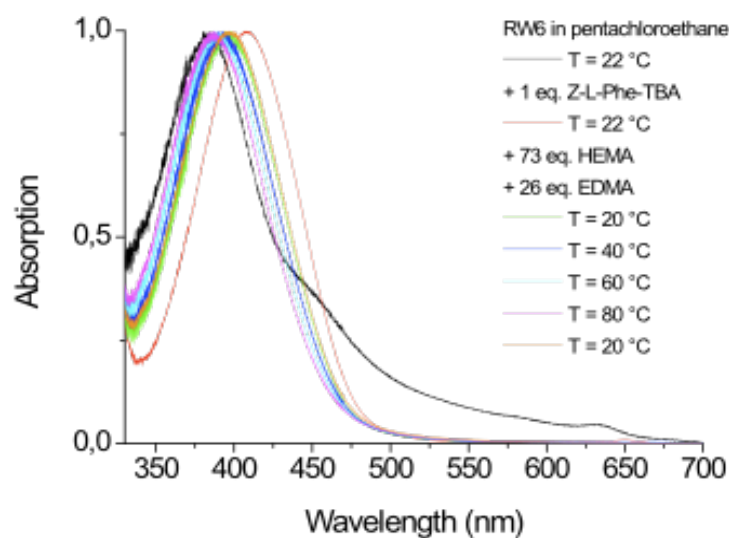


Figure 12.11: Absorption spectra of monomer 1, and the pre-polymerisation mixtures in pentachloroethane at varying temperatures

The functional monomer **1** was dissolved in pentachloroethane. This solution shows an absorption maximum at $\lambda = 383$ nm. Upon addition of TBA-Z-L-Phe the monomer-template complex is formed resulting in an absorption band at $\lambda = 408$ nm. The solution was evaluated at elevated temperatures. From the shift of the absorption maximum towards the wavelength of the free monomer it can be concluded that elevation of the temperature weakens the monomer-template complex and leads to dissociation. However, the dissociation upon temperature increase is reversible.

Furthermore, the complex is significantly weakened (dissociation about 50%) upon addition of the co-monomer HEMA and the cross-linker EDMA. This might be due to the high polarity of these reagents.

According to the tested pre-polymerisation mixture polymer films were prepared in pentachloroethane employing monomer **1** as functional monomer, HEMA as co-monomer and EDMA as cross-linker. In order to gain information regarding the influence of the polymerisation temperature on the performance of the films each set of films was prepared in two different ways:

- 3 h polymerisation at 50 °C
- 4 times 10 s at 110°C and subsequently 1 h at 60 °C

The following diagrams display the normalized fluorescence emission intensity of the obtained films recorded in pure ACN and upon addition of increasing concentration of TBA-Z-L-Phe (excitation wavelength 380 nm; emission wavelength range: 395 – 650 nm).

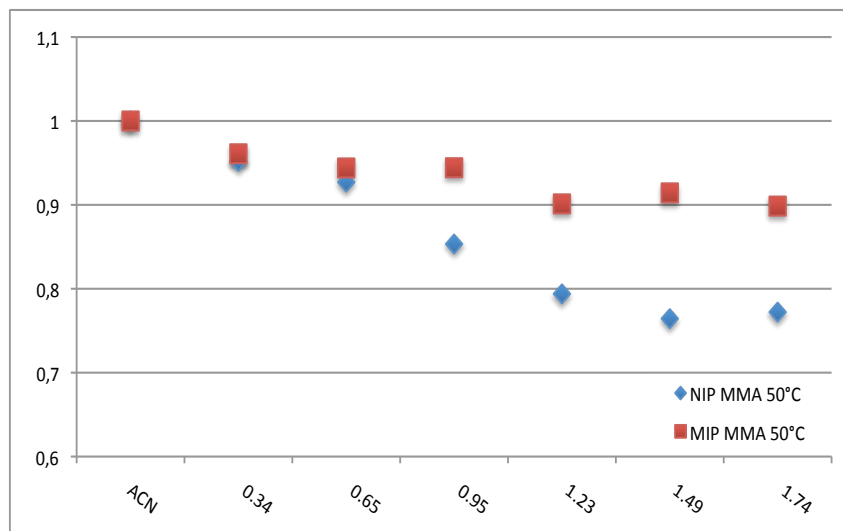


Figure 12.12: Normalised fluorescence emission intensity of NIP and MIP MMA (50°C) upon addition of TBA-Z-L-Phe

For the MMA/EDMA film polymerised at 50°C a slight quenching of the fluorescence emission intensity can be observed. The quenching is more pronounced on the NIP than on the MIP.

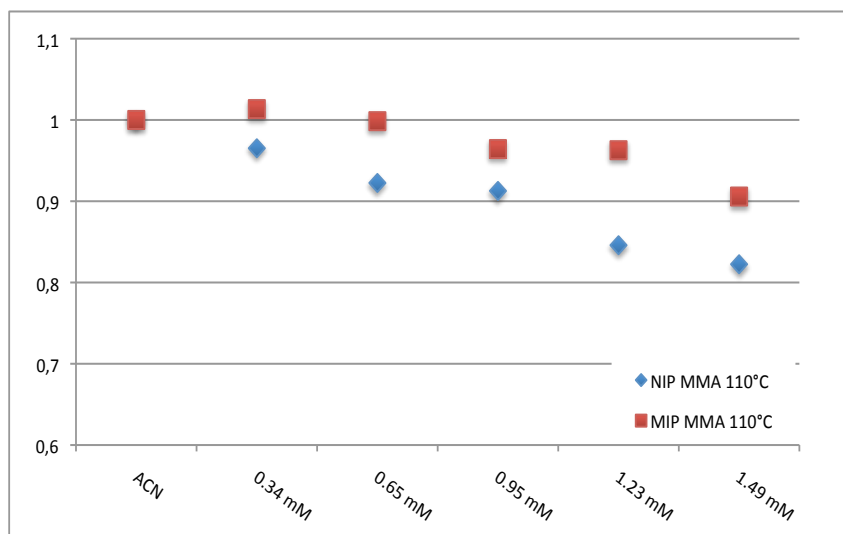


Figure 12.13: Normalised fluorescence emission intensity of NIP and MIP MMA (110°C) upon addition of TBA-Z-L-Phe

In the case of the MMA/EDMA system the polymerisation temperature has no influence on the degree of the fluorescence quenching. Also in this case the quenching is more pronounced on the NIP than on the MIP.

The films prepared from HEMA/EDMA at 50°C show no systematic response of the fluorescence emission intensity upon addition of increasing concentration of the analyte TBA Z-L-Phe.

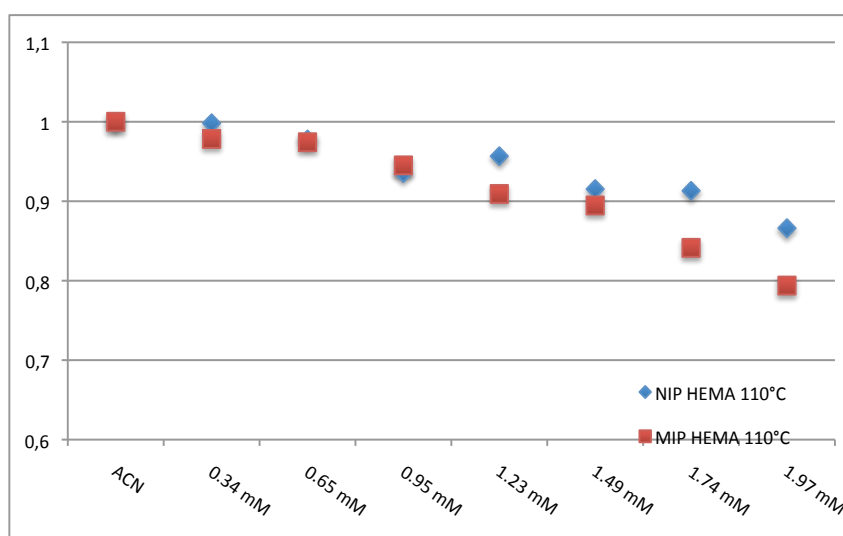


Figure 12.14: Normalised fluorescence emission intensity of NIP and MIP HEMA (110°C) upon addition of TBA-Z-L-Phe

Of all the investigated films only in case of the HEMA/EDMA films prepared at 110°C the quenching on the MIP is more pronounced than on the NIP.

It was evaluated for all films if the change of the fluorescence emission intensity is linked to a change in the excitation spectra. The following diagrams display representatively the excitation spectra of the HEMA/EDMA and the MMA/EDMA films prepared at 50 °C at the start point of the titration in pure ACN, at the middle point and at the end point recorded at three different emission wavelength.

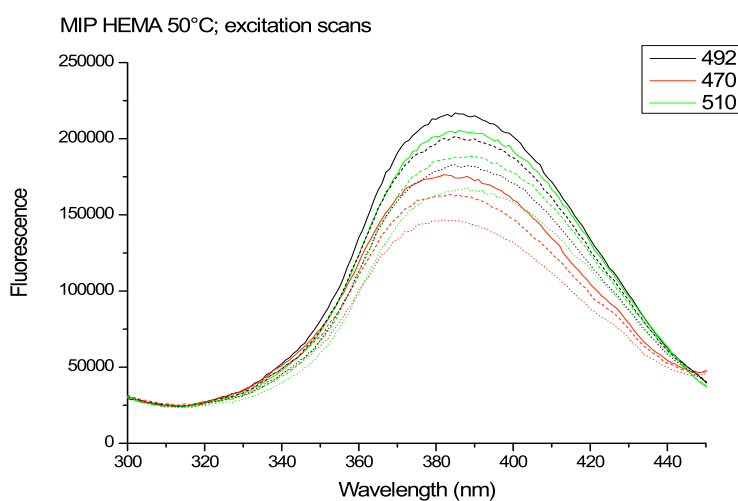


Figure 12.15: Excitation spectra of polymer film MIP HEMA/EDMA 50°C, $\lambda_{em} = 470, 492, 510$ nm; $\lambda_{ex} = 300 - 475$ nm

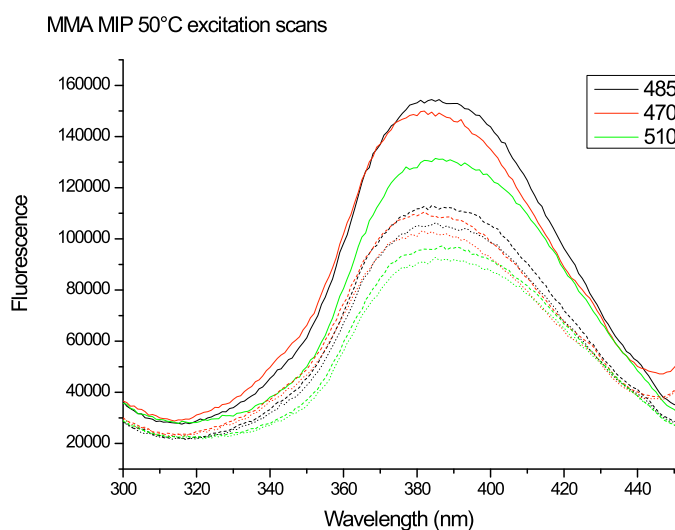


Figure 12.16: Excitation spectra of polymer film MIP MMA/EDMA 50°C, $\lambda_{em} = 470, 485, 510$ nm; $\lambda_{ex} = 300 - 470$ nm

The excitation spectra of all analysed polymer films do not shift during the titration. Thus, the monomer stays intact upon addition of the analyte.

Conclusion:

Polymer films employing monomer **1** as functional monomer, MMA respectively HEMA as co-monomer and EDMA as cross-linker were prepared at 50 °C and at 110°C in order to investigate the influence of the polarity of the environment and the temperature on the performance on molecularly imprinted polymer films.

In all cases no pronounced fluorescence quenching could be observed. The evaluated systems seem to be too polar to allow stable complex formation between the monomer and the template during the whole polymerization process. This might be due to the high polarity of the employed co-monomers, cross-linkers and solvent. The solution study of the pre-polymerisation mixtures at elevated temperatures indicate that elevated temperatures are non-favourable for the complex-stability.

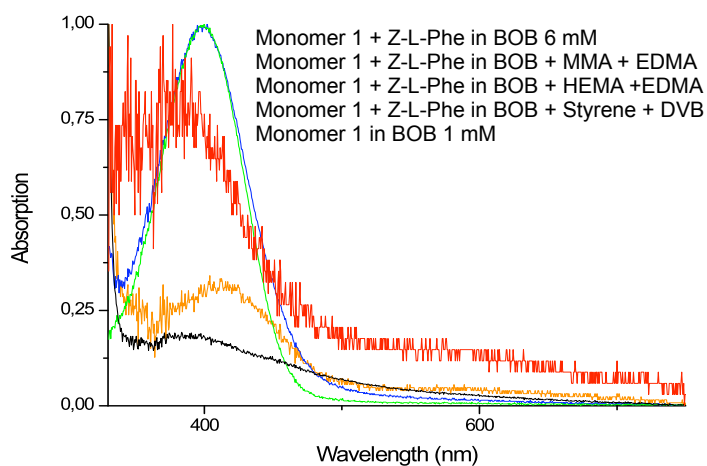
12.1.2. Solvent optimisation

Based on the above mentioned conclusions and the assumption that the polarity of the environment is crucial for successful imprinting toluene and di-n-butylether were chosen as solvents for further evaluation. Both solvents inherit favourable characteristics being less polar than pentachloroethane (E_T^N Pentachlorethane: 0.176, toluene: 0.099, di-n-butylether: 0.071) and of low volatility (BP toluene: 110.6 °C, di-n-butylether: 140.3 °C). Low volatility is an essential requirement for a solvent employed in polymer film synthesis.

The following diagrams display the results obtained for the solution studies of the pre-polymerisation mixtures with systems listed in **Table 12.14** in di-n-butylether and toluene.

Table 12.14: Pre-polymerisation compositions investigated in di-n-butylether and toluene

Functional Monomer	Template	Co-Monomer	Cross-linker
1	TBA-Z-L-Phe	MMA	EDMA
1	TBA-Z-L-Phe	HEMA	EDMA
1	TBA-Z-L-Phe	Styrene	DVB

**Figure 12.17:** Absorption spectra of monomer 1, and the pre-polymerisation mixtures in di-n-butylether

As can be seen from the solution by naked-eye and the pronounced scattering in the absorption spectra the solubility of the monomer in di-n-butylether is very poor. This counts also for the monomer-template complex. Only the addition of the polar co-monomers and crosslinker MMA/EDMA and HEMA/EDMA enhances the solubility. Since the application of polar reagents impedes the idea to keep the system as non-polar as possible the solvent di-n-butylether was not employed in the film synthesis.

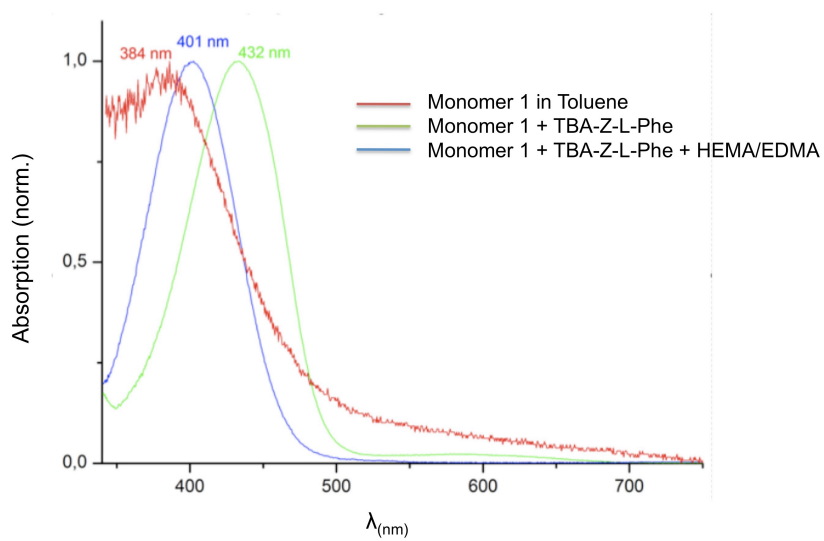


Figure 12.18a: Absorption spectra of monomer 1, and the pre-polymerisation mixtures (HEMA/EDMA) in toluene

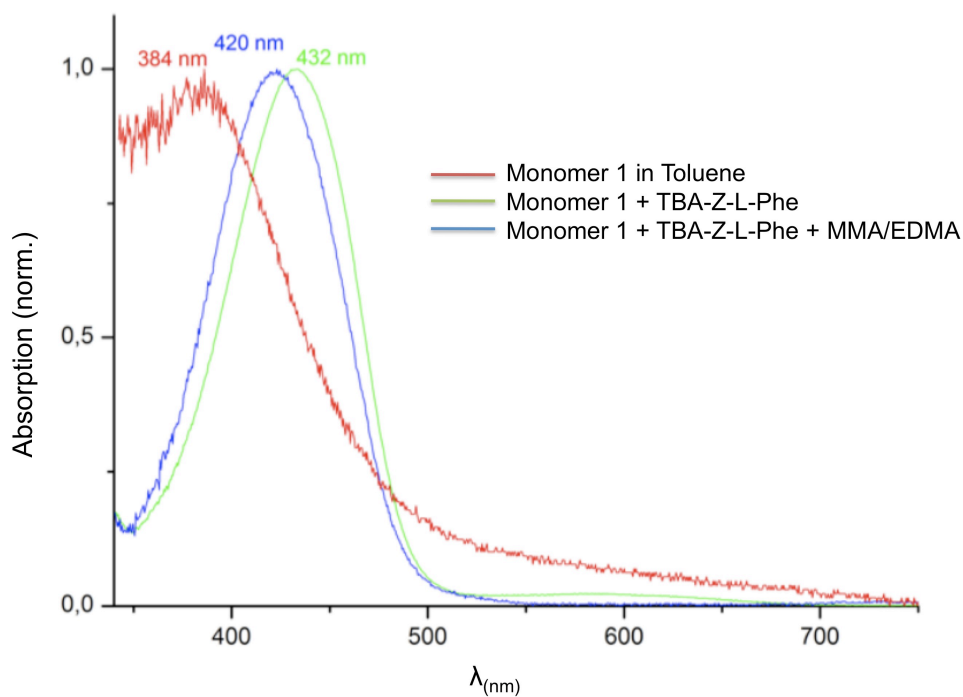


Figure 12.18b: Absorption spectra of monomer 1, and the pre-polymerisation mixtures (MMA/EDMA) in toluene

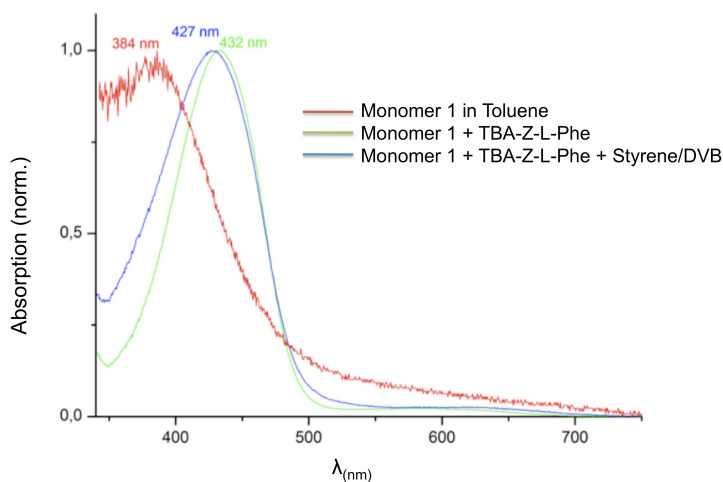


Figure 12.18c: Absorption spectra of monomer **1**, and the pre-polymerisation mixtures (Styrene/DVB) in toluene

Also in the case of toluene low solubility of the monomer can be concluded from the high scattering. The absorption maximum of the monomer in toluene lies at $\lambda = 383$ nm. Upon addition of TBA-Z-L-Phe the absorption maximum shifts to $\lambda = 433$ nm. Thus, formation of the monomer-template complex can be assumed. The absorption maximum shifts back in the direction of the one of the free monomer in solution in agreement with the polarity of the added reagents. In presence of HEMA/EDMA the strongest shift is observed (433 nm to 400 nm). The addition of MMA/EDMA induces a shift from 433 nm to 422 nm. The shift upon addition of Styrene/DVB is the least from 433 nm to 426 nm. This observation supports the assumption that the stability of the pre-polymerisation complex between monomer and template is strongly depended on the polarity.

12.1.3. Thin-film MIPs on glass cover-slips

Based on these promising results polymer films in toluene were synthesized with the MMA/EDMA system and the Styrene/DVB system both on coverslips modified with a linker and on slips carrying the RAFT agent.

Polymer films were prepared to the following ratio and immobilised on coverslips. The sys-

tems tested are:

- System 1: Functional monomer **1**, MMA, EDMA at 110 °C on RAFT coverslips
- System 2: Functional monomer **1**, MMA, EDMA at 50 °C
- System 3: Functional monomer **1**, MMA, EDMA at 110 °C
- System 4: Functional monomer **1**, Styrene, DVB at 50°C

The coverslips were carefully extracted via soxhlet extraction in MeOH and evaluated spectroscopically. The following diagrams display the background-corrected relative fluorescence emission intensity of the slides upon addition of increasing concentration of the guest molecule TBA-Z-L-Phe:

System 1:

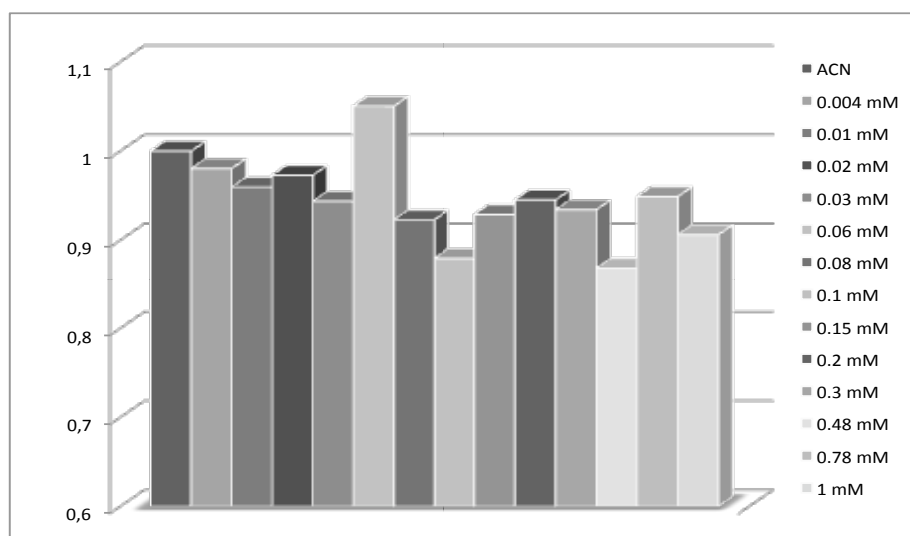


Figure 12.19: Background corrected fluorescence emission intensity of MMA/EDMA MIP film prepared on RAFT cover-slip at 110°C in toluene in presence of increasing concentration of the template TBA Z-L-Phe in ACN

The recipe of this polymer film is the same like for polymer VI presented in the RAFT chapter. Only the solvent was changed from ACN to the less polar toluene and the polymerisation temperature was elevated to 110°C.

The evaluation of the fluorescence emission intensity of the MIP film prepared in tolu-

ene on the RAFT-modified coverslip shows that in this case the change of the solvent employed during the polymerisation does not improve the recognition properties of the film visible as a quenching of the fluorescence emission intensity. The quenching is less pronounced than in case of the films prepared in ACN.

System 2:

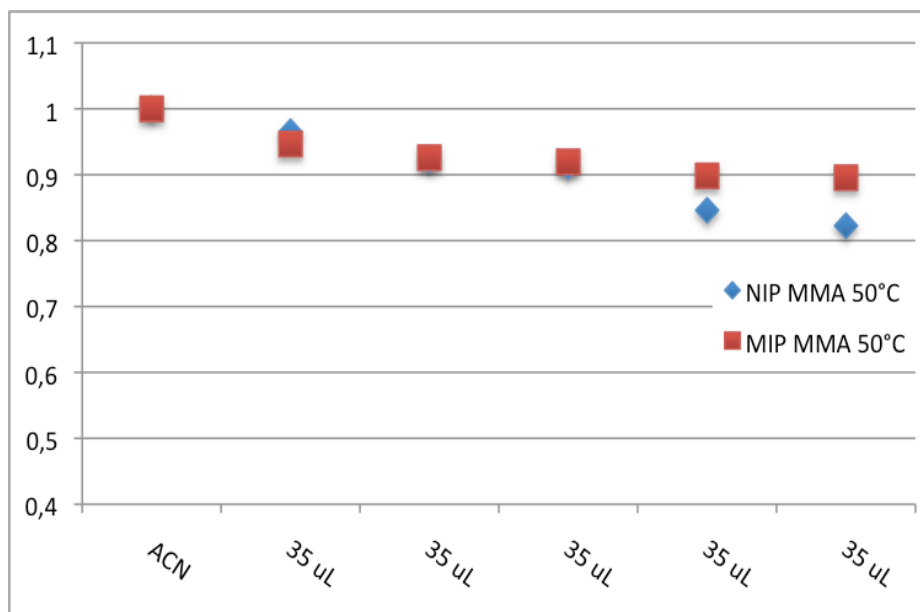


Figure 12.20 Background corrected fluorescence emission intensity of MMA/EDMA MIP film prepared at 50°C in toluene in presence of increasing concentration of the template TBA Z-L-Phe in ACN

The MMA/EDMA films prepared at 50 °C show fluorescence quenching. The quenching is more pronounced on the NIP than on the MIP.

System 3:

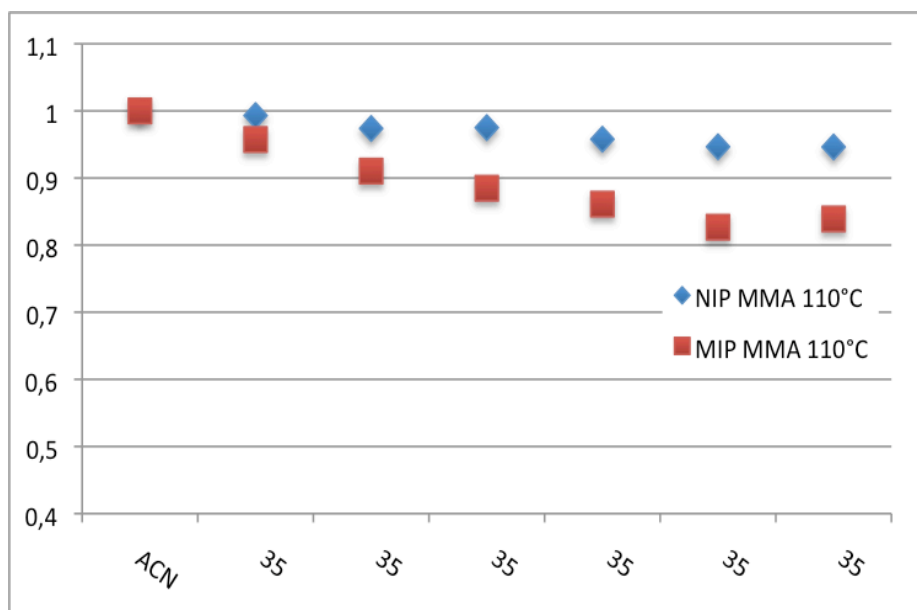


Figure 12.21: Background corrected fluorescence emission intensity of MMA/EDMA MIP film prepared at 110°C in toluene in presence of increasing concentration of the template TBA Z-L-Phe in ACN

The MMA/EDMA films prepared at 110 °C show fluorescence quenching. The quenching is more pronounced on the MIP than on the NIP. This is also displayed by the values listed in **Table 12.15**:

Table 12.15: Imprinting factors of System 3 calculated from fluorescence quenching in ACN upon addition of TBA Z-L-Phe

	IF _Q
0.34 mM	0.964
0.65 mM	0.935
0.95 mM	0.907
1.23 mM	0.899
1.49 mM	0.873
1.74 mM	0.887

With increasing concentration the imprinting factor is diminished.

System 4:

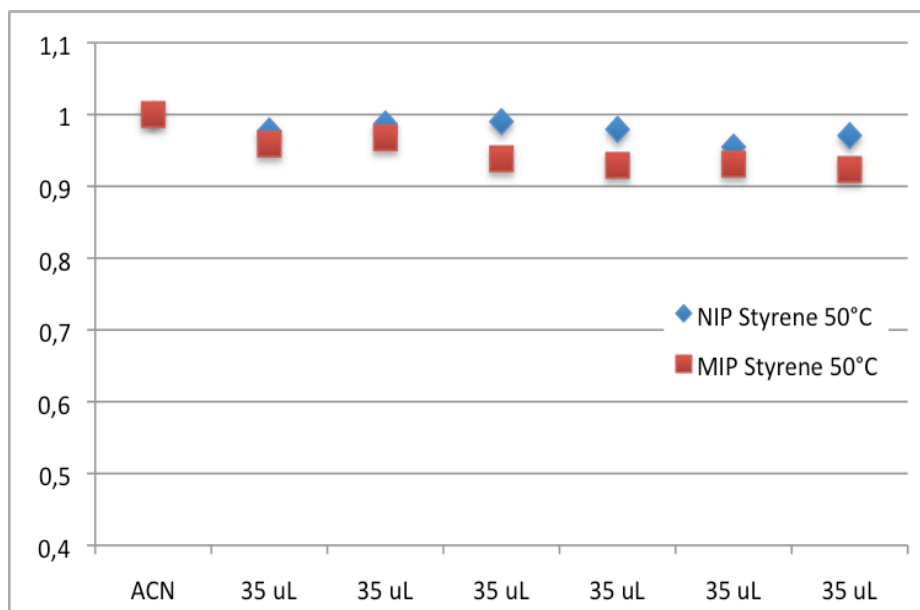


Figure 12.22: Background corrected fluorescence emission intensity of Styrene/EDMA MIP film prepared at 110°C in toluene in presence of increasing concentration of the template TBA Z-L-Phe in ACN

Conclusion:

Polymer films according to the above mentioned compositions were prepared in toluene and evaluated spectroscopically in presence of solutions of TBA Z-L-Phe in ACN of increasing concentration. The 110°C MMA/EDMA system shows quenching upon addition of the analyte solutions. The quenching is more pronounced on the MIP than on the NIP. Thus, successful imprinting can be assumed.

12.1.3.1. MMA/ EDMA 110°C film prepared in Toluene

From the tested polymer compositions the MMA/EDMA system polymerised at 110°C in toluene was identified as the most promising one. Thus, the film synthesis was repeated in bigger scale and the obtained polymers were extensively tested.

Stability/ Comparability test

Molecularly imprinted polymers with a low cross-linking level (lower than ca. 50 %) are

known to be of poor stability and prone to loose their recognition properties upon washing and reuse.

Several measurements were thus performed in order to assess the stability of the films and the comparability of films prepared from the same pre-polymerisation mixture and different batches.

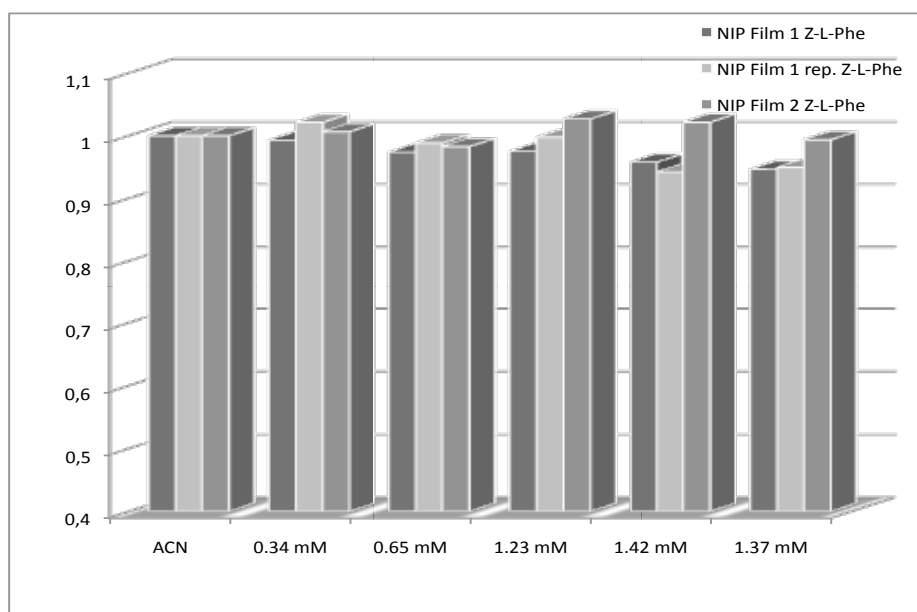


Figure 12.23: Comparison of background-corrected fluorescence emission intensity of NIP films prepared in different batches and upon reuse after soxhlet extraction

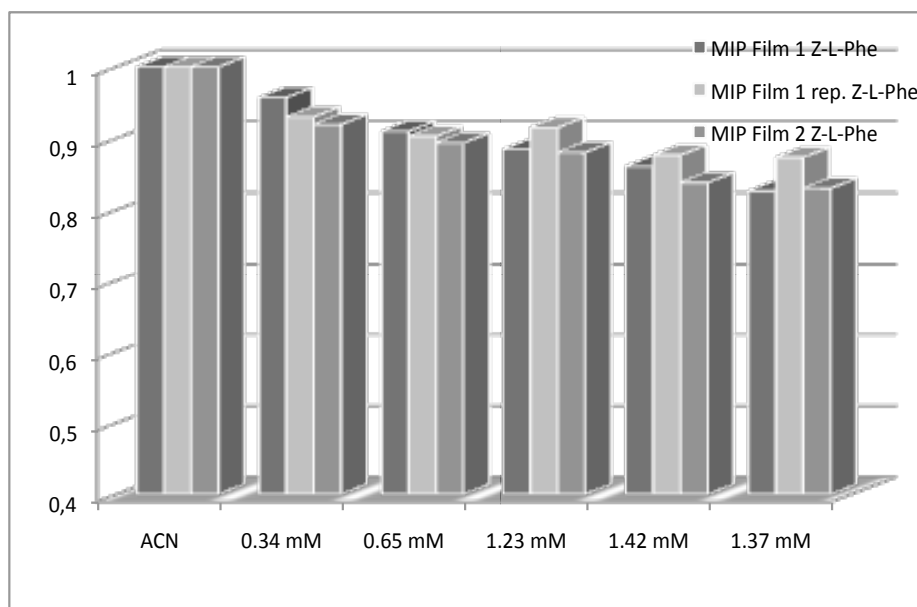


Figure 12.24: Comparison of background-corrected fluorescence emission intensity of MIP films prepared in different batches and upon reuse after soxhlet extraction

In both cases (NIP and MIP) the deviation between the data points for the repeated measurements on film 1 and also for the comparison with film 2 is always below 5 %. It can thus be concluded that the film synthesis is reproducible and the films are stable upon washing and reuse.

Solvatochromism of the polymer films

Due to the fact that the built-in functional monomer **1** is a solvatochromic dye, conclusions about the environment that the monomer encounters in the polymer can be drawn from the position of the maximum emission wavelength in solvents of different polarity. In case that the monomer is well accessible by the solvent and the polymer-backbone does not change the polarity of the media, the emission maxima of the free monomer in solution and of the polymer film should have roughly the same position. Since the monomer exhibits positive solvatochromism, also the polymer films should show a shift of the maximum emission wavelength towards longer wavelength.

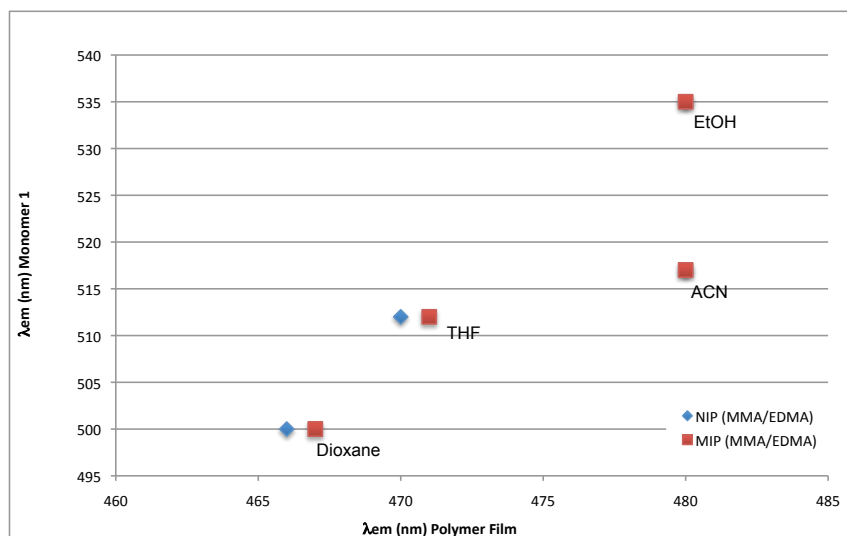


Figure 12.25: Maximum emission wavelength of free monomer in solution plotted against maximum emission wavelength of the MMA/EDMA polymer films prepared at 110°C in toluene measured in Dioxane, THF, ACN and EtOH

The displayed values show that the integration of the functional monomer into the polymer backbone severely changes the position of the maximum emission wavelength. Like the free monomer in solution the polymer films exhibit positive solvatochromism. Neverthe-

less, the absolute positions of the fluorescence emission maximum are shifted to shorter wavelengths. This indicates an environment of significantly lower polarity for the monomer upon being integrated into the polymer. This assumption is supported by the fact that no shift in the maximum emission wavelength can be observed upon changing from ACN to EtOH. Being shielded by the polymer-backbone of low polarity the monomer might not be accessible by a highly polar solvent and thus no shift of the emission maximum is induced. The low polarity may be a result of the high content on pMMA.

As a result of the low polarity of the system, the accessibility of the cavities in the polymer for polar solvents/ compounds might be hindered.

Selectivity test

In order to test the success of the imprinting process the fluorescence emission properties of the films were investigated in presence of increasing concentration of the template TBA Z-L-Phe and its D-enantiomer as solutions in ACN.

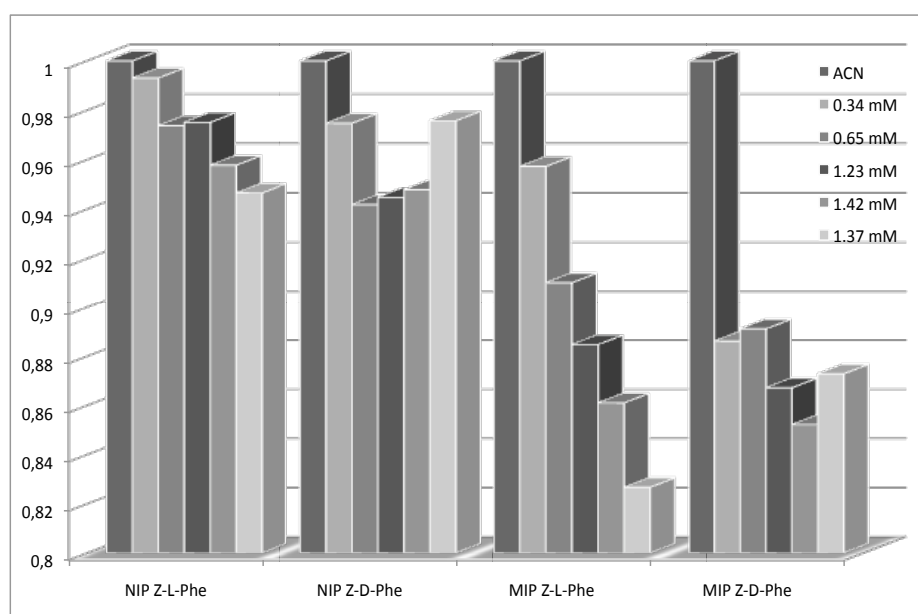


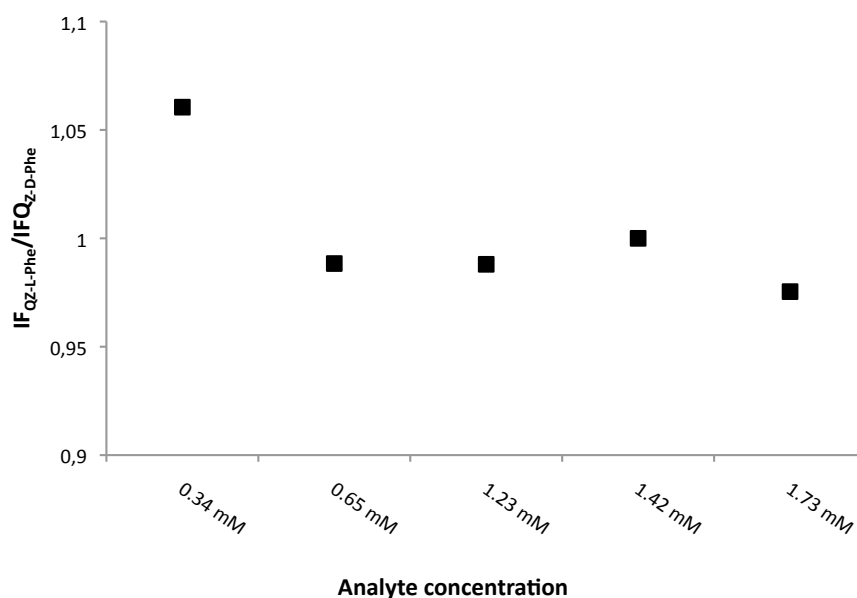
Figure 12.26: Normalised and background corrected fluorescence emission intensity of MMA/EDMA NIP and MIP films prepared in Toluene at 110°C in presence of increasing concentration of TBA Z-L-Phe and TBA Z-D-Phe

Table 12.16: IF_Q and QF of MMA/EDMA films

	IF _Q		QF	
	Z-D-Phe	Z-L-Phe	NIP	MIP
0.34 mM	0.909	0.964	1.019	1.080
0.65 mM	0.946	0.935	1.034	1.021
1.23 mM	0.918	0.907	1.032	1.020
1.42 mM	0.899	0.899	1.010	1.010
1.73 mM	0.895	0.873	0.970	0.957

In order to display better the enantiomeric resolution properties of the polymers or respectively their cross-selectivity a separation factor α_Q was introduced as:

$$\alpha_Q = \text{IF}_{Q\text{Template}} / \text{IF}_{Q\text{Cross-Analyte}} \quad (12.2)$$

**Figure 12.27:** α_Q for Z-L-Phe and Z-D-Phe on MMA/EDMA MIP

Taking into account the deviation of about five percent no pronounced difference in the fluorescence emission intensity of the MIP can be observed upon addition of Z-L-Phe and Z-D-Phe. Nevertheless, the quenching is more pronounced for the MIP than for the NIP resulting in imprinting factors below 1.

The titrations were thus repeated starting from lower concentrations of Z-L-Phe and Z-D-Phe.

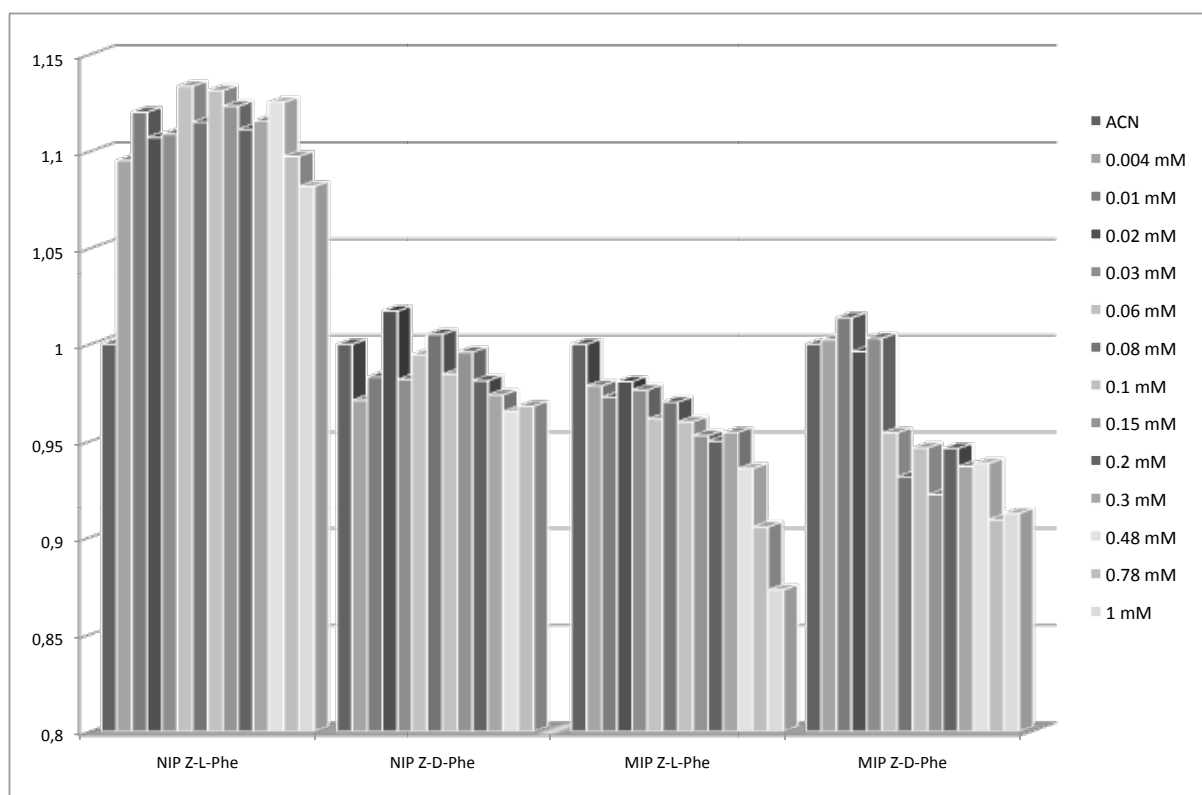


Figure 12.28: Normalised and background corrected fluorescence emission intensity of MMA/EDMA NIP and MIP films prepared in Toluene at 50°C in presence of increasing concentration of TBA Z-L-Phe and TBA Z-D-Phe

Table 12.17: Imprinting and quenching factor for MMA/EDMA films prepared in Toluene

	IF _Q		QF	
	Z-D-Phe	Z-L-Phe	NIP	MIP
0.004 mM	1.032	0.893	1.128	0.976
0.01 mM	1.031	0.868	1.139	0.959
0.02 mM	0.979	0.886	1.088	0.985
0.03 mM	1.022	0.881	1.129	0.973
0.06 mM	0.959	0.848	1.139	1.008
0.08 mM	0.927	0.870	1.109	1.041
0.1 mM	0.961	0.849	1.149	1.014
0.15 mM	0.926	0.848	1.128	1.033
0.2 mM	0.964	0.855	1.132	1.004

	IF _Q		QF	
0.3 mM	0.962	0.856	1.145	1.019
0.48 mM	0.972	0.831	1.166	0.997
0.78 mM	0.939	0.825	1.134	0.996
1 mM	/	0.807	/	0.957

The obtained data clearly shows that the imprinting step was successful.

The calculated imprinting factors show that the fluorescence quenching of the MIP in presence of the template *Z-L-Phe* is significantly stronger than on the NIP. Furthermore, as displayed by the quenching factors, the NIP is not discriminating between the two enantiomers, whereas the fluorescence of the MIP quenches more in presence of the template than of the *D*-enantiomer.

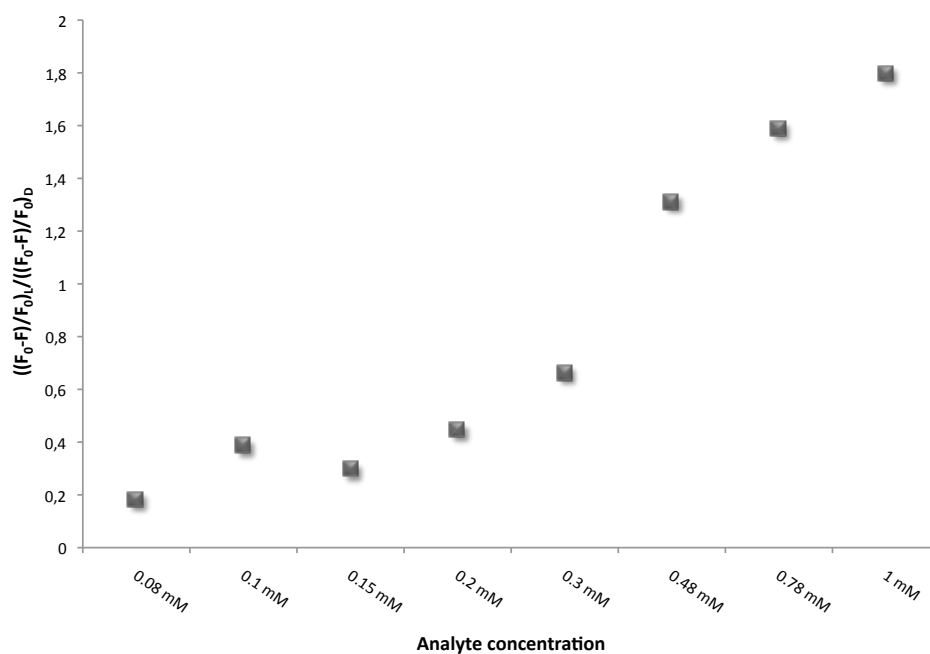


Figure 12.29: Quotient of titration curves of MMA/EDMA MIP in presence of *Z-L-Phe* and *Z-D-Phe*

Upon direct comparison of the titration curves of the MIP in presence of *Z-L-Phe* and *Z-D-Phe* the polymer is clearly discriminating between its template and the cross-analyte resulting in a quenching twice as strong in presence of the template.

12.1.3.2. Benzyl methacrylate/ EDMA 110°C films prepared in Toluene against TBA Z-L-Phe

Apart from the functional monomer **1**, all building blocks of the polymers are aliphatic compounds. The template is thus only able to interact with the polymer via functional group interactions. It is assumed that the integration of an aromatic co-monomer should lead to an amplified interaction between the polymer film and the analyte containing an aromatic group due to π - stacking. The co-monomer MMA was thus replaced with benzyl methacrylate.

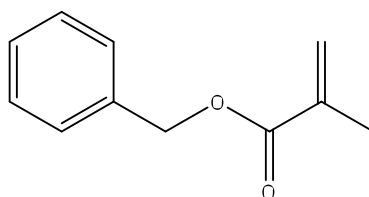


Figure 12.30: Benzyl methacrylate

Solvatochromism

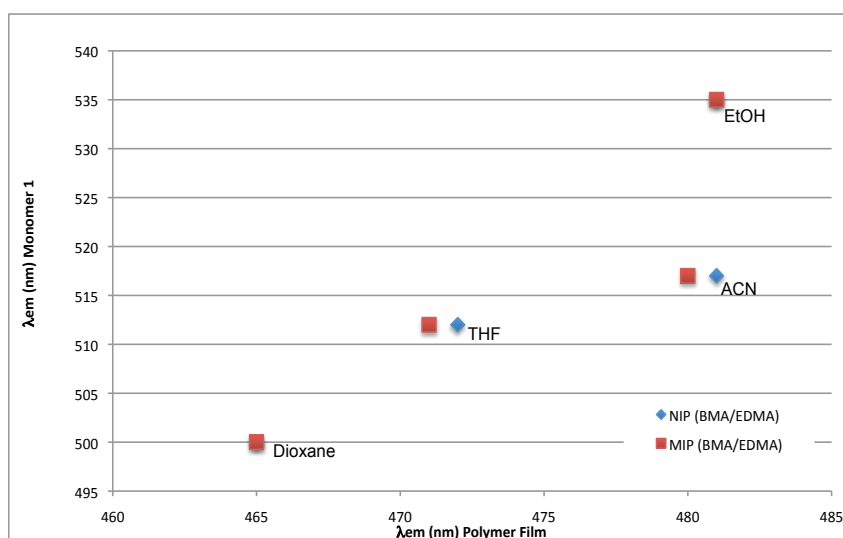


Figure 12.31: Maximum emission wavelength of free monomer in solution plotted against maximum emission wavelength of the BMA/EDMA polymer films prepared at 110°C in toluene measured in Dioxane, THF, ACN and EtOH

In case of the BMA/EDMA system the positions of the maximum emission wavelength are severely shifted to shorter wavelengths in comparison with the free monomer in solution, means that the monomer is shielded from the solvent by a non-polar environment.

The positions are stronger blue-shifted than for the MMA/EDMA system, which indicates an even lower polarity of the BMA/EDMA system. Taking into account the structures of MMA and BMA it can be expected that the BMA/EDMA system is less polar. Nevertheless, a positive solvatochromism is observed for the polymer films. This means that the solvatochromic monomer and thus the binding sites are accessible.

Selectivity test

The selectivity of the obtained films was tested in different solvent systems starting from pure ACN.

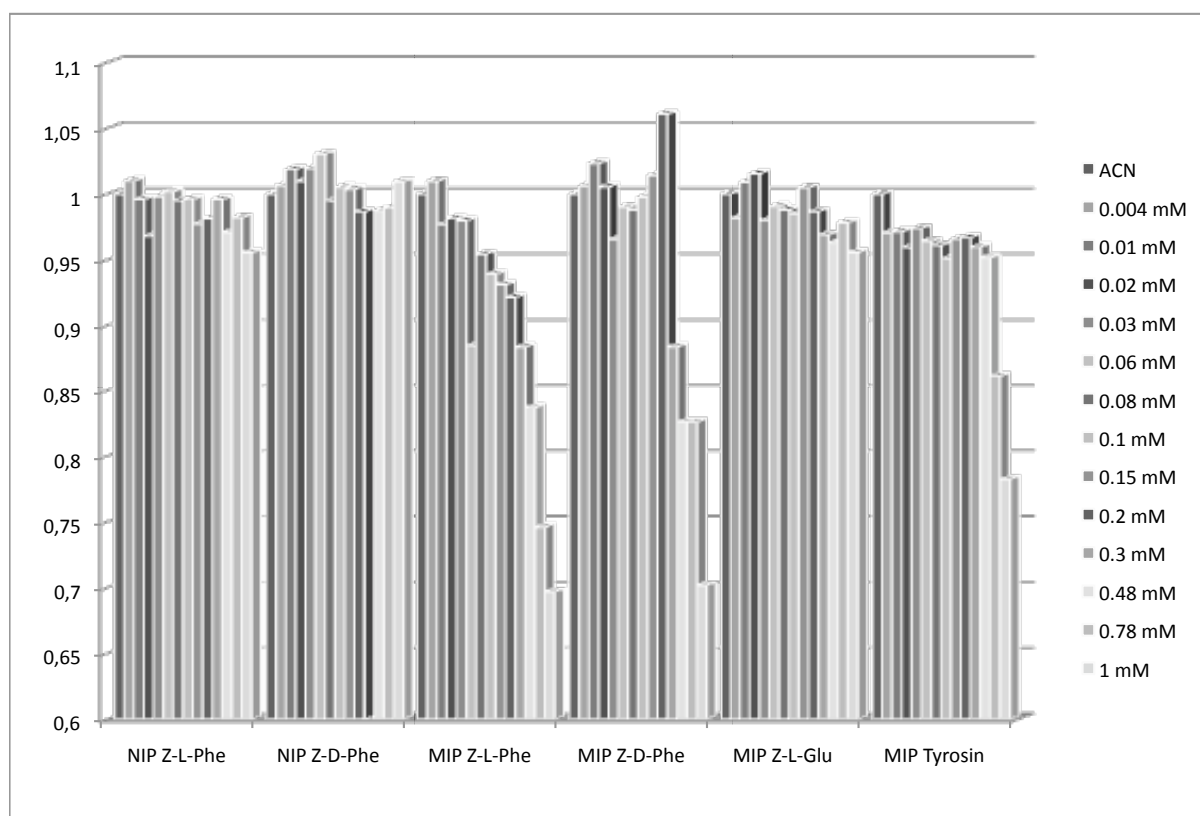


Figure 12.32: Normalised and background corrected fluorescence emission intensity of BMA/EDMA NIP and MIP films prepared in Toluene at 110°C in presence of increasing concentration of TBA Z-L-Phe and TBA Z-D-Phe, TBA-Z-L-Glu, TBA-Z-L-Tyr

Table 12.18: Imprinting factors for BMA/ EDMA films prepared in Toluene

	IF _Q	
	Z-D-Phe	Z-L-Phe
0.004 mM	0.999	0.999
0.01 mM	1.004	0.981
0.02 mM	0.996	1.014
0.03 mM	0.947	0.982
0.06 mM	0.961	0.883
0.08 mM	0.993	0.959
0.1 mM	0.993	0.943
0.15 mM	1.010	0.953
0.2 mM	1.075	0.939
0.3 mM	/	0.887
0.48 mM	0.837	0.862
0.78 mM	0.835	0.759
1 mM	0.695	0.729

Upon addition of increasing concentration of the template TBA *Z-L-Phe* and its D-enantiomer TBA *Z-D-Phe* no quenching of the fluorescence emission intensity can be observed for the NIP. The fluorescence emission intensity of the MIP is quenched upon addition of both TBA-*Z-Phe* enantiomers. With increasing concentration of the analytes the quenching becomes more pronounced on the MIP. This is displayed in the lower imprinting factors. The differences in the imprinting factors for the D- and the L-enantiomer are within the error range of the measurement; means that the MIP is not discriminating between the two enantiomers.

The difference in quenching degree between NIP and MIP is bigger for the BMA/EDMA system than for the MMA/EDMA system. This might be due to the amplified interaction between the template and the polymer backbone based on pi -stacking.

For further analysis of the cross-selectivity two other amino-acids were tested:

- TBA-Z-L-Glutamic acid (aliphatic, two carboxylic-functionalites)
- TBA-Z-L-Tyrosin (aromatic)

These cross-analytes were chosen in order to evaluate what the fluorescence quenching of the MIP is based on. If the fluorescence quenching was based only on the presence of carboxylic functionalites and thus the formation of hydrogen bonds, strong quenching should be observed for TBA-Z-L-Glu as well. If the quenching was mainly due to interactions of the aromatic side-groups it should be observed also for TBA-Z-L-Tyrosin.

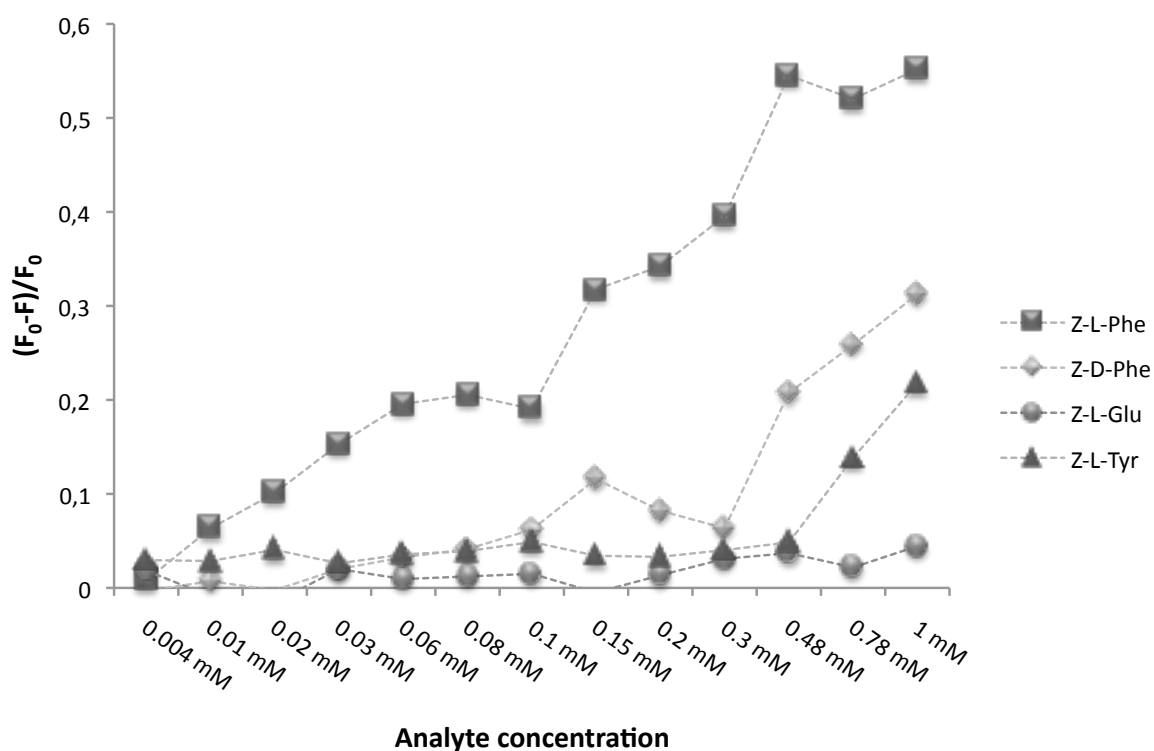


Figure 12.33: Titration curves of BMA/EDMA MIP in presence of Z-L-Phe, Z-D-Phe, Z-L-Glu and Z-L-Tyr

The BMA/EDMA MIP clearly discriminates between the analytes (Figure 12.33). Throughout the titration experiment the quenching in presence of the template Z-L-Phe is twice as strong as the quenching in presence of Z-D-Phe, revealing strong enantioselective discrimination. In case of the aliphatic amino-acid Z-L-Glu no fluorescence quenching could be observed and also the quenching upon addition of another aromatic amino acid Z-L-Tyr is much less pronounced than in case of the template.

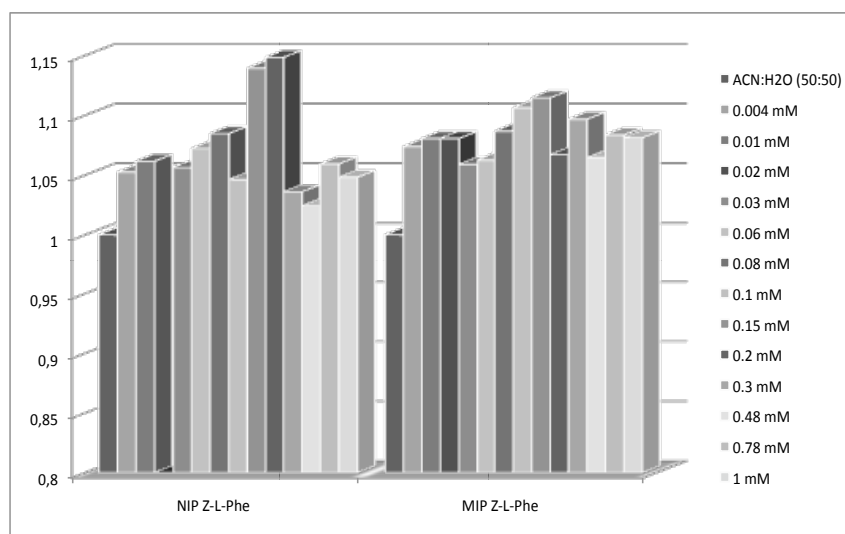
Evaluation in ACN:H₂O (50:50)

Figure 12.34: Normalised and background corrected fluorescence emission intensity of BMA/EDMA NIP and MIP films prepared in Toluene at 110°C in presence of increasing concentration of TBA Z-L-Phe and in ACN:H₂O (50:50)

In the 50:50 mixture of acetonitrile and water no quenching of the fluorescence emission intensity can be observed upon addition of Z-L-Phe both for the NIP and for the MIP. This behaviour corresponds to the results from the HPLC analysis. Only poor retention of Z-L-Phe could be achieved on the Z-L-Phe imprinted column in the acetonitrile/ water mixture.

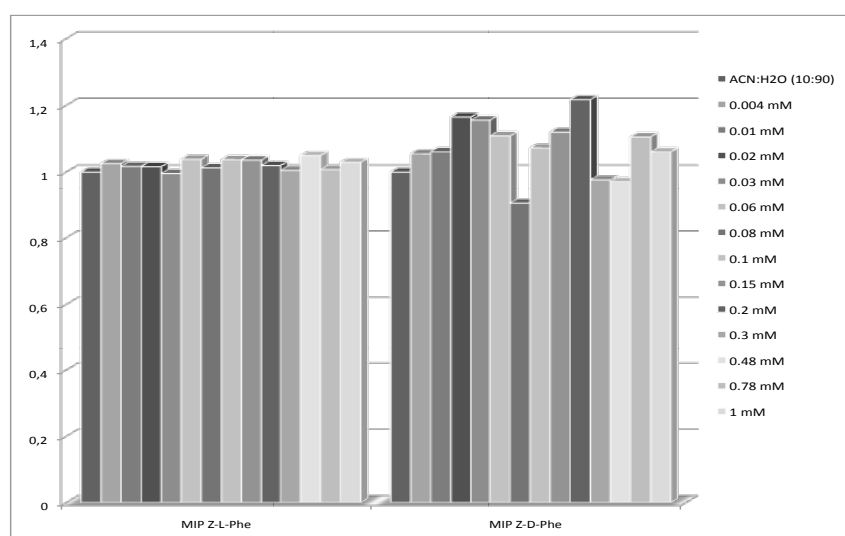
Evaluation in ACN:H₂O (10:90)

Figure 12.35: Normalised and background corrected fluorescence emission intensity of BMA/EDMA MIP films

prepared in Toluene at 110°C in presence of increasing concentration of TBA Z-L-Phe and TBA Z-D-Phe
ACN:H₂O (10:90)

In the 10:90 mixture of ACN and water no quenching could be obtained on the MIP
for both analytes, the template TBA Z-L-Phe and the D-enantiomer.

Evaluation in ACN:TEA (99:1)

In order to gain information whether the remarkable discrimination behaviour of the BMA/EDMA polymer can be improved by the addition of a base modifier, the titration experiments were repeated in an ACN:TEA (99:1) mixture.

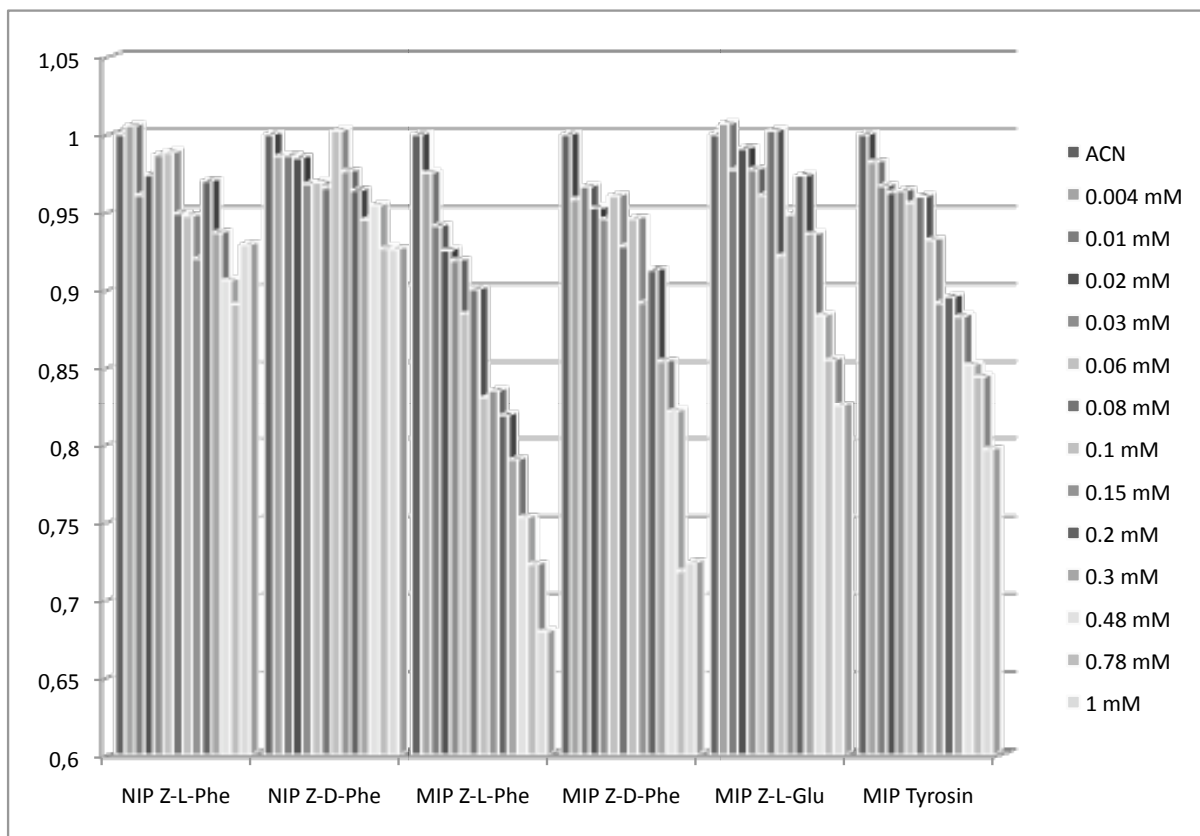


Figure 12.36: Normalised and background corrected fluorescence emission intensity of BMA/EDMA NIP and MIP films prepared in Toluene at 110°C in presence of increasing concentration of TBA Z-L-Phe, TBA Z-D-Phe, TBA Z-L-Glu and TBA Z-L-Tyrosin ACN:TEA (99:1)

In case of the base-modified system fluorescence quenching was also observed for the NIP and for MIP in presence of TBA-Z-L-Glu. Thus, in this solvent system deprotonation of the functional monomer might play a role regarding the fluorescence quenching. Nevertheless, the fluorescence quenching of the MIP is most pronounced in presence of the template TBA-Z-L-Phe.

Table 12.20: Imprinting factors calculated for BMA/EDMA films prepared in Toluene in ACN:TEA (99:1)

	IF	
	Z-D-Phe	Z-L-Phe
0.004 mM	0.972	0.969
0.01 mM	0.979	0.979
0.02 mM	0.967	0.949
0.03 mM	0.977	0.931
0.06 mM	0.991	0.895
0.08 mM	0.961	0.959
0.1 mM	0.944	0.877
0.15 mM	0.913	0.908
0.2 mM	0.947	0.844
0.3 mM	0.904	0.844
0.48 mM	0.860	0.830
0.78 mM	0.775	0.811
1 mM	0.781	0.731

The calculated imprinting factors are similar for the D-enantiomer and the L-enantiomer. This indicates that the films are not discriminating between the two enantiomers. Nevertheless, the quenching of the MIP is more pronounced upon addition of the analytes than of the NIP.

Table 12.21: Quenching factors calculated for BMA/EDMA films prepared in Toluene in ACN:TEA (99:1)

	QF		
	Z-L-Phe/Z-D-Phe	Z-L-Phe/Z-L-Glu	Z-L-Phe/Z-L-Tyr
0.004 mM	1.018	0.969	0.993
0.01 mM	0.974	0.963	0.973
0.02 mM	0.972	0.934	0.961
0.03 mM	0.972	0.940	0.953
0.06 mM	0.921	0.920	0.925
0.08 mM	0.970	0.898	0.938
0.1 mM	0.878	0.901	0.891
0.15 mM	0.937	0.881	0.937
0.2 mM	0.897	0.841	0.914
0.3 mM	0.925	0.844	0.895
0.48 mM	0.917	0.852	0.884
0.78 mM	1.006	0.846	0.856
1 mM	0.938	0.823	0.853

In case of the base-modified solvent system a slight enantio-selective discrimination can be observed for some concentration. The MIP clearly discriminates between the template *Z-L-Phe* and the cross-analytes Glutamic acid and Tyrosin.

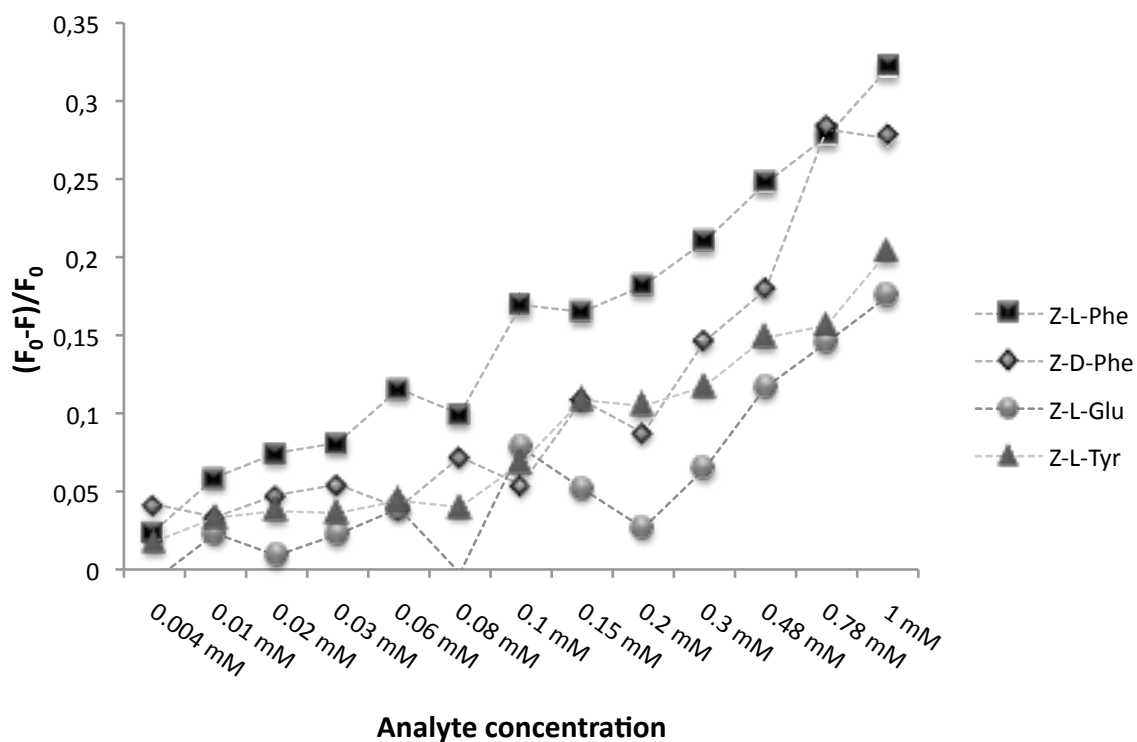


Figure 12.37: Titration curves of BMA/EDMA MIP in presence of Z-L-Phe, Z-D-Phe, Z-L-Glu and Z-L-Tyr

The difference in quenching upon addition of the template and the cross-analytes is not as pronounced as in the non-modified ACN. Figure 12.37 supports the fact stated above that the functional monomer is deprotonated in presence of the base. This behaviour corresponds to the observations made for the bulk polymers.

1. Benzyl methacrylate/ EDMA 110°C films prepared in Toluene against Penicillin G potassium salt

Apart from the films imprinted on TBA *Z-L*-Phe also films against Penicillin G potassium salt were prepared. Also in this case monomer **1** was employed as functional monomer, BMA as co-monomer and EDMA as cross-linker. The cross-linking level was adjusted to 25 %.

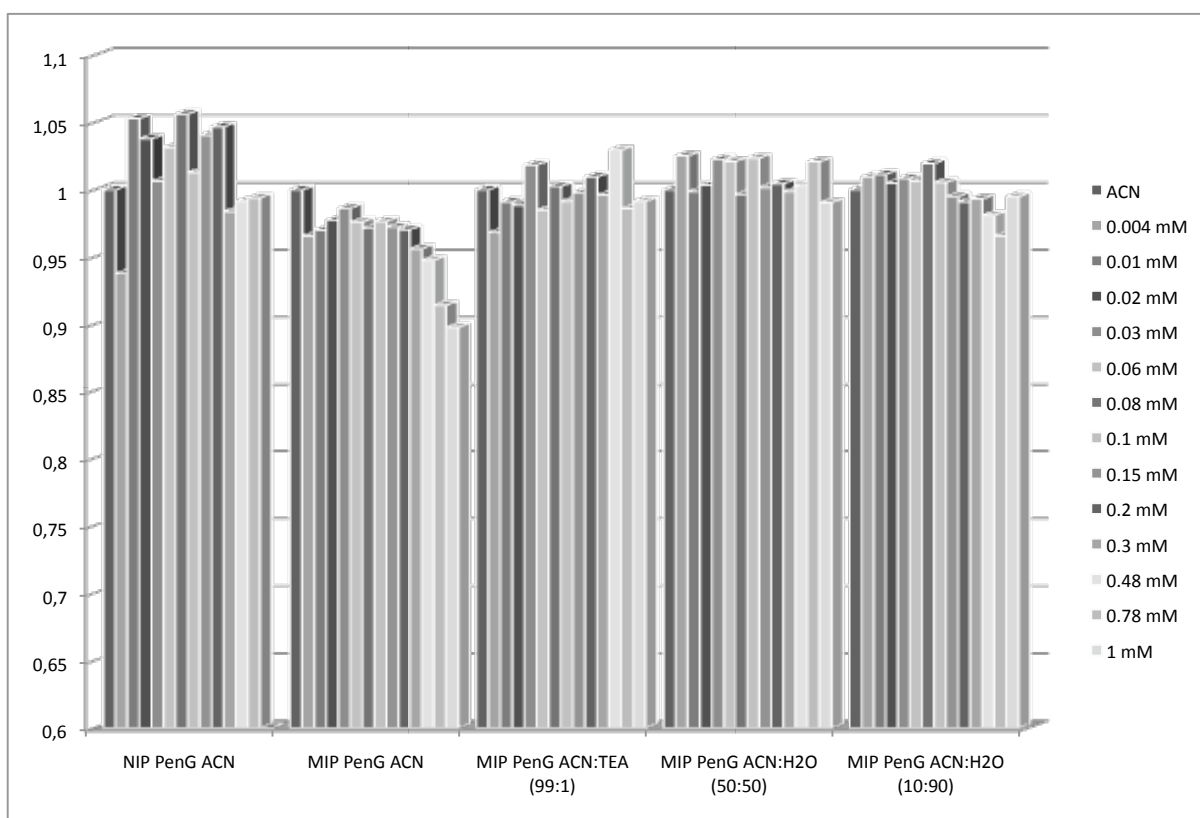


Figure 12.38: Normalised, background corrected fluorescence emission intensity of BMA/EDMA NIP and MIP films prepared in Toluene at 110°C in presence of increasing concentration of PenG pot in ACN

The films imprinted on Penicillin G were tested in four different solvent systems. Only in pure ACN a fluorescence quenching can be observed for the MIP.

Table 12.22: Imprinting factors calculated for PenG pot BMA/EDMA films prepared in Toluene in ACN

	IF
0.004 mM	1.029
0.01 mM	0.921
0.02 mM	0.942
0.03 mM	0.980
0.06 mM	0.946
0.08 mM	0.919
0.1 mM	0.964
0.15 mM	0.934
0.2 mM	0.927
0.3 mM	0.972
0.48 mM	0.956
0.78 mM	0.919
1 mM	/

The imprinting factors confirm that the quenching is more pronounced on the MIP than on the NIP. A more pronounced quenching of up to 11 % can be observed upon addition of increasing concentration of penicillin G as its potassium salt in ACN (5 % water). In all other mobile phases no quenching was induced. This behaviour might be due to the low polarity of the polymer.

Conclusion

In parallel to the RAFT-approach, also thin-film formation without the help of an additional agent was tested. In order to design this approach as rational as possible, the possible pre-polymerisation mixtures and the influence of different solvents were carefully studied with regard to the complex stability and the deprotonation of monomer 1. The goal was to limit down the amount of trial-and-error and to predict the goodness of a film system with regard to stability and selectivity.

Polymer films composed of monomer **1**, the co-monomer benzyl-methacrylate and the cross-linker EDMA imprinted on TBA-*Z-L*-Phe and PenicillinG potassium salt were prepared in toluene and evaluated spectroscopically in different solvents.

The tests of solvatochromism reveal a severely less polar environment for the monomer built-into the polymer films. Nevertheless, the films exhibit positive solvatochromism indicating good accessibility of the monomer.

The selectivity tests indicate that the imprinting of the films was successful. In ACN and ACN:TEA (99:1) the films imprinted on TBA *Z-L*-Phe discriminate between the template and aliphatic and structurally closely-related cross-analytes, namely TBA *Z-L*-Glu and TBA *Z-L*-Tyrosine. The titration experiments performed in ACN revealed remarkable enantio-selective discrimination. In the base modified system the MIP shows slight enantio-selective discrimination. The films imprinted on PenicillinG show quenching upon addition of the template in pure ACN.

13. Conclusion

Monomers

A polymerisable naphthalimide-based monomer **1** was designed, synthesised and spectroscopically evaluated. The monomer shows the typical favourable spectral features of amino-substituted naphthalimides, namely broad and strongly Stokes' shifted absorption and emission bands.

Evaluation in different solvents revealed positive solvatochromism in agreement with formally published findings for naphthalimides. Furthermore, titrations against oxyanionic guests show that the nature of the induced events (complex formation or deprotonation) is dependent on the employed solvent as well as the basicity of the guest molecule. Monomer **1** proved to be a promising candidate for the integration into molecularly imprinted polymers with signaling properties.

A new polymerisable indole-based monomer **2** was designed and synthesised and evaluated regarding its affinity towards oxyanionic guests, namely TBA-benzoate and its spectroscopical properties.

In NMR titration experiments monomer **2** showed high affinity towards TBA-benzoate. The absorption range of this monomer lies outside the spectral range suitable for sensing applications. Nevertheless, due to the high affinity towards oxyanions, monomer **2** can be of great value for separation applications and was thus included into the bulk synthesis for chromatographic analysis.

Polymers

Monomer **1** was successfully employed as building block in the synthesis of molecularly imprinted polymers in bulk and thin-film format against templates of biological or environmental importance. The bulk format is highly suitable for chromatographic evaluation whereas the thin, transparent polymer-films are ideal for spectroscopical applications.

Monolithic polymers in bulk format

Depending on the template employed, polymers of different colours were obtained in bulk synthesis. The colour-differences obtained imprinting on different templates hint at partial deprotonation of monomer **1**. Nevertheless, **chromatographic evaluation** proved the successful imprinting of the polymers. The polymers displayed the ability to enantio-selectively discriminate between their respective template and the D-enantiomer in case of *P_{1Glu}* and *P_{1Phe}* and complete retention of the template in case of the polymer imprinted on Penicillin G. The influence of the mobile-phase composition on the chromatographic evaluation was extensively studied. Base modification of the mobile phase leads to reduced retention, supporting the assumption that the rather acidic secondary amine of the urea- monomer exhibits gradual deprotonation under basic conditions.

The bulk polymers with a 99 % cross-linking level employing monomer **1** as functional monomer and EDMA as cross-linker were **spectroscopically evaluated** regarding their fluorescence emission properties in varying solvents. The response towards their template, basic conditions and cross-analytes was investigated. The polymers show no change in fluorescence emission intensity in organic solvents. Nevertheless, the accessibility of the dye-monomer **1** was confirmed by solvatochromic tests employing solvents of different polarity. In water remarkable quenching could be observed upon addition of the analyte and PMP for the MIP (30 %), whereas the quenching on the NIP (10%) was much less pronounced. Significant darkening of the polymer colour indicates that monomer **1** deprotonates at least partially under these conditions. In order to exclude swelling phenomena as a reason for the fluorescence quenching in water swelling tests were performed.

Comparison of the results from chromatographic analysis and the spectroscopic evaluation revealed show that a polymer aiming at separation applications has to be designed differently than a polymer suitable for sensing purposes. The fact that the sensing abilities of the free monomer in solution were preserved in the bulk polymers but observed in a less pronounced manner can be a result of the changed microenvironment that the monomer encounters upon polymerisation.

Cross-linking study

The influence of changing microenvironment on the spectral answer of the polymers employing monomer **1** as signalling unit was thus evaluated in cross-linking studies. In this case MMA was employed as co-monomer to adjust the cross-linking level and EDMA as cross-linker were prepared with different cross-linking levels and different dye-monomer loads and evaluated spectroscopically.

The spectroscopic response towards an oxyanionic guest was investigated in presence of increasing concentration of TBA Benzoat. All polymers employing the high dye-monomer load apart from polymer 6 (98 % cross-linking level) showed fluorescence quenching in presence of (high concentration) of TBA Benzoat. The strongest fluorescence quenching was observed for polymer 1 (0 % CL) and polymer 5 (69 % CL). This result is supported by the evaluation of the solvatochromism. Polymers with a very low cross-linking level and a high one seem to guarantee the best accessibility of monomer **1** for polar substances, whereas the very high cross-linking level of 99 % seems to prevent the interaction. The colour changes observed for the polymers without cross-linker and with low cross-linking level indicates that at least partial deprotonation of monomer **1** takes place in these polymers. It is assumed that the altered microenvironment in the polymers with higher cross-linking level (> 30 %) stabilises the protonated form of monomer **1**.

The polymers in the low-load study are rather non-responsive regarding fluorescence quenching and colour-change visible to naked-eye towards TBA Benzoat. This might be due to the fact that in the high-load polymers five times more dye-monomer contributes to the fluorescence emission intensity.

Polymers in thin-film format

In the developed thin-film format two approaches were tested. The first films were successfully synthesised via **RAFT polymerisation**. The obtained results show that all slides exhibit a positive solvatochromism, which is -in most cases- more pronounced in the MIP than in the NIP. The solvation of the polymer seems to be influenced by the amount of porogen used in the synthesis and by the polymerisation time. Higher dilution of the system during

polymerisation leads to a stronger bathochromic shift, which is an indication for better solvation. This observation is in agreement with the expectations, because a higher dilution should lead to a better accessibility of the built-in monomer.

The polymerisation time influences the position of the maximum emission wavelength. In the cases when the polymerisation was quenched after 30 minutes, the maximum emission is obtained at longer wavelengths than in the cases where the polymerisation was quenched after 2 h. The values obtained after 30 minutes are closer to the ones obtained for the free monomer in solution.

For the most promising polymer composition **VI** extensive titration experiments were performed in ACN revealing that the imprinting step in the preparation of the MIPs was successful. The MIP discriminates enantioselectively between its template *Z*-L-Phe and the *D*-enantiomer, whereas no enantioselective discrimination was observed for the NIP.

In parallel to the RAFT-approach, also thin-film formation without the help of an additional agent was tested. In order to design this approach as rational as possible, the possible pre-polymerisation mixtures and the influence of different solvents were carefully studied with regard to the complex stability and the deprotonation of monomer **1**. The goal was to limit down the amount of trial-and-error and to predict the goodness of a film system with regard to stability and selectivity.

Based on the assumption that the polarity of the environment should severely influence the stability of the monomer-template complex and thus the success of the imprinting step, extensive solution-studies of pre-polymerisation mixtures of varying polarity were performed. These tests revealed toluene to be the most promising solvent for thin-film polymers.

According to the solution studies, films were synthesised and extensively spectroscopically investigated. The most promising system is composed of monomer **1**, the comonomer benzyl-methacrylate and the cross-linker EDMA. Films were prepared imprinted on TBA-*Z*-L-Phe and PenicillinG potassium salt in toluene and evaluated spectroscopically in different solvents.

The tests of solvatochromism reveal a severely less polar environment for the monomer built-into the polymer films. Nevertheless, the films exhibit positive solvatochromism indicating good accessibility of the monomer.

The selectivity tests reveal that the imprinting of the films was successful. In ACN and ACN:TEA (99:1) the films imprinted on TBA *Z-L*-Phe clearly discriminate between the template and aliphatic and structurally closely-related cross-analytes, namely TBA *Z-L*-Glu and TBA *Z-L*-Tyrosine. The MIP shows remarkable ability to discriminate enantioselectively in ACN. Throughout the titration experiment the quenching in presence of the template *Z-L*-Phe is twice as strong as the quenching in presence of *Z-D*-Phe. In case of the aliphatic amino acid *Z-L*-Glu no fluorescence quenching could be observed and also the quenching upon addition of another aromatic amino acid *Z-L*-Tyr is much less pronounced than in case of the template. The films imprinted on PenicillinG show quenching upon addition of the template in pure ACN.

14. Experimental part

14.1. Synthesis

14.1.1. Chemicals

4-Bromo-1,8-naphthalic anhydride, ethylamine, hydrazine x H₂O, 1,4-dioxane, pyridine, ethylchloroformate, triethylamine, hydrochloric acid, tetrabutylammonium hydroxide, Disperse Yellow 9 and the RAFT agent were purchased from Aldrich (Steinheim).

Tetrahydrofuran, n-hexane, formaldehyde, ethanol and sodium hydroxide from AppliChem (Darmstadt). p-bromomethylbenzoic acid from Chemos (Regenstauf), tri-phenylphosphine, thionylchloride and acetone from Merck (Darmstadt) and benzoic acid and diethyl ether were obtained from Acros Organics (Geel). DMSO-d₆ was purchased from Deutero-GmbH (Kastellaun). 5-Amino-2-(trifluoromethyl)benzimidazole was bought from Alfa Aesar (Karlsruhe, Germany). 2,3-Dimethyl-7-nitro-1 *H*-indole dry acetonitrile was purchased from Acros Organics (Geel, Belgium); Methanol (MeOH, p.a.) and tetrahydrofurane (THF, stabilised) KMF Optichem (Lohmar, Germany). Nitrogen (4.6) was purchased from Air Liquide (Düsseldorf, Germany). HPLC grade acetonitrile and methanol were purchased from Merck KGaA (Darmstadt, Germany). HPLC water was purified using a Milli-Q system (Millipore, Bedford, MA). Anhydrous solvents, tetrahydrofuran, Pyridine were stored over appropriate molecular sieves. Other solvents were of reagent grade or higher.

14.1.2. Apparatus and instruments

¹H-NMR spectra were measured on a Bruker Avance DRX Spectrometer and evaluated using Mestrelab or SpinWorks Software. FT-APCI-MS spectra were recorded with a LTQ-Orbitrap spectrometer (Thermo Fischer).

Elemental Analysis (EA): Carbon, hydrogen and nitrogen contents were determined at the "Institut für Organische Chemie", Johannes Gutenberg Universität Mainz using a Heraeus CHN-rapid analyser (Hanau, Germany).

Synthesis of 1- Isocyanato-4-vinylbenzene

Step 1: (4-carboxybenzyl)triphenylphosphonium bromide

The synthesis of the isocyanate follows a modified procedure of Porcal et al.⁸⁸

p-bromomethylbenzoic acid (11.50 g, 54 mmol) and triphenylphosphine (14.10 g, 54 mmol) were dissolved in 250 mL acetone and refluxed for 3 h. The warm mixture was precipitated from 1 L diethyl ether. The precipitated salt was filtered off and dried under vacuum.

Yield: 97 %.

¹H-NMR (300 MHz, DMSO-d₆) δ: 5.26 (d, 2H, *J*=12 Hz), 7.09 (q, 2H), 7.74 (m, 14H), 7.92 (m, 3H), 13.11 (s, 1H).

MS, *m/z* found: 397.14 g mol⁻¹ [M-Br]⁻, calc. mass: 397.14 g mol⁻¹.

Step 2: 4-vinylbenzoic acid

(4-carboxyphenyl)methyl-triphenyl-phosphonium bromide (24.6 g, 50 mmol) was dissolved in 100 mL formaldehyde in water (37 %). The solution was cooled to 0 °C. Subsequently, 100 mL 0.5 M NaOH were added drop wise. The mixture was stirred 48 h at room temperature. The solid was removed by filtration and washed with 1 M NaOH solution. The filtrate was acidified with 10 % HCl solution to precipitate the product. The product was dried and recrystallised from ethanol/water 3:7.

Yield: 89 %.

¹H-NMR (300 MHz, DMSO-d₆) δ: 5.37 (d, 1H, *J*=9 Hz), 5.94 (d, 1H, *J*=12 Hz), 6.80 (dd, 1H), 7.54 (d, 2H, *J*=6 Hz), 7.89 (d, 2H, *J*=6 Hz), 8.39 (s, 1H). ¹³C-NMR (DMSO-d₆) δ: 117.86, 127.08, 130.51, 130.77, 136.69, 142.13, 167.87.

MS, *m/z* found mass: 148.55 g mol⁻¹, calc. mass: 148.16 g mol⁻¹.

Step 3: 1-isocyanato-4-vinylbenzene

In agreement with a protocol published by Luebke et al.⁸⁹ 4-vinylbenzoic acid was transformed into 1- isocyanato-4-vinylbenzene, using ethyl chloroformate as the chlorination agent and NaN₃.

Yield: 62 %.

¹H-NMR (CDCl₃) δ: 5.24 (dd, 1H), 5.71 (dd, 1H), 6.65 (dd, 2H), 7.02 (d, 2H), 7.34 (d, 2H);

MS, *m/z* found mass: 145.10 g mol⁻¹, calc. mass: 145.01 g mol⁻¹

Synthesis of 1

Step 1: (6-Bromo-2-ethyl-benzo[de] isoquinoline- 1,3-dione)

This synthesis step follows Gunnlaugsson et al.⁹⁰ 6-Bromo-1,8-naphthalic anhydride (1 g, 3.61 mmol) and Ethylamine (70% in water) (excess) were refluxed in 50 mL 1,4 Dioxane for 20 h. After cool-down to room-temperature the reaction mixture was poured into water. The precipitated solid was collected by filtration, washed with water, dried and purified by column chromatography.

m = 0.944 g (3.11 mmol, 86 %) cream-white solid

¹H-NMR (300 MHz, CDCl₃) δ: 1.31 (t, 3 H), 4.22 (q, 2 H), 7.83 (dd, 1 H), 8.02 (d, 1 H), 8.40 (d, 1 H), 8.55 (dd, 1 H), 8.65 (dd, 1 H)

MS, Calcd. for [M+ H]⁺ 303.99, found 303.99

Step 2: 2-Ethyl-6-hydrazino-benzo[de]isoquinoline-1,3-dione

(6-Bromo-2-ethyl-benzo[de] isoquinoline- 1,3-dione) (120 mg, 0.39 mmol) was dissolved in 30 mL of 1,4-dioxane. Subsequently, 2.5 mL Hydrazine monohydrate were added drop wise. and the solution was stirred at 60 °C for 18 h. After cool-down to room temperature, the reaction mixture was poured into water. The precipitated solid was collected by filtration, washed with water and dried, yielding a yellow solid.

Yield = 90 mg (0.35 mmol, 90 %).

¹H-NMR (300 MHz, DMSO-d₆) δ: 1.14 (t, 3H), 4.01 (q, 2H), 4.63 (s, 2H), 7.20 (d, 1H), 7.58 (dd, 1H), 8.24 (d, 1H), 8.37 (d, 1H), 8.56 (dd, 1H), 9.07 (s, 1H).

MS, Calcd. for [M+ H]⁺ 256.10, found 256.10

Step 3: N-Ethyl-4-(N-[4-vinylphenyl]hydrazinecarboxamidyl)-1,8- naphthalimide (1)

The reaction was carried out under inert gas atmosphere.

(2-Ethyl-6-hydrazino-benzo[de]isoquinoline-1,3-dione) (150 mg, 0.59 mmol) was dissolved in 12 mL THF/pyridine (50:50, v/v). 1-Isocyanato-4-vinylbenzene (85 mg, 0.59 mmol) dissolved in 12 mL THF/pyridine (50:50, v/v) was added drop wise. The solution was stirred at 28 °C for two days under inert atmosphere, precipitated from n-hexane, filtrated and dried, yielding a yellow solid.

Yield = 136.88 mg (0.34 mmol, 58 %).

^1H NMR (400 MHz, *DMSO* d_6) δ ppm 1.15 (t, $J = 7.0$ Hz, 3H), 4.03 (q, $J = 7.0$ Hz, 2H), 5.08 (d, $J = 11.7$ Hz, 1H), 5.64 (d, $J = 17.6$ Hz, 1H), 6.60 (dd, $J = 17.7, 10.8$ Hz, 1H), 7.01 (d, $J = 8.5$ Hz, 1H), 7.39 (q, $J = 29.6, 8.5$ Hz, 4H), 7.73 (m, 1H), 8.33 (d, $J = 8.4$ Hz, 1H), 8.46 (d, $J = 6.7$ Hz, 1H), 8.64 (s, 1H), 8.68 (d, $J = 8.6$ Hz, 1H), 9.04 (s, 1H), 9.55 (s, 1H).

^{13}C NMR (500 MHz, *DMSO* d_6) δ ppm 13.3, 34.2, 103.9, 107.3, 112.0, 118.0, 118.4, 121.7, 124.0, 126.6, 128.2, 129.2, 130.4, 130.8, 134.1, 136.2, 139.3, 152.2, 153.1, 162.6, 163.5.

HRMS, Calcd. for $\text{C}_{23}\text{H}_{21}\text{O}_3\text{N}_4$ $[\text{M} + \text{H}]^+$ 401.1608, found 401.1608.

4-Bromo-2-butyl-benzo[de]isoquinoline-1,3-dione

4-Bromo-1,8-naphthalic anhydride (0.300 g, 1.08 mmol) and n-Butylamine (0.095 g, 1.30 mmol, 1.2 eq) were dissolved in Ethanol (17 mL) and stirred under reflux for 18 h. The reaction mixture was poured into water, the Ethanol was removed under reduced pressure and the solid collected by filtration, yielding a yellow-white solid. This compound has been published before in.⁹¹

Yield = 261 mg (0.79 mmol, 73 %)

^1H -NMR (300 MHz, *DMSO*- d_6) δ : 0.88 (t, 3 H), 1.31 (m, 2 H), 1.58 (m, 2H), 3.99 (t, 2H), 7.97 (t, 1 H), 8.19 (d, 1 H), 8.30(dd, 1 H), 8.53 (dd, 2 H)

2-Butyl-6-hydrazino-benzo[de]isoquinoline-1,3-dione

4-Bromo-2-butyl-benzo[de]isoquinoline-1,3-dione (100 mg, 0.301 mmol) and Hydrazine Monohydrate (4.7 mL, excess) were dissolved in 6 mL THF. The solution was stirred at 60°C for 24 h, precipitated from water, filtrated and dried.

m = 81.02 mg (0.29 mmol, 95 %) orange solid

^1H -NMR (300 MHz, *DMSO*- d_6) δ : 0.88 (t, 3 H), 1.29 (m, 2 H), 1.55 (m, 2H), 3.99 (t, 2H), 4.64 (s, 2H), 7.21 (d, 1H), 7.60 (t, 1 H), 8.25 (d, 1 H), 8.37 (d, 1 H), 8.57 (d, 1 H), 9.08 (s, 1 H)

(2-Butyl-6-[4-tolylcarbamoil])-benzo[de]isoquinoline-1,3-dione

Prior to reaction the apparatus was heated out and flushed extensively with nitrogen.

2-Butyl-6-hydrazino-benzo[*de*]isoquinoline-1,3-dione (30 mg, 0.106 mmol) was dissolved in 10 ml THF/ Pyridine (50:50, v/v). A solution of 1- Isocyanato-4-vinylbenzene (18.37 mg, 0.106 mmol) in 10 ml THF/ Pyridine (50:50, v/v) was added dropwise. The mixture was stirred at 30 °C for five days under nitrogen atmosphere, precipitated from Hexane, filtrated and dried yielding a reddish solid.

Yield = 44.93 mg (0.105 mmol, 99 %)

¹H-NMR (300 MHz, DMSO-*d*₆) δ: 0.88 (t, 3 H), 1.29 (m, 2 H), 1.56 (m, 2 H), 3.99 (t, 2 H), 5.08 (d, 1H), 5.65 (d, 1H), 6.60 (q, 1 H), 7.01 (d, 1 H), 7.32 (d, 2 H), 7.47 (d, 2 H), 7.73 (t, 1 H), 8.32 (d, 1H), 8.45 (d, 1 H), 8.68 (d, 2 H), 9.04 (s, 1 H), 9.55 (s, 1 H)

m/z 429 (m + H)⁺

M.p. (DSC): 296 °C

Purity (DSC): 95.73 %

IR (KBr) ν_{\max} (cm⁻¹): 3291, 1691, 1643, 1582, 1530, 1387, 1309, 1235, 1191, 1083, 989, 900, 843, 769, 755

Synthesis of 2

Step 1: 2,3-Dimethyl-1 H-indol-7-amine

2,3-Dimethyl-7-nitro-1 *H*-indole (556 mg, 2.92 mmol) was dissolved in 20 mL MeOH/ Toluene (50:50, v/v). Pd/C was then added as catalyst and the system was flushed extensively with H₂ to remove present oxygen. The suspension was stirred overnight at ambient temperature under hydrogen atmosphere. Afterwards the catalyst was removed by filtration. Evaporation of the solvent yielded the product as a deep-purple solid.

Yield = 480 mg (> 100 %)

¹H NMR (DMSO) δ 2.05 (s, 3H), 2.25 (s, 3H), 4.78 (s, 2H), 6.19 (dd, 1H), 6.60 (m, 2H), 10.11 (s, 1H)

m/z 161 (m + H)⁺

Step 2: 1-(2,3-Dimethyl-1H-indol-7-yl)-3-(4-vinyl-phenyl)-urea

Prior to reaction the apparatus was heated out and flushed extensively with nitrogen.

2,3-Dimethyl-1 *H*-indol-7-amine (50 mg, 0.312 mmol) was dissolved in THF/ Pyridin (6 mL, 50:50, v/v). 1-Isocyanato-4-vinyl-benzene (43.47 μL, 0.312 mmol) was dissolved in 6 mL of

the same mixture and added to the 2,3-Dimethyl-1 *H*-indol-7-amine- solution dropwise. After 48 h stirring at 28 °C under nitrogen atmosphere the solution was poured into n-Hexane, filtered and dried yielding a grey-reddish solid.

Yield = 89.45 mg (0.293 mmol, 94 %)

¹H-NMR (300 MHz, DMSO-d₆) δ: 2.10 (s, 3 H), 2.28 (s, 3 H), 5.09 (d, 1H), 5.65 (d, 1H), 6.62 (q, 1 H), 6.84 (t, 1 H), 6.97 (d, 1 H), 7.08 (d, 1 H), 7.35 (d, 2 H), 7.44 (d, 2H), 8.28 (s, 1 H), 8.80 (s, 1 H), 10.23 (s, 1 H)

MS, Calcd. for C₁₉H₁₉N₃O [M+ H]⁺ 306.152, found 306.15

The synthesis of compounds 4 and 5 has been described in the Ph.D. thesis of Issam Lazraq.⁹²

1-(4-(2,4-dinitrophenylamino)phenyl)-3-(4-vinylphenyl)urea (4)

Prior to reaction the apparatus was heated out and flushed extensively with nitrogen.

N-(2,4-dinitrophenyl)benzene-1,4-diamine (500 mg, 1.192 mmol) was dissolved in 20 mL THF/ Pyridine (50:50, v/v). A solution of 1-Isocyanato-4-vinylbenzene (173.06 mg, 1.192 mmol) was added drop-wise. The reaction mixture was stirred at 32 °C for 72 h under nitrogen atmosphere and subsequently precipitated from n-Hexane. The precipitated solid was collected by filtration and recrystallised from Methanol yielding an ochre solid.

Yield = 374.94 mg (0.894 mmol, 75 %)

¹H-NMR (300 MHz, DMSO-d₆) δ: 5.10 (d, 1H), 5.67 (d, 1H), 6.63 (dd, 1H), 7.01(d, 1H), 7.26 (d, 2H), 7.32 (m, 4H), 7.55 (d, 2H), 8.18(dd, 1H), 8.53 (s, 1H), 8.77 (s, 1H), 8.85 (m, 1H), 10.09 (s, 1H)

MS, Calcd. [m + H]⁺ 420.13, found 420.12.

1-(2-(trifluoromethyl)-1H-benzimidazol-5-yl)-3-(4-vinylphenyl)urea (5)

Prior to reaction the apparatus was heated out and flushed extensively with nitrogen.

To a solution of 5-Amino-2-(trifluoromethyl)benzimidazole (1.50 mg, 7.46 mmol) in 50 mL THF:Pyridine (50:50, v/v), were added (1.08 mg, 7,46 mmol) of 1-isocyanato-4-vinylbenzene dissolved in 50 ml of the same solvent mixture drop-wise. The reaction mixture was stirred

for 60 h at 32 °C under nitrogen atmosphere and subsequently precipitated from n-Hexane. The precipitated solid was collected by filtration and dried yielding a red-brown solid.

Yield = 1.598 g (4.614 mmol, 62%)

¹H-NMR (300 MHz, DMSO-d₆) δ: 5.10 (d, 1H), 5.62 (d, 1H), 6.61 (dd, 1H), 7.20 (d, 1H), 7.40 (m, 3H), 7.61 (d,1H), 8.00 (s, 1H), 8.55 (s, 1H), 8.78 (s, 1H), 8.40 (s, 1H)

Bulk polymer synthesis

The synthesis procedure is here displayed in an exemplaric way for the glutamic-acid imprinted polymer.

The imprinted polymer **P_{MGlu}** was prepared in the following manner., The template Z-L-Glu (0.25 mmol), PMP (0.5 mmol), the functional monomer **1** (0.5 mmol) and EDMA (20 mmol) were dissolved in DMF (5.6 mL). After addition of the initiator ABDV (1 % w/w total monomers) the pre-polymerisation solution was transferred to a glass polymerisation tube and purged with a flow of dry nitrogen for 10 min. The tube was flame-sealed and placed in a polymerisation bath at 45°C. After 24 h the tube was broken and the polymer monolith lightly crushed. The template molecule was removed by soxhlet extraction with MeOH: HCl (0.5 mM) (80:20 v/v) for 24 h and 24 h with MeOH. Thereafter, the particles were further crushed and sieved to obtain particles in the size range 25-50 μm.

(The polymers imprinted on Z-L-Phe **P_{Mphe}** and Penicillin G Procaine salt **P_{MPen}** were prepared accordingly, but in a template: monomer ratio 1:1. A non-imprinted polymer **P_N** was prepared in the same way, but with the omission of the template and PMP.)

The success of the polymer synthesis was evaluated via elemental analysis:

Polymers prepared based on **1**:

Anal. calc. for **P_{MGlu}**: C, 61.00; H, 7.02; N, 0.67. Found: C, 60.24; H, 7.51; N, 0.70

Anal. calc. for **P_{Mphe}**: C, 61.00; H, 7.02; N, 0.67. Found: C, 60.57; H, 7.54; N, 0.75

Anal. calc. for **P_{MPenG}**: C, 61.00; H, 7.02; N, 0.67. Found: C, 60.43; H, 7.74; N, 0.76

Anal. calc. for **P_N**: C, 61.00; H, 7.02; N, 0.67. Found: C, 60.30; H, 7.43; N, 0.75

Polymers prepared based on **4**:

Anal. calc. for **P_{MGlu}**: C, 60.57; H, 6.97; N, 0.84. Found: C, 60.11; H, 7.63; N, 0.82

Anal. calc. for **P_{MPhc}**: C, 60.57; H, 6.97; N, 0.84. Found: C, 59.11; H, 7.46; N, 0.83

Anal. calc. for **P_{MPenG}**: C, 60.57; H, 6.97; N, 0.84. Found: C, 60.09; H, 7.69; N, 0.79

Anal. calc. for **P_N**: C, 60.57; H, 6.97; N, 0.84. Found: C, 59.89; H, 7.48; N, 0.75

Polymers prepared based on **5**:

Anal. calc. for **P_{MGlu}**: C, 60.52; H, 6.98; N, 0.68. Found: C, 59.51; H, 7.25; N, 0.67

Anal. calc. for **P_{MPhc}**: C, 60.52; H, 6.98; N, 0.68. Found: C, 59.69; H, 7.33; N, 0.65

Anal. calc. for **P_{MPenG}**: C, 60.52; H, 6.98; N, 0.68. Found: C, 59.98; H, 7.21; N, 0.68

Anal. calc. for **P_{MGlu}**: C, 60.52; H, 6.98; N, 0.68. Found: C, 59.99; H, 7.42; N, 0.59

All polymers show good agreement between measured and calculated values. Thus, it can be concluded that the polymer synthesis was successful and the monomers were integrated into the polymers quantitatively.

Polymers with varying cross-linking level

High load polymers:

The polymers were prepared in the following manner. The functional monomer **1** (0.5 mmol), MMA and EDMA (20 mmol) were dissolved in DMF (5.6 mmol). After addition of the initiator ABDV (1 % w/w total monomers) the pre-polymerisation solution was purged with a flow of dry nitrogen for 10 min. The tube was placed in a polymerisation bath at 45°C. Subsequently the polymers were removed from the tubes, lightly crushed and purified by extraction using methanol.

(The NIPs were prepared accordingly but in absence of the template molecule.)

Low load polymers

The functional monomer **1**, the template TBA-Benzoate and varying ratios of MMA and EDMA were dissolved in DMF. After addition of the initiator ABDV (1 % w/w total monomers) the pre-polymerisation solution was purged with a flow of dry nitrogen for 5 min. The polymerisation-tubes were kept in a polymerisation bath at 45°C for 24 h and at 60 °C for 24 h.

Subsequently the polymers were removed from the tubes, lightly crushed and purified by extraction using methanol.

(The NIPs were prepared accordingly but in absence of the template molecule.)

Elemental analysis of low load polymers:

NIPs:

Anal. calc. for **P_{N1}**: C, 60.16; H, 7.99; N, 0.27. Found: C, 58.26; H, 7.30; N, 0.40

Anal. calc. for **P_{N2}**: C, 60.24; H, 7.86; N, 0.25. Found: C, 57.64; H, 7.07; N, 0.32

Anal. calc. for **P_{N3}**: C, 60.26; H, 7.81; N, 0.25. Found: C, 58.97; H, 6.57; N, 0.30

Anal. calc. for **P_{N4}**: C, 60.39; H, 7.59; N, 0.21. Found: C, 58.37; H, 6.95; N, 0.26

Anal. calc. for **P_{N5}**: C, 60.50; H, 7.40; N, 0.19. Found: C, 58.37; H, 6.94; N, 0.25

Anal. calc. for **P_{N6}**: C, 60.58; H, 7.26; N, 0.16. Found: C, 58.42; H, 6.79; N, 0.23

Anal. calc. for **P_{N7}**: C, 60.68; H, 7.10; N, 0.14. Found: C, 58.41; H, 7.01; N, 0.24

MIPs:

Anal. calc. for **P_{M1}**: C, 60.33; H, 7.70; N, 0.23. Found: C, 57.38; H, 7.53; N, 0.30

Anal. calc. for **P_{M2}**: C, 60.48; H, 7.44; N, 0.19. Found: C, 58.26; H, 6.87; N, 0.24

Anal. calc. for **P_{M3}**: C, 60.53; H, 7.35; N, 0.18. Found: C, 58.44; H, 6.79; N, 0.22

Anal. calc. for **P_{M4}**: C, 60.58; H, 7.26; N, 0.16. Found: C, 58.44; H, 6.96; N, 0.20

Film systems

RAFT system

Cover Glasses with a diameter of 5 mm and nominal thickness of 0.145 mm were purchased from Thermo Scientific, Menzel GmbH & Co. KG.

Pretreatment/ Activation

Prior usage the glass slides were washed with saturated KOH, 1.67 mM HCl and subsequently with 15 mL 30 % H₂O₂ and 90 mL H₂O. The slides were then rinsed twice with copious amounts of water and with acetone and dried.

Aminolysation

2 g of the activated glass slides were rinsed with dry toluene and then refluxed in presence of (3-aminopropyl)triethoxysiloxane (2.267 g, 0.010 mM) in 250 mL of dry toluene for 24 h.

Immobilisation of the RAFT agent (4-cyanopentanoic acid dithiobenzoate)

Prior to usage the apparatus consisting of a three neck flask equipped with an overhead stirrer and a dropping funnel was heated out and flushed extensively with N₂. It was kept under nitrogen for the whole reaction time.

The RAFT agent (321.008 mg, 1.149 mM), 124.689 μ L (1.149 mM) Ethylchloroformate and 116.26 μ L (1.149 mM) Triethylamin were dissolved in 50 mL dry THF in a three neck flask equipped with an overhead stirrer and a dropping funnel. The reaction mixture was cooled to -78 °C using a liquid-nitrogen- ethanol bath and stirred for 30 min at this temperature. Subsequently the functionalized glass slides were added and the mixture was stirred another 3 h at -78 °C. The reaction mixture was then kept at RT overnight.

The glass slides were separated from the reaction mixture via filtration and washed extensively with THF and MeOH to remove the precipitate. Subsequently they were dried under vacuum at RT and stored under inert conditions at 8 °C.

Thin - film formation via „grafting from“

1. Drop method

The template Z-L-Glutamic acid (0.703 mg, 0.003 mM) and PMP (0.779 mg, 0.005 mM) were dissolved in 1.3 mL of solvent (DMF, CHCl₃, ACN, ACN: Toluene (50:50 (v/v))). Subse-

quently the functional monomer 1 (2.201 mg, 0.022 mM), the co- monomer MMA (116.710 mg, 1.166 mM), the cross-linker EDMA (991.100 mg, 5 mM) and the initiator ABDV (1 w%) were added and the pre-polymerisation mixture was flushed with nitrogen for 5 min.

4 μ L of the pre-polymerisation mixture were dropped on a RAFT modified glass slide mounted in the lid of an Eppendorf vessel. The glass slide was covered with an unmodified slide. After flushing with nitrogen the Eppendorf vessel was sealed and kept at 45 °C for the desired reaction time (30, 60, 90, 180 min). Subsequently the cover slide was removed and the obtained films were rinsed with Chloroform in order to remove unreacted pre-polymerisation mixture. The slides were then evaluated via optical microscopy and using a 96 well plate reader.

1. Dip method

The polymerisation was initiated thermally at 45 °C in an incubator.

In this approach the glass slides were kept completely covered in the pre-polymerisation mixture during the whole reaction time. In order to avoid macrogelation, four different methods were tested:

- Dilution of the system upon increasing the amount of solvent
- Reduction of the amount of added initiator
- Addition of soluble RAFT agent in 1/1 ratio with respect to the initiator
- Quench polymerisation reaction at low conversion

The pre-polymerisation mixture follows the recipe displayed in **Table 15.1**.

	Z-L-Glu [mmol]	PMP [mmol]	n_{Urea} [mmol]	n_{MMA} [mmol]	n_{EDMA} [mmol]
NIP	-	-	0.022	4.663	20
MIP	0.011	0.022	0.022	4.663	20

Table 14.1: *Polymer composition*

The ratios displayed in **Table 14.1** result in a cross-linking level of 81 %. This cross-linking level showed the most significant change in the life time of the bulk polymers upon addition of increasing concentration of the guest TBA Benzoat.

The different approaches to avoid macrogelation are displayed in **Table 14.2**:

	Z-L-Phe [mmol]	PMP [mmol]	ABDV/RAFT [mg]	1 [mmol]	MMA [mmol]	EDMA [mmol]
Dilution 1x						
NIP I	/	/	8/0	0.022	4.663	20
MIP I	0.022	0.022	8/0	0.022	4.663	20
NIP II	/	/	8/8	0.022	4.663	20
MIP II	0.022	0.022	8/8	0.022	4.663	20
NIP III	/	/	0.8/0	0.022	4.663	20
MIP III	0.022	0.022	0.8/0	0.022	4.663	20
NIP 30 I	/	/	8/0	0.022	4.663	20
MIP 30 I	0.022	0.022	8/0	0.022	4.663	20
Dilution 2x						
NIP IV	/	/	8/0	0.022	4.663	20
MIP IV	0.022	0.022	8/0	0.022	4.663	20
NIP V	/	/	8/8	0.022	4.663	20
MIP V	0.022	0.022	8/8	0.022	4.663	20
NIP VI	/	/	0.8/0	0.022	4.663	20
MIP VI	0.022	0.022	0.8/0	0.022	4.663	20
NIP 30 II	/	/	8/0	0.022	4.663	20
MIP 30 II	0.022	0.022	8/0	0.022	4.663	20

Table 15.2: Approaches to avoid macrogelation

The pre-polymerisation mixtures were prepared in ACN.

The template Z-L-Phenylalanine (1.645 mg, 0.006 mmol) and PMP (0.853 mg, 0.006 mmol) were dissolved in 1.4 mL (respectively 2.8 mL) anhydrous ACN. Subsequently, the functional monomer 1 (2.200 mg, 0.006 mmol), the co-monomer MMA (116.575 mg, 1.166 mmol) and the cross-linker EDMA (991.100 mg, 5.000 mmol) were added. After addition of the azo-initiator ABDV (1 w-%) (and RAFT agent in stoichiometric amount with respect to ABDV) the pre-polymerisation solution was flushed for 5 min with nitrogen. Thereafter the RAFT-modified glass slides were put into the pre-polymerisation mixture and the polymerization was initiated thermally at 50 °C in an incubator equipped with a roller.

In case of the polymers labeled with a “30” the polymerization was interrupted after 30 min.

In the cases where the pre-polymerisation mixture macrogelated the film-formation was repeated and polymerization was interrupted after 2 h. This led to film formation.

After the removal from heat the glass-slides were taken out from the polymerisation mixture and rinsed carefully with CHCl_3 in order to remove unreacted monomers from the surface of the immobilized films without removing the template.

Polymer films immobilised with 3-Methacryloxypropyltrimethoxysilane:

Preparation of the coverslips:

300 coverslips were pre-cleaned for 12 h with conc. KOH solution and subsequently carefully rinsed with water. For activating the surface the coverslips were left in piranha acid overnight and rinsed with water, acetone and toluene and dried.

The linker 3-Methacryloxypropyltrimethoxysilane was immobilised by stirring the coverslips in a solution of the linker (20 mL) and triethylamine (7mL) in toluene (150 mL). Subsequently, the coverslips were washed with Toluene and MTBE and dried.

Polymer films were prepared to the following ratio and immobilised on coverslips with 3-Methacryloxypropyltrimethoxysilane. **1** (0.06 mg, 0.15 μmol), TBA-Z-L-Phe (equimolar to **1**), (Hydroxyethyl)methacrylate (HEMA, 12.86 μL , 0.11 mmol) and ethylene glycol dimethacrylate (EDMA, 8.58 μL , 0.04 mmol) were dissolved in 25 μL pentachlorethane, respectively toluene. The NIP was prepared accordingly without the template. After the oxygen was removed with an Argon flow ABDV was added. 2 μL of the solutions were dropped on a glass slide and covered with a 3-Methacryloxypropyltrimethoxysilane-modified coverslip. Polymerisation was initiated thermally, either by heating with a heat-gun three times for 10 seconds and subsequently in the oven at 70 °C, or at 50°C in the oven for 3 h.

Films employing MMA and BMA instead of HEMA were prepared accordingly.

The coverslips were subsequently extracted via soxhlet extraction in MeOH and evaluated spectroscopically.

The thickness of the obtained films was determined by SEM:

PenG NIP	PenG MIP	MMA NIP	MMA MIP	BMA NIP	BMA MIP
1,935 ± 0,035	1,925 ± 0.045	2,235 ± 0.055	1,721 ± 0.048	1.384 ± 0.064	2.03 ± 0

14.2.Evaluation

14.2.1.Apparatus and instruments

Chromatographic evaluations were performed using a Hewlett-Packard instrument (HP 1050) equipped with a quaternary pump, an autosampler, a diode array detector and HP workstation. Spectrophotometric analysis of the bulk polymers was performed using a multifunctional plate reader SAFIRE, From Tecan Deutschland GmbH (Crailsheim, Germany). (Wavelength measurement accuracy ± 1 nm). Absorption spectra and UV/VIS-spectrometric titrations were performed on a Specord 210 Plus absorption spectrometer (Analytik Jena). Fluorescence measurements were performed on FluoroMax 4 spectrofluorometer (Horiba Jobin Yvon).

HPLC analysis of bulk polymers

The 25-50 μm particle size fraction was repeatedly sedimented (80/20 methanol/millipore water) to remove fine particles and then slurry-packed into stainless-steel HPLC columns (2.5 x 0.4 cm) using the same solvent mixture as pushing solvent. Prior to usage the columns were first washed with methanol to ensure the complete template removal. Subsequent analysis of the polymers was performed using an Agilent HP1050 system equipped with a diode array-UV detector and a workstation. Analyte detection was performed at 205 and 260 nm (Z-Glu, Z-Phe) and 220 nm PenG. In order to evaluate the polymers ability to discriminate between its template, other enantiomer of the template and a non-template, solutions of Z-L-Glutamic acid, Z-D-Glutamic acid and Z-L-Phenylalanine were injected. The Glutamic acid solutions were prepared in the corresponding mobile phases, concentration 10 mM, injection volume 10 μl . Due to the poor solubility of Z-L-Phenylalanine in mobile phases with high water content, the concentration was lowered to 1 mM, injection volume 100 μl .

Swelling test of bulk polymers

A fraction of the ground monolithic polymer was filled into an NMR tube. The height of the polymer layer was measured. The tube was filled with 1 mL of the respective solvent system.

After 24 h the height of the swollen polymer in the tube was measured again. The swelling factor is calculated as the quotient of the polymer height after swelling divided by the polymer height before swelling.

Fluorescence monitored batch rebinding

To define the optimum excitation wavelength for the polymer an emission spectrum was recorded at the maximum absorption wavelength for the employed monomer. The emission wavelength associated to the maximum emission intensity was used to perform an excitation scan. The maximum of the resulting excitation spectrum was then chosen as optimum excitation wavelength for the measurements.

12 times 10 mg of \mathbf{P}_N and 24 times \mathbf{P}_{MGlu} were weighed into a 96 well-plate and incubated for 4 h with 12 different concentrations (between 0-2 mM) of Z-D-Glu and Z-L-Glu solutions in H₂O (respectively DMSO). After 3 h emission scans of all wells were performed (emission wavelength range: 390 – 800 nm; excitation wavelength: 377 nm).

In order to determine the uncertainty generated from using different wells another measurement principle was tested.

2 times 10 mg of \mathbf{P}_{MGlu} and its corresponding NIP were weight into a 96 well-plate and incubated with 200 μ l ACN: H₂O (50:50, v/v). Z-L-GLu (respectively Z-D-Glu) was added from a highly concentrated stock solution in small portions to yield the concentrations 1 μ M, 10 μ M, 100 μ M, 500 μ M and 1 mM. After each addition the fluorescence emission intensity was measured after 10 min, 30 min and 50 min (emission wavelength range: 400 - 800 nm; excitation wavelength: 405 nm). The change of fluorescence emission intensity was monitored time-resolved and dependent on the concentration.

Evaluation of the RAFT slides

After gain optimisation the fluorescence emission intensity (λ_{ex} : 420 nm; λ_{em} : 435 – 700 nm, bandwidth 7.5/7.5, step-size 2 nm) of the polymer films was evaluated in ACN and in presence of increasing concentration of Z-L-Phe and Z-D-Phe in ACN. Prior to analysis the measurement error was defined by measuring one polymer slide six times in a row according to

exactly the same principle. From these measurements the standard deviation was calculated to be less than 2 %.

Thin-layer polymer films

The obtained polymer films were extracted using a soxhlet apparatus with MeOH. Subsequently, they were mounted in a custom-made quartz-glass cuvette equipped with a teflon holder. The fluorescence emission of the films was monitored during titrations with increasing concentration of selected analytes between 0 and 1 mM (excitation wavelength: 380 nm, emission wavelength range: 395 - 550 nm). The obtained results were background corrected with respect to the starting fluorescence.

15. References

- 1 Sellergren, B., *Angew. Chem. Int. Ed.*, **2000**, *39*, 1031-1037
- 2 Sellergren, B.,(ed) *Molecularly imprinted polymers. Man made mimics of antibodies and their applications in analytical chemistry*, Elsevier Science B.V., Amsterdam, 2001
- 3 Danielsson, B., *Adv. Biochem. Engin/ Biotechnol.*, **2008**, *109*, 97-122
- 4 Sellergren, B., The non-covalent approach to molecular imprinting. In *Molecularly imprinted polymers. Man made mimics of antibodies and their applications in analytical chemistry*; Sellergren, B., Elsevier Science B.V., Amsterdam, 2001; p 161
- 5 Mohanraj, V.J., Chen, Y., *Tropical Journal of Pharmaceutical Research*, **2006**, *5,1*, 561 - 573
- 6 films mass transfer sensing applications
- 7 Al-Kindy, S., Badína, R., Suárez-Rodríguez, J. L., Díaz-García, M. E., *Crit. Rev. in Anal. Chem.*, **2000**, *30*, 291-309
- 8 Saha, S., Samanta, A., *J. Phys. Chem. A*, **2002**, *106*, 4763 - 4771
- 9 IUPAC. Compendium of Chemical Terminology, 2nd ed. (the "Gold Book"). Compiled by A. D. McNaught and A. Wilkinson. Blackwell Scientific Publications, Oxford (1997). XML on-line corrected version: <http://goldbook.iupac.org> (2006-) created by M. Nic, J. Jirat, B. Kosata; updates compiled by A. Jenkins. ISBN 0-9678550-9-8. [doi:10.1351/goldbook](https://doi.org/10.1351/goldbook), accessed 4.5.2012
- 10 IUPAC. Compendium of Chemical Terminology, 2nd ed. (the "Gold Book"). Compiled by A. D. McNaught and A. Wilkinson. Blackwell Scientific Publications, Oxford (1997). XML on-line corrected version: <http://goldbook.iupac.org> (2006-) created by M. Nic, J. Jirat, B. Kosata; updates compiled by A. Jenkins. ISBN 0-9678550-9-8. [doi:10.1351/goldbook](https://doi.org/10.1351/goldbook), accessed 4.5.2012
- 11 Hulanicki, A., Geab, S., Ingman, F., *Pure & Appl. Chem.*, **1991**, *63*, 9, 1247 - 1250 (IUPAC)
- 12 Hulanicki, A., Geab, S., Ingman, F., *Pure & Appl. Chem.*, **1991**, *63*, 9, 1247 - 1250 (IUPAC)
- 13 Rurack, K., Resch-Genger, U., *Chem. Soc. Rev.*, **2002**, *31*, 116-127
- 14 Suksai, C., Tuntulani, T., *Chem. Soc. Rev.*, **2003**, *32*, 192-202
- 15 Gunnlaugsson, T., Kruger, P., E., Jensen, P., Tierney, J., Ali, H. D. P., Hussey, G. M., *J. Org. Chem.*, **2005**, *70*, 10875-10878
- 16 Gale, P.A., *Coord. Chem. Rev.*, **2003**, *240*, 191-221
- 17 Gale, P. A., *Chem. Soc. Rev.*, **2010**, *39*, 3746-3771
- 18 Martínez-Máñez, R., Sancenón, F., *Chem. Rev*, **2003**, *103*, 4419-4476
- 19 Piletsky, S.A., Piletsaya, E.V., El'skaya, A.V., Levi, R., Karube, I., *Anal. Lett.*, **1997**, *30*, 445
- 20 Martínez-Máñez, R., Sancenón, F., *Chem. Rev*, **2003**, *103*, 4419-4476

- 21 Suksai, C., Tuntulani, T., *Chem. Soc. Rev.*, **2003**, 32, 192-202
- 22 Bissell, R. A., Prasanna de Silva, A., Gunaratne, H. Q. N., Lynch, P. L. M., Maguire, G. E. M., Sandanayake, K. R. A. S., *Chem. Soc. Rev.*, **1992**, 187-195
- 23 Manesiotis, P., Hall, A. J., Emgenbroich, M., Quaglia, M., De Lorenzi, E., Sellergren, B., *Chem. Commun.*, **2004**, 2278-2279
- 24 Hall, A.J., Manesiotis, P., Emgenbroich, M., Quaglia, M., De Lorenzi, E., Sellergren, B., *J. Org. Chem.*, **2005**, 70, 1732-1736
- 25 Nicholls, I.A., Andersson, H. S., Thermodynamic principles underlying molecularly imprinted polymer formulation and ligand recognition. In *Molecularly imprinted polymers. Man made mimics of antibodies and their applications in analytical chemistry*; Sellergren, B., Elsevier Science B.V., Amsterdam, 2001; p 59
- 26 Wulff, G., Biffis, A., Molecular imprinting with covalent or stoichiometric non-covalent interactions, In *Molecularly imprinted polymers. Man made mimics of antibodies and their applications in analytical chemistry*; Sellergren, B., Elsevier Science B.V., Amsterdam, 2001; p 102
- 27 Wulff, G., Sarhan, A., *Angew. Chem. internat. Edit.*, **1972**, Vol.11, No. 4
- 28 Wulff, G., Sarhan, A., Zabrocki, K., *Tetrahedron Letters*, **1973**, 44, 4329 - 4332
- 29 Komiyama, M., Takeuchi, T., Mukawa, T., Asamuma, H.,(ed) *Molecular Imprinting. From Fundamentals to applications*, Wiley-VCH, 2003, p. 16
- 30 Shea, K.J., Sasaki, D.Y., *J. Am. Chem. Soc.*, **1989**, 111, 3442-3444
- 31 Dickey, F.H., *Proc. Natl. Acad. Sci. USA*, **1949**, 35 after Andersson, H. S., Nicholls, I. A., A historical perspective of the development of molecular imprinting, In *Molecularly imprinted polymers. Man made mimics of antibodies and their applications in analytical chemistry*; Sellergren, B., Elsevier Science B.V., Amsterdam, 2001; p 6
- 32 Andersson, L., Sellergren, B., Mosbach, K., *Tetrahedron Letters*, **1984**, 25, (45), 5211 - 5214
- 33 Komiyama, M., Takeuchi, T., Mukawa, T., Asamuma, H.,(ed) *Molecular Imprinting. From Fundamentals to applications*, Wiley-VCH, 2003
- 34 Komiyama, M., Takeuchi, T., Mukawa, T., Asamuma, H.,(ed) *Molecular Imprinting. From Fundamentals to applications*, Wiley-VCH, 2003, p. 37
- 35 Sellergren, B., Lepistö, M., Mosbach, K., *J. Am. Chem.Soc.*, **1988**, 110, 5853 - 5860
- 36 Wulff, G., Schönfeld, R., *Adv. Mater.*, **1998**, 10, 12, 957 - 959
- 37 Moad, G., Rizzardo, E., Thang, S. H., *Accounts*, **2008**, 41, 9, 1133 - 1142
- 38 Pérez-Moral, N, Mayes, A. G., *Bioseparation*, **2002**, 10, 287-299
- 39 IUPAC. Compendium of Chemical Terminology, 2nd ed. (the "Gold Book"). Compiled by A. D. McNaught and A. Wilkinson. Blackwell Scientific Publications, Oxford (1997). XML on-line corrected version: <http://goldbook.iupac.org> (2006-) created by M. Nic, J. Jirat, B. Kosata; updates compiled by A. Jenkins. ISBN 0-9678550-9-8. [doi:10.1351/goldbook](https://doi.org/10.1351/goldbook).

- 40 Jenkins, A. D., Jones, R. G., Moad, G, *Pure Appl. Chem.* **2010**, 82, 2, 483 - 491 (IUPAC)
- 41 Wang, J.-S., Matyjaszewski, K., *Macromol.*, **1995**, 28, 7901 - 7910
- 42 Moad, G., Chiefari, J., Chong, YK, Krstina, J., Mayadunne, R. T. A., Postma, A., Rizzardo, E., Thang, S. H., *Polym, int.*, **2000**, 49, 993 - 1011
- 43 Chiefari, J., Chong Y. K., Ercole, F., Krstina, J., Jeffery, J., Le, T. P. T., Maydunne, R. R. A., Meijs, G. F., Moad, C. L., Moad, G. Rizzardo, E., Thang, S.-H., *Macromol.*, **1998**, 31, 5559 - 5562
- 44 Moad, G., Chiefari, J., Chong, YK, Krstina, J., Mayadunne, R. T. A., Postma, A., Rizzardo, E., Thang, S. H., *Polym, int.*, **2000**, 49, 993 - 1011
- 45 Mohanraj, V.J., Chen, Y., *Tropical Journal of Pharmaceutical Research*, **2006**, 5,1, 561 - 573
- 46 Nematollahzadeh, A., Sun, W., Aureliano, C. S. A.; Luetkemeyer, D., Stute, J., Abdekhodaie, M. J.; Shojaei, A., Sellergren, B., *Angewandte Chemie, Int. Ed.*, **2011**, 50, 2, 495-498
- 47 Descalzo, A. B., Marcos, M. D., Monte, C., Martinez - Manez, R., Rurack, K., *J. Mater. Chem.*, **2007**, 17, 4716 - 4723 after *Topics in Fluorescence Spectroscopy*, ed. J. R. Lakowicz, Plenum, New York, 1992–2004, vol. 1–8
- 48 Al-Kindy, S., Badína, R., Suárez-Rodríguez, J. L., Díaz-García, M. E., *Crit. Rev. in Anal. Chem.*, **2000**, 30, 291-309
- 49 Sellergren, B., The non-covalent approach to molecular imprinting, In *Molecularly imprinted polymers. Man made mimics of antibodies and their applications in analytical chemistry*; Sellergren, B., Elsevier Science B.V., Amsterdam, 2001; p 116
- 50 Sellergren, B., Lepistö, M., Mosbach, K., *J. Am. Chem., Soc.*, **1988**, 110, 5853-5860
- 51 Sellergren, B., Hall, A., Molecular imprinting with covalent or stoichiometric non-covalent interactions, In *Molecularly imprinted polymers. Man made mimics of antibodies and their applications in analytical chemistry*; Sellergren, B., Elsevier Science B.V., Amsterdam, 2001; p 35
- 52 Cormack, P. A. G., Zurutuza Elorza, A., *J. Chromatogr. B*, **2004**, 804, 173-182
- 53 Wulff, G., *Angew. Chem. Int. Ed. Engl.*, **1995**, 34, 1812-1832
- 54 Sellergren, B., Lepistö, M., Mosbach, K., *J. Am. Chem.Soc.*, **1988**, 110, 5853- 5860
- 55 Cormack, P. A. G., Zurutuza Elorza, A., *J. Chromatogr. B*, **2004**, 804, 173-182
- 56 Goossens, H., Ferech, M., Stichele, R. v.d., Elseviers, M., *Lancet*, **2005**, 365, 579 - 587
- 57 Turnage, *Lancet*, **2005**, 365, 579 - 587

- 58 Sellergren, B., Hall, A., Fundamental aspects on the synthesis and characterisation of imprinted network polymers , In *Molecularly imprinted polymers. Man made mimics of antibodies and their applications in analytical chemistry*; Sellergren, B., Elsevier Science B.V., Amsterdam, **2001**; p 35
- 59 Sellergren, B., Hall, A., Fundamental aspects on the synthesis and characterisation of imprinted network polymers , In *Molecularly imprinted polymers. Man made mimics of antibodies and their applications in analytical chemistry*; Sellergren, B., Elsevier Science B.V., Amsterdam, **2001**; p 35
- 60 Wulff, G., *Angew. Chem. Int. Ed. Engl.*, **1995**, *34*, 1812-1832
- 61 Sellergren, B., Hall, A., Fundamental aspects on the synthesis and characterisation of imprinted network polymers , In *Molecularly imprinted polymers. Man made mimics of antibodies and their applications in analytical chemistry*; Sellergren, B., Elsevier Science B.V., Amsterdam, **2001**; p 36
- 62 Sellergren, B., Hall, A., Fundamental aspects on the synthesis and characterisation of imprinted network polymers , In *Molecularly imprinted polymers. Man made mimics of antibodies and their applications in analytical chemistry*; Sellergren, B., Elsevier Science B.V., Amsterdam, **2001**; p 38
- 63 Komiyama, M., Takeuchi, T., Mukawa, T., Asamuma, H.,(ed) *Molecular Imprinting. From Fundamentals to applications*, Wiley-VCH, **2003**)
- 64 Wulff, G., Biffis, A., Molecular imprinting with covalent or stoichiometric non-covalent interactions, In *Molecularly imprinted polymers. Man made mimics of antibodies and their applications in analytical chemistry*; Sellergren, B., Elsevier Science B.V., Amsterdam, 2001; p 78
- 65 Guyot, A., In *Synthesis and separations using functional polymers*; Sherington, D. C., Hodge, P., ed., John Wiley & Sons Ltd., 1988
- 66 Manesiotis, P., Hall, A.J., Emgenbroich, M., Quaglia, M., De Lorenzi, E., Sellergren, B., *Chem. Commun*, **2004**, 2278 - 2279
- 67 Hall, A. J., Manesiotis, P., Emgenbroich, M., Quaglia, M., De Lorenzi, E., Sellergren, B., *J. Org. Chem*, **2005**, *70*, 1732 - 1736
- 68 Descalzo, A. B., Marcos, M. D., Monte, C., Martinez - Manez, R., Rurack, K., *J. Mater. Chem.*, **2007**, *17*, 4716 - 4723
- 69 Ghosh, P. B., Whitehouse, M. W., *Biochem. J.*, **1968**, *108*, 155 - 156
- 70 Brown, A., Ngai, T. Y Barnes, M. A., Key, J. A., Cairo, C. W., *J. Phys. Chem. A*, **2012**, *116*, 46 - 54

- 71 Wu, H.-H., Sun, Y.-L., Wan, C.-F., Yang, S.-T., Chen, S.-J., Hu, C.-H., Wu, A.-T., *Tetrahedron Letters*, **2012**, *53*, **9**, 1169 - 1172
- 72 Yu, H.-T., Colucci, W. J., McLaughlin, M. L., Barkley, M. D., *J. Am. Chem. Soc.*, **1992**, *114*, 8449 - 8454
- 73 Schwander, H., Hendrix, P., *Fluorescent dyes*, Ullmann's encyclopedia of industrial chemistry, **2005**
- 74 Gunnlaughsson, T., Kruger, P. E., Jensen, P., Tierney, J., Ali, H. D. P., Hussey, G. M., *J. Org. Chem.*, **2005**, *70*, 10875 - 10878
- 75 Grabchev, I., Qian, X., Xiao, Y., Zhang, R., *New J. Chem*, **2002**, *26*, 920 - 925
- 76 Wulff, G., Vesper, W., Grobe-Einsler, R., Sarhan, A., *Makromol. Chem.*, **1977**, *178*, 2799-2816
- 77 Cormack, P. A. G., Zurutuza Elorza, A., *J. Chromatogr. B*, **2004**, *804*, 173-182
- 78 Dickert, F. L., Hayden, O., Non-covalent molecularly imprinted sensors for vapours, polyaromatic hydrocarbons and complex mixtures, In *Molecularly imprinted polymers. Man made mimics of antibodies and their applications in analytical chemistry*; Sellergren, B., Elsevier Science B.V., Amsterdam, 2001; p 521
- 79 Komiyama, M., Takeuchi, T., Mukawa, T., Asamuma, H.,(ed) *Molecular Imprinting. From Fundamentals to applications*, Wiley-VCH, **2003**
- 80 Sellergren, B., The non-covalent approach to molecular imprinting, In *Molecularly imprinted polymers. Man made mimics of antibodies and their applications in analytical chemistry*; Sellergren, B., Elsevier Science B.V., Amsterdam, 2001; p 168
- 81 Sellergren, B., The non-covalent approach to molecular imprinting, In *Molecularly imprinted polymers. Man made mimics of antibodies and their applications in analytical chemistry*; Sellergren, B., Elsevier Science B.V., Amsterdam, 2001; p 177
- 82 Z. Shen, H. Röhr, K. Rurack, H. Uno, M. Spieles, B. Schulz, G. Reck, N. Ono, *Chem. Eur. J.* **2004**, *10*, 4853-4871
- 83 U. Resch, K. Rurack, *Proc. SPIE-Int. Soc. Opt. Eng.*, **1997**, *3105*, 96-103
- 84 Saha, S., Samanta, A., *J.Phys. Chem. A*, **2002**, *106*, 4763-4771
- 85 Saha, S., Samanta, A., *J.Phys. Chem. A*, **2002**, *106*, 4763-4771
- 86 Harriman, A.; Mallon, L. J.; Elliot, K. J.; Haefele, A.; Ulrich, G.; Ziessel, R. *J. Am. Chem. Soc.* **2009**, *131*, 13375-13386
- 87 Shea, K. J., Stoddard, G. J., *Macromolecules*, **1991**, *24*, 1207
- 88 Porcal, W.; Hernández, P.; Aguirre, G.; Boiani, L.; Boiani, M.; Merlino, A.; Ferreira, A.; Di Maio, R.; Castro, A.; González, M.; Cerecetto, H. *Bioorg. Med. Chem.* **2007**, *15*, 2768.
- 89 Luebke, M.; Whitcombe, M. J.; Vulfson, E. N. *J. Am. Chem. Soc.* **1998**, *120*, 13342.

- ⁹⁰ Gunnlaughsson, T., Kruger, P. E., Jensen, P., Tierney, J., Ali, H. D. P., Hussey, G. M., *J. Org. Chem.*, **2005**, *70*, 10875 - 10878
- ⁹¹ Gunnlaughsson, T., Kruger, P. E., Jensen, P., Tierney, J., Ali, H. D. P., Hussey, G. M., *J. Org. Chem.*, **2005**, *70*, 10875 - 10878
- ⁹² Lazraq, I., *Host monomers for stoichiometric imprinting of oxyanions: Chromogenic and fluorogenic receptors designed for possible sensing applications*, (Ph.D. thesis), **2008**